FROM MUTATIONS TO DISEASE MECHANISM IN RETT SYNDROME, BREAST CANCER, AND CONGENITAL HYPOTHYROIDISM

by

İbrahim Barış

B.S., Molecular Biology and Genetics, Boğaziçi Univesity, 2000

M.S., Molecular Biology and Genetics, Boğaziçi Univesity, 2002

Submitted to the Institute for Graduate Studies in
Science and Engineering in partial fulfillment of
the requirements for the degree of
Doctor of Philosophy

Graduate Program in Molecular Biology and Genetics

Boğaziçi University

2008

to my family

ACKNOWLEDGEMENTS

I would like to express my sincere gratitude to my thesis supervisor Assoc. Prof. Esra Battaloğlu for her endless support and intimate encouragement throughout my thesis.

My appreciation is also extended to the members of my thesis committee Prof. A. Nazlı Başak, Prof. Hande Çağlayan, Prof. Uğur Özbek, and Assoc. Prof. Müge Türet Sayar for allocating their time to evaluate this work.

I would like to extend my gratitude to Boğaziçi University, Scientific Research Projects Fund for funding the expenses of my thesis (Project No: 03S101 and 08B103D).

I am grateful to the CMT members Duygu, Çiğdem, İrem, Başak, and Dr. Rezan who has provided a warm environment in the lab. I am also thankful to all Retina and plant group members for creating best laboratory environment ever. I am grateful to my dear friends Dr. Birdal Bilir and Dr. Yeşim Özmen for their valuable and wonderful friendship. I would to extend my thanks to all my dear friends (Kader, İnanç, Sibel, and Murat) in the department.

I wish to thank all of the academic staff, among whom I would like to mention Prof. Kuyaş Buğra, Assoc. Prof. Muge Türet Sayar, and Assoc. Prof. Nesrin Özeren for their kind support and encouragement.

I would like to express my great thanks to each of my family member, especially to my parents for standing by my side at all time. I am grateful to my wife Tuğba who has always supported, appreciated and encouraged me with his endless love and patience throughout my life. Additionally, I would not complete my thesis work on time without her help in DNA sequencing and quantitative analyses.

ABSTRACT

FROM MUTATIONS TO DISEASE MECHANISM IN RETT SYNDROME, BREAST CANCER, AND CONGENITAL HYPOTHYROIDISM

Epidemiological studies provide the correlative data to understand the etiology of human inherited diseases and develop efficient genetic testing assays. Additionally, the accumulated data of genetic and epigenetic findings, expression profiling, and proteomics allows disease diagnosis, to understand the molecular mechanisms leading to the disease pathogenesis, and to develop efficient therapeutic approaches. In the framework of this thesis, we have investigated genetic and epigenetic changes and performed genotype-phenotype correlations to unravel the molecular mechanisms that lead to three different diseases, Rett Syndrome, breast cancer, and congenital hypothyroidism.

The genetic basis of Rett Syndrome (RTT) was investigated in a total of 71 RTT patients. A heterogeneous spectrum of disease-causing *MECP2* mutations was identified in 68.2 per cent of a clinically well defined group of cases whereas in only 12.5 per cent of the patients referred for differential diagnosis suggesting that this gene does not represent a major cause of the disease among patients with Rett-like features. For the first time, we have identified gene duplications as causative mutations in female atypical RTT cases. Consistent with the animal models, our results support the possibility that duplication of MECP2 that leads to increased expression might underlie some cases of X-linked delayed-onset neurobehavioral disorders including Rett Syndrome. Our results showed that exon rearrangements that could not be detected by standard techniques contribute to 19.3 per cent of these MECP2 mutations, and should be considered in especially RTT variants in order to determine the actual significance of the gene in the etiology of RTT. Genotype/phenotype correlation was performed based on comparison of severity score of patients with the type and location of the mutation and the XCI pattern. The results did not reveal a statistically significant correlation, but, the patients with exon deletions were

found to be more severely affected than patients with all other types of mutations and patients with exon duplications to present with severe eye contact problems. Additionally, we have developed and validate a novel multiplexed amplification refractory mutation system (ARMS) assay for identification of seven common mutations that accounts for almost 65 per cent of all MECP2 gene mutations. The validation studies revealed that our novel assay is an efficient, reliable, and cost-effective screen for molecular genetic testing of patients with RTT. Furthermore, we tested the effect of DNA concentration on reliablity and reproducibility of SYBR green dye-based Real Time PCR analysis to detect the MECP2 exon rearrangments. The results suggested that Real Time PCR analysis is reliable for determination of the exon copy number if the DNA amount is in the range of 1-50 ng.

To our knowledge, there are no known reports investigating the role of methylation of hHR23A and hHR23B genes in the tumor tissues. We have characterized the 5' flanking region of the hHR23A and hHR23B genes using web-based analysis and investigated the involvement of methylation status of putative promoter region of hHR23A and hHR23B genes in breast carcinogenesis. The observations of the hypermethylation of hHR23A gene and the presence of methylated conserved motifs and transcription binding sites in hHR23B gene among the analyzed tumor tissues suggested the involvement of methylation of hHR23 genes in the breast carcinogenesis. Investigation of epigenetic changes in tumor samples of breast cancer patients was a pioneering work since available literature implicates its presence only in cell lines.

Since our CH patient was the first case with Bamforth Syndrome and suffered the plasma cholinesterase deficiency, the genetic mechanisms leading to congenital hypothyroidism and prolonged paralysis after mivacurium were investigated. In contrast to other reported two patients with TTF2 gene mutation, the presence of thyroid tissue in our patient suggested further phenotypic heterogeneity associated with human TTF-2 mutations. The functional study with a collaborative work also helped to understand the genetic mechanisms and provided original evidence that implicated differential effects of TTF-2 mutations on downstream target genes required for normal human thyroid organogenesis.

ÖZET

RETT SENDROMU, MEME KANSERİ, VE KONJENİTAL HİPOTİROİDİZMDE MUTASYONLARDAN HASTALIK MEKANİZMASINA

Epidemiyolojik çalışmalar, insan kalıtsal hastalıklarının etiyolojisinin anlaşılması ve genetik testlerin geliştirilmesi için, karşılaştırmalı veriler sağlar. Bunun yanı sıra, genetik ve epigenetik bulgular, anlatım profilleri ve proteomiksden elde edilen bilgi birikimi, hastalık tanısına, hastalık patogenezine neden olan moleküler mekanizmaların anlaşılmasına ve doğru töropatik yaklaşımların geliştirilmesine ışık tutar. Bu tez çalışması kapsamında, üç farklı hastalığa, Rett Sendromu (RTT), meme kanseri ve Konjenital Hipotiroidizme (CH), neden olabilecek mekanizmaları aydınlatmak amacıyla genetik ve epigenetik değişimler incelendi ve genotip-fenotip karşılaştırması yapıldı.

RTT'nin genetik temeli toplam 71 hastada incelendi. Kesin klinik tanı alan hastaların yüzde 68.2'sinde heterojen dağılım gösteren ve hastalığa neden olduğu bilinen MECP2 gen mutasyonları tanımlanırken, ayırımcı tanı amacıyla yönlendirilen hastaların sadece yüzde 12.5'inde mutasyonların belirlenmesi, sözkonusu genin, RTT-benzeri özellikler gösteren hastalar için majör neden olamayacağını düşündürdü. Atipik RTT olgularında, ilk defa, gen duplikasyon mutasyonlarının hastalığa neden olabileceği gösterildi. Hayvan modellerindeki bulgularla örtüşen sonuçlar, duplikasyonların, MECP2 anlatımının artmasına ve Rett Sendromunu da içeren bazı X'e bağlı geç-başlangıçlı nörodavranışsal hastalıklara neden olabileceği olasılığını destekledi. Sonuçlar, standart teknikler ile tanımlanamayan ekson düzenlenme bozukluklarının, mutasyonların yüzde 19.3'ünü kapsadığını ve sözkonusu genin RTT etiyolojisine gerçek katkısının belirlenmesi açısından özellikle RTT varyantlarında araştırılması gerektiğini gösterdi. Hastalık şiddeti skorları ile mutasyonların tipi ve konumlarının, ve XCI paterninin karşılaştırılması temeline dayanan genotip/fenotip korelasyonu gerçekleştirildi. Bulgular istatiksel olarak anlamlı bir korelasyonu desteklemese de ekson delesyonu taşıyan hastaların diğer tüm mutasyon

tiplerini taşıyan hastalardan daha şiddetli etkilendikleri ve ekson duplikasyonu olan hastalarda şiddetli göz kontağı problemi olduğu bulundu. Ayrıca bilinen tüm MECP2 gen mutasyonlarının yüzde 65'ini oluşturan ve en sık görülen yedi mutasyonun tanımlanması amacıyla yeni bir multipleks amplifikasyon refrakter mutasyon tanımlama sistemi (ARMS) geliştirildi ve geçerliliği sınandı. Yeni metodun RTT hastalarının moleküler genetik analizinde kullanılabilecek elverişli, güvenilir, ve düşük maliyetli bir test olduğu gösterildi. Bunun yanı sıra, DNA konsantrasyonunun, MECP2 ekson düzenleme bozukluklarının belirlenmesinde kullanılan SYBER yeşili boya-bazlı Gerçek Zamanlı PCR analizinin güvenilirliği ve tekrarlanabilirliği üzerindeki etkisi irdelendi. Ayrıca, ekson kopya sayısının belirlenmesi çalışmalarında, DNA miktarının 1-50 ng aralığında olduğu durumlarda Gerçek Zamanlı PCR analizinin güvenilir sonuçlar verdiği gösterildi.

Bilgimiz dahilinde, tümör dokularında hHR23A and hHR23B gen metilasyonlarının rolünü araştıran raporlar bulunmamaktadır. Bu konuda katkı sağlamak amacıyla sözkonusu genlerin 5' uçları web tabanlı analiz kullanılarak karakterize edildi ve olası promotör bölgelerinin metilasyon durumunun meme karsinogenezindeki rolü incelendi. Analiz edilen tümör dokularında hHR23A gen hipermetilasyonunun gözlenmesi ve hHR23B geninde korunmuş metilasyon motifleri ve transkripsiyon bağlanma bölgelerinde metilasyon bulunması hHR23 genlerinin metilasyonunun meme kanseri oluşumunda yer alabileceğini düşündürdü. Literatürde epigenetik değişimlerin sadece hücre hatlarında gösterilmiş olması nedeniyle meme kanseri hastalarının tümör dokularında bu değişimlerin araştırılması öncü bir çalışma niteliğindedir.

Tez kapsamında incelenen konjenital hipotiroidizm (CH) hastası ilk Bamford Sendromlu olgu olması ve plazma kolin esteraz yetersizliği göstermesi nedeniyle CH'e ve mivacurim kullanımı sonrası uzun paralize neden olan mekanizmanın aydınlatılması amacıyla incelendi. TTF2 gen mutasyonu olduğu bilinen diğer iki hastanın aksine hastamızda tiroid bezinin varlığının belirlenmesi insanda TTF2 mutasyonları ile ilişkili fenotipik heterojenliğin bilinenden fazla olduğunu ortaya çıkardı. Uluslararası ortak bir çalışma ile gerçekleştirilen işlevsel analizler de genetik mekanizmanın anlaşılmasına yardımcı oldu ve TTF2 mutasyonlarının normal insan tiroid organogenezinde rol alan hedef genler üzerindeki farklı etkilerine işaret eden özgün kanıt sağladı.

TABLE OF CONTENTS

LIST OF FIGURES

LIST OF TABLES

LIST OF SYMBOLS / ABBREVIATIONS

R	Arginine
T4	Thyroxine
W	Tryptophan
X	Stop
5meC	5- methyl cytosine
APS	Ammoniumpersulfate
ARMS	Amplification refractory mutation system
AS	Angelman syndrome
BChE	Butyrylcholinesterase
BDNF	Brain-derived neurotrophic factor
BER	Base excision repair
Bp	Base pair
BSA	Bovine serum albumine
C	Cysteine
cAMP	Cyclic adenosine 5'-monophosphate
CDKL5	cyclin-dependent kinase like 5
cDNA	Complementary deoxyribonucleic acid
CH	Congenital hypothyroidism
CNS	Central nervous system
CT	Computed tomography
CREB	Cyclic AMP-responsive element binding
CRH	Corticotropin-releasing hormone
DCIS	Ductal carcinoma *in situ*
DLX5	Distal-less homeobox 5
DNA	Deoxyribonucleic acid
DNMT	DNA methyltransferase
dNTP	Deoxynucleosidetriphosphate
ECG	Electrocardiography
EEG	Electroencephalogram

H	Histone
FHD	Forkhead domain
Fkbp5	FK506-binding protein 5
GG-NER	Global genome nucleotide excision repair
GST	Glutathione S-transferase
HATs	Histone acetyltransferases
HDACs	Histone deacetylases
IDC	Invasive (infiltrating) ductal carcinoma
ILC	Invasive lobular carcinomas
KD	Knockdown
KO	Knockout
LCIS	Lobular carcinoma *in situ*
LTP	Long-term potentiation
MBD	Methyl binding domain
MDM2	Mouse double minute 2
MECP2	methyl-CpG-binding protein 2
Mecp2	mause methyl-CpG-binding protein 2
$Mecp2^{-/-}$	*Mecp2*-null female
$Mecp2^{-/y}$	*Mecp2*-null male
$MgCl_2$	Magnesium Chloride
mM	Milimolar
mRNA	Messenger ribonucleic acid
MRX	X-linked mental retardation
NER	Nucleotide excision repair
NIS	Sodium iodide transporter
NLS	Nuclear localization signals
Nm	nanometer
OD_{260}	Optical density at 260 nm
PAGE	Poly acrylamide gel electrophoresis
PChE	Pseudocholinesterase
PCR	Polymerase chain reaction
PRNP	Prion protein
PSV	Preserved speech variant

QF-PCR	Quantitative fluorescent multiplex PCR
RBC	Red blood cell
RNA	Ribonucleic acid
ROS	Reactive oxygen species
Rpm	Revolution per minute
RTT	Rett syndrome
SDS	Sodium dodecyl sulfate
Sgk1	Serum glucocorticoid-inducible kinase 1
SSCP	Single strand conformation polymorphism
STI1	Stress-induced phosphoprotein
STK9	Serine/threonine kinase 9
T3	Triiodothyronine
TBE	Tris-base- boric Acid- Edta
TC-NER	Transcription-coupled nucleotide excision repair
TE	Tris-Edta
TEMED	N,N,N',N'-Tetramethylethylenediamine
TFC	Follicular cells
TFIIH	Transcription factor IIH
TG	Thyroglobulin
TPO	Thyroid peroxidase
TRD	Transcription repression domain
TSHR	TSH receptor
TTF	Thyroid transcription factors
UBA	Ubiquitin-associated
UBE3A	Ubiquitin ligase E3A
UBL	Ubiquitin-like
UV	Ultraviolet
XCI	X-chromosome inactivation
XPC	Xeroderma pigmentosum group C
YB1	Y box-binding protein 1

1. INTRODUCTION

1.1. Epigenetics

1.1.1. Epigenetics

Epigenetics refers to stable and heritable changes in gene expression that are not directly attributable to DNA sequence alterations. These changes may affect the expression of a gene or the properties of its product. Epigenetic mechanisms provide an "extra" level of transcriptional control and include DNA methylation, histone modifications, chromatin configuration changes, imprinting, and RNA-associated silencing (Rodenhiser and Mann, 2006). The human genome contains approximately 23 000 genes that should be expressed in specific cell types at precise times and this is known to be achieved via two pathways. The first pathway is the immediate control by transcriptional activators and repressors that have various nuclear concentrations, covalent modifiers, and subunit associations. It is the traditional model of genetics in which the regulation of transcription and messenger RNA (mRNA) stability are directly influenced by the genomic DNA sequence and any sequence changes present. The second pathway is the epigenetic regulation by altering chromatin structure through covalent modification of DNA and histones. The epigenetic pattern can be transmitted from parent cell to daughter cell maintaining a specific epigenotype within cell lineages. Thus, the phenotype is a result of the genotype, the specific DNA sequence, and the epigenotype.

1.1.2. DNA Packaging

DNA is wrapped around clusters of globular histone proteins to form nucleosomes. Nucleosomes consist of short segments of a 146-bp DNA wrapped tightly around a set of conserved basic proteins known as histones (H2A, H2B, H3, and H4) (Margueron *et al.*, 2005). Each nucleosome consists of histone octamers (2 of each protein), and these basic histone proteins allow interaction with acidic DNA. These repeating nucleosomes of DNA and histones are organized into chromatin (Figure 1.1). The structure of chromatin is not static, and influences the gene expression. Transcriptionally inactive DNA is characterized by a highly condensed conformation and is associated with regions of the genome that

undergo late replication during S phase of the cell cycle. Transcriptionally active DNA has a more open conformation, is replicated early in S phase, and has relative weak binding by histone molecules (Figure 1.1). These dynamic chromatin structures are controlled by reversible epigenetic patterns of DNA methylation and histone modifications (Feinberg *et al*., 2004). Enzymes involved in this process include DNA methyltransferases (DNMTs), histone acetyltransferases (HATs), histone deacetylases (HDACs), histone methyltransferases, and the methyl-binding domain proteins (Rodenhiser and Mann, 2006; Strachan *et al*., 2003).

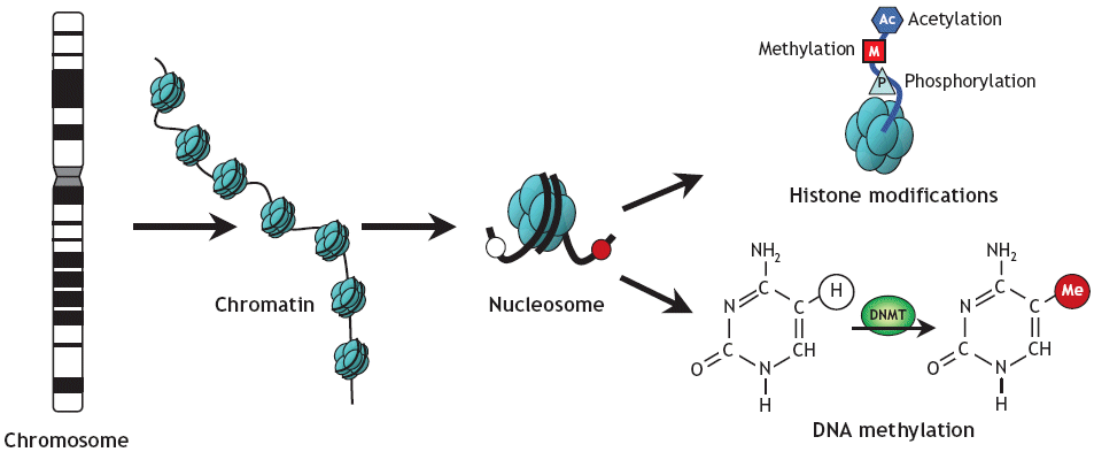

(a)

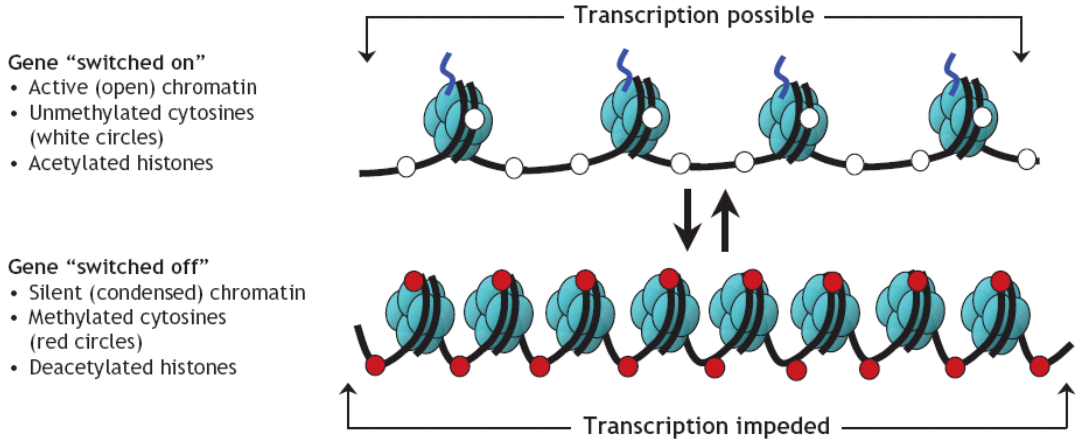

(b)

Figure 1.1. Schematics of epigenetic modifications (a) and reversible changes in chromatin organization (b) that influence the gene expression (Rodenhiser and Mann, 2006).

1.1.3. Epigenetic Modifications

1.1.3.1. CpG and non-CpG Methylation. DNA methylation refers to the covalent addition of a methyl group derived from S-adenosyl-L-methionine to the fifth carbon of the cytosine ring to form the 5- methyl cytosine (5meC) (Ehrlich *et al*., 1981). Across eukaryotic species, methylation occurs predominantly in cytosines located 5′ of guanines, known as CpG dinucleotides. In the mammalian genome, the distribution of CpG dinucleotides is nonrandom (Antequera and Bird, 1993). They are greatly under-represented in the genome because of evolutionary loss of 5meCs through deamination to thymine. However, clusters of CpGs known as CpG islands are preserved in 1–2 per cent of the genome. Briefly, CpG islands are defined as the region of DNA ranging from 200 bp to 5 kb in size and with greater than 55 per cent GC content. More than 40 per cent of mammalian genes have CpG islands (Bird *et al*., 2002). About 70 per cent of CpG islands are located in the promoter, the first exon, and the first intron of the genes, suggesting that they are important for gene regulation. Typically, unmethylated clusters of CpG dinucleotides are located at the upstream of tissue specific genes and essential "housekeeping" genes that are required for cell survival and are expressed in most tissues. These unmethylated CpG islands are targets for proteins that initiate gene transcription. However, methylated CpGs are associated with silent DNA and cause stable heritable transcriptional silencing. The establishment and maintenance of DNA methylation patterns is provided by DNA methyltransferases (DNMTs) and accessory proteins (Dnmt1, Dnmt3a, Dnmt 3b, Dnmt2, and Dnmt 3L) (Egger *et al*., 2004). Two mechanisms have been proposed to explain the inhibitory effect of CpG methylation on gene expression (Figure 1.2). First, it might inhibit the binding of transcription factors to their recognition sites. Many factors are known to bind CpG-containing sequences, and some of these fail to bind when the CpG is methylated (Bell and Felsenfeld, 2000). The second and more prevalent mechanism involves proteins with high affinity for methylated CpGs, such as the methyl-CpG-binding protein MeCP2, the methyl-CpG-binding-domain proteins MBD1, MBD2 and MBD4, and Kaiso. These proteins induce the recruitment of protein complexes (co-repressor Sin3a and HDACs) that are involved in histone modification and chromatin remodeling.

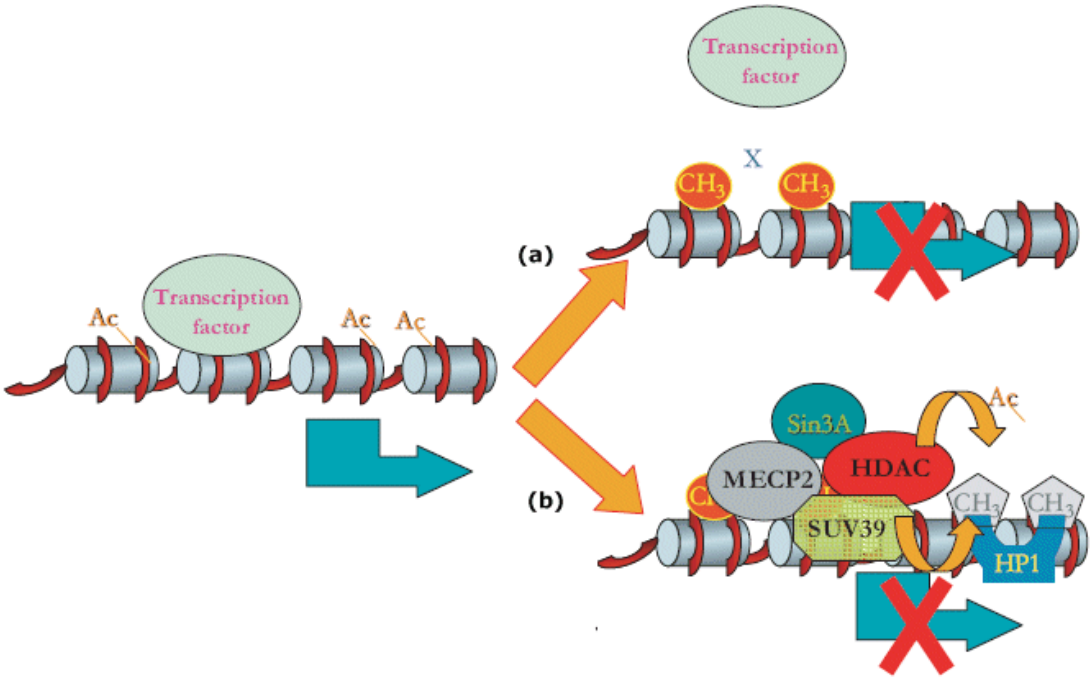

Figure 1.2. DNA methylation can silence genes by either direct (a) or indirect mechanisms (b) (SZYF, 2006).

Cytosine methylation of non-CpG (CpA, CpC and CpT) dinucleotides are commonly observed in embryonic stem cells and plants (Ramsahoye *et al*., 2000). Grandjean *et al.* (2007) has reported that Cre-LoxP recombination as well as other non homologous recombination types (Rassoulzadegan *et al*., 2002) are strongly inhibited in non-CpG methylated regions. It is also consistent with previous observations that showed *in vivo* involvement of extensively non-CpG methylated oligo C sequences in inactivation of transposons and integrated viral genomes (Dodge *et al*., 2002; Brooks *et al*., 2004).

The exact mechanism(s) responsible for *de novo* CpG and non-CpG methylation process is only partly known. Most of the currently available information concerns methylation in the symmetrical CpG dinucleotides. Much less is known of the somatic and germ line maintenance of the non CpG methylation pattern observed in animal and plant cells (Finnegan *et al*., 2000; Chan *et al*., 2005). Recent data indicate that the proteins Dnmt3a and Dnmt3b may be responsible for *de novo* methylation whereas Dnmt1 maintain established patterns of methylation (Okano *et al*., 1999; Oka *et al*., 2005). *De novo* methylation of both CpG and non-CpG sites is believed to occur during embryogenesis by post implantation expression of DNMT3s (Dnmt3b or 3l) (Grandjean *et al*., 2007). After

the repression of DNMT3 expression, Dnmt1 maintains the methylation of CpGs but not on other methylated C residues, resulting in the loss of non-CpG methylation (Ramsahoye *et al*., 2000). In tumor cells, de novo CpG and non-CpG methylation is observed and most likely the results of reactivation of DNMT3 expression (Oka *et al*., 2005; Kouidou *et al*., 2005).

1.1.3.2. Histone Modification. In addition to DNA methylation, changes to histone proteins affect the DNA structure and gene expression (Peterson *et al*., 2004). These modifications, including acetylation, methylation, phosphorylation, ubiquitination, and poly–adenosine diphosphate ribosylation, ensure that DNA is accessible for transcription or targeted for silencing. Among them, acetylation and methylation of lysine residues in the amino termini of histones H3 and H4 are highly correlated with transcriptional activities. HATs add acetyl groups to lysine residues close to the N terminus of histone proteins, neutralizing the positive charge. The acetylated N termini then form tails that protrude from the nucleosome core. Because the acetylated histones are thought to have a reduced affinity for DNA and possibly for each other, the chromatin may be able to adopt a more open structure, make DNA more accessible to the transcriptional machinery, and facilitate localized transcription. HDACs promote repression of gene expression, presumably because the chromatin can become more condensed upon deacetylation. Changes in chromatin structure mediated by equilibrium between HAT and HDACs affect regulation of transcription (Strachan *et al*., 2003; Ausio *et al*., 2003) Histone methylation can be a marker for both active and inactive regions of chromatin. Methylation of lysine 9 on the N terminus of histone H3 is a hallmark of silent DNA and is globally distributed throughout heterochromatic regions such as centromeres, telomeres and silenced promoters. In contrast, methylation of lysine 4 of histone H3 denotes activity and is found predominantly at promoters of active genes. Combinations of acetylation, methylation, and other posttranslational processing events lead to enormous variation of histone modifications (Egger *et al*., 2004).

Epigenetic mechanisms are involved in control of gene expression, including tissue-specific expression, imprinting, silencing of repetitive elements, correct organization of chromatin and X-chromosome inactivation. Perturbations in the patterns of DNA methylation and histone modifications can lead to congenital disorders, multisystem

pediatric syndromes, neurodevelopmental disorders (e.g. Rett Syndrome) or predispose people to acquired disease such as sporadic cancers and neurodegenerative disorders.

1.2. Rett Syndrome

Rett syndrome (RTT; OMIM 312750) is an X-linked dominant postnatal progressive neurodevelopmental disorder and the second most common cause of mental retardation affecting females (Rett, 1966; Hagberg *et al*., 1983).

1.2.1. Historical Background

In 1965, Dr. Andreas Rett, an Austrian physician, investigated two disabled girls having abnormal hand movements like winging, washing and clapping. One year later, he reported 22 girls with these abnormal clinical features (Rett, 1966). However, the report would not be recognized in the medical community for 17 years. In 1983, Dr. Bengt Hagberg, a Swedish neurologist, and his colleagues reported the clinical description of 35 cases (Hagberg *et al*., 1983). He recognized that his patients showed overlapping phenotype with Dr. Rett's and called the disease as Rett Syndrome to honor the first description by Dr. Rett.

1.2.2. Clinical and Neuropathological Charecteristics

After normal development up to the age of 6 to 18 months, RTT patients show a regression of motor and mental abilities. The clinical manifestations in the classical form of RTT are characterized by cognitive deterioration with autistic features, loss of acquired skills such as language and hand usage, stereotypical hand wringing movements, and gait ataxia (Weaving *et al*., 2005). Behavioral abnormalities include teeth grinding, night laughing or crying, screaming fits, low mood, and anxiety episodes elicited by distressful external events (Mount *et al*., 2001). Patients suffer generalized rigidity, dystonia, and worsening of scoliosis. Autistic features include expressionless face, hypersensitivity to sound, lack of eye-to-eye contact, indifference to the surrounding environment, and unresponsiveness to social cues (Segawa and Nomura, 2005). Most girls with RTT suffer

breathing anomalies, including breath-holding, aerophagia, forced expulsion of air and saliva, apnea, and hyperventilation.

Patients with RTT develop postnatal microcephaly. The major morphological abnormalities detected in the central nervous system (CNS) are an overall decrease in the size of the brain and of individual neurons. Autopsy studies revealed a 12–34 per cent reduction in brain weight and volume in patients with RTT, the effect most pronounced in the prefrontal, posterior frontal, and anterior temporal regions (Armstrong *et al*., 2005). The RTT brain shows no obvious degeneration, atrophy, or inflammation, and there are no signs of gliosis or neuronal migration defects (Jellinger *et al*., 1988; Reiss *et al*., 1993). These observations indicate that RTT is a disorder of postnatal neurodevelopment rather than a neurodegenerative process. In addition, dendritic spines of the RTT frontal cortex are sparse and short, with no other apparent abnormalities (Belichenko *et al*., 1994). Although neuronal size is reduced in the cortex, thalamus, basal ganglia, amygdala, and hippocampus, there is an increase in neuronal cell packing in the hippocampus (Kaufmann and Moser, 2000).

Neurophysiological studies of mouse models and patients with RTT revealed that both the CNS and the autonomous nervous system contribute to the pathophysiology of the disease. Altered somatosensory evoked potentials and abnormal electroencephalogram (EEG) findings of focal, multifocal, and generalized epileptiform discharges and the occurrence of rhythmic slow theta activity, all suggest altered cortical excitability in the RTT brain. Electrocardiographic recordings (ECG) demonstrate long corrected QT intervals and suggest perturbation of the autonomic nervous system (Glaze *et al*., 2005). Mouse models reveal abnormalities in long-term potentiation (LTP) and impaired synaptic plasticity. LTP is reduced in Mecp2$^{-/Y}$ and Mecp2$^{308/Y}$ cortical slices whereas LTP is enhanced in hippocampal slices of mouse with MeCP2 overexpression (*MECP2*^{Tg}) (Asaka *et al*., 2006; Moretti *et al*., 2006; Collins *et al*., 2004). In addition, reduced spontaneous activity in cortical slices of null mice was observed due to a decrease in the total excitatory synaptic drive and an increase in the total inhibitory drive (Dani *et al*., 2005). Synaptic outputs in glutamatergic neurons showed 50 per cent reduction and 100 per cent enhancement in Mecp2$^{-/Y}$ and *MECP2*^{Tg}, respectively (Chao *et al*., 2007).

Altogether, these findings indicate that MeCP2 is essential in modulating synaptic function and plasticity, and that MeCP2 function is critical in regulating the number of excitatory synapses during early postnatal development (Chahrour and Zoghbi, 2007).

1.2.3. Phenotypic Variability in RTT

Atypical variants of RTT are also commonly observed, and five distinct categories have been delineated on the bases of clinical criteria: Infantile (early) seizure onset, congenital forth, 'forme fruste', preserved speech variant (PSV), and late childhood regression form (Hagberg *et al*., 2002). These variants range from milder forms with a later age of onset to more severe manifestations. 'Forme fruste' comprises the most common group (with 80 per cent) of atypical variants. These patients have surprisingly well preserved, yet somewhat dyspraxic, hand function, as well as absence of the classic hand wringing stereotypies (Hagberg, 2002). The PSV variant is characterized by the ability of patients to speak a few words, although not necessarily in context. PSV patients have a normal head size and are usually overweight and kyphotic (Zappella *et al*., 2001). Early seizure onset type and congenital forth are the more severe variants of RTT. Early seizure onset type is characterized by a lack of early normal period due to presence of seizures whereas congenital forth patients lack the early period of normal development (Chahrour and Zoghbi, 2007). A definite loss of acquired hand skill is not found in congenital forth cases, instead an improvement with age in their most primitive early bilateral hand use is seen (Hagberg *et al*., 2002). Classical and atypical RTT phenotypes vary in severity and onset between different patients and in the same patient over time.

1.2.4. Genetic Basis of RTT

RTT has an incidence of 1/10,000 to 1/22,000 female live births (Percy, 2002). However, since more than 99 per cent of RTT cases are sporadic, it was very hard to map the disease locus by traditional linkage analysis. Using information from rare familial cases, exclusion mapping identified the Xq28 candidate region, and subsequent screening of candidate gene, methyl-CpG-binding protein 2 (MECP2; MIM# 300005), revealed mutations in RTT patients (Amir *et al*., 1999). Several recent studies identified mutations in the CDKL5 gene (OMIM 300203) encoding cyclin-dependent kinase like 5 in patients

with an atypical, early onset seizure variant of RTT (Weaving *et al*., 2005; Evans *et al*., 2005; Scala *et al*., 2005). The disruption of NTNG1 gene, encoding the axon guiding molecule Netrin G1, by a balanced chromosome translocation was described in one female patient with atypical RTT and early-onset seizures (Borg *et al*., 2005). However, this might be an isolated case because *NTNG1* screening in a cohort of *MECP2* and *CDKL5* mutation-negative patients with RTT failed to identify any pathogenic mutations in this gene (Archer *et al*., 2006).

RTT was initially thought to affect exclusively females and germline *MECP2* mutations were considered to be lethal in males. Recently, several investigators have reported MECP2 mutations in males with classic RTT, nonfatal nonprogressive encephalopathy, nonspecific X-linked mental retardation (MRX), language disorder, or schizophrenia (Orrico *et al*., 2000; Cohen *et al*., 2002; Kleeftra *et al*., 2004; Masuyama *et al*., 2005). Males with MECP2 mutations fall into three main categories: boys with Rett syndrome; boys with severe encephalopathy and infantile death; and boys with less severe neurological and/or psychiatric manifestations. Boys in the first category have a 47,XXY karyotype or are somatic mosaic and carry the same *MECP2* mutations that cause classic Rett syndrome in girls. Males in the second group carry *MECP2* mutations identical to those found in females; these mutations are generally thought to disrupt DNA binding or nuclear localization of the MECP2 protein. In the third group are boys with mutations that are not found in girls with Rett syndrome, presumably because their effects are mild in heterozygosity. Recent data indicate that increased *MECP2* gene-dosage can disrupt normal brain function. Interestingly, submicroscopic duplications in Xq28 region encompassing the *MECP2* gene were identified in a boy with severe mental retardation and clinical features of Rett syndrome, several patients with severe mental retardation and progressive spasticity, and male with non-specific X-linked mental retardation (Meins *et al*., 2005; van Esch *et al*., 2005; de Gaudio *et al*., 2006; Friez *et al*., 2006).

1.2.5. MECP2 Gene

The MECP2 gene is located on chromosome Xq28 and consists of four exons that code for two different isoforms of the protein, due to alternative splicing of exon 2. Two MeCP2 isoforms differ only in their N-terminus. The first identified isoform, MeCP2-e2

(MeCP2A, 486 amino acids) uses a translational start site within exon 2, whereas the new isoform, MeCP2-e1 (MeCP2B, 498 amino acids) is derived from an mRNA in which exon 2 is excluded and starts from ATG located within exon 1. MeCP2-e1 isoform is more abundant and contains 24 amino acids encoded by exon 1 and lacks the 9 amino acids encoded by exon 2 (Dragich *et al*., 2007; Kriaucionis and Bird, 2004; Mnatzakanian *et al*., 2004). In addition, *MECP2* has a large, highly conserved 3'-untranslated region that contains multiple polyadenylation sites, which can be alternatively used to generate four different transcripts. Expression studies in mice showed that the longest transcript is the most abundant in brain, with higher expression during embryonic development, followed by postnatal decline, and subsequent increase in expression levels later in adult life (Pelka *et al*., 2005; Shahbazian *et al*., 2002b). Although the MeCP2 is almost ubiquitously expressed, it is relatively more abundant in the brain, primarily in mature postmigratory neurons (Jung *et al*., 2003). MeCP2 protein levels are low during embryogenesis and increase progressively during the postnatal period of neuronal maturation (Balmer *et al*., 2003; Cohen *et al*., 2003; Kishi and Macklis, 2004; Mullaney *et al*., 2004; Shahbazian *et al*., 2002b). Both MeCP2 isoforms are nuclear and colocalize with methylated heterochromatic foci in mouse cells. Since *MeCP2* is expressed in mature neurons and its levels increase during postnatal development, it may play a role in modulating the activity or plasticity of mature neurons. Consistent with this, *MECP2* mutations do not seem to affect the proliferation or differentiation of neuronal precursors.

MeCP2 is a member of the family of related proteins that bind specifically to symmetrically methylated CpG dinucleotides via a conserved methyl binding domain (MBD) (Bird, 2002). Besides a methyl binding domain (MBD, residues 78–162), the protein includes a transcription repression domain (TRD, residues 207–310) involved in transcriptional repression through recruitment of co-repressors and chromatin remodeling complexes, two nuclear localization signals (NLS, residues173-193 and 255–271), and a 63 residue group II WW binding domain in C-terminal (from 325 to 388) (Figure 1.3). The C-terminus facilitates MeCP2 binding to naked DNA and to the nucleosomal core, and it also contains evolutionarily conserved poly-proline runs that can bind to group II WW domain splicing factors (Buschdorf and Stratling, 2004).

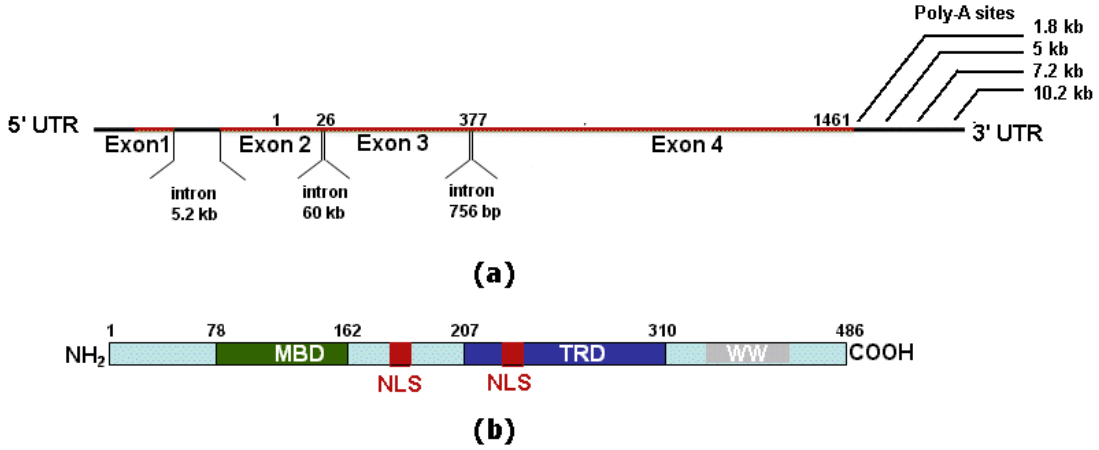

Figure 1.3. The MECP2 gene (a) and its protein product (MeCP2A) with conserved domains (b).

1.2.6. CDKL5 Gene

CDKL5 gene, previously known as serine/threonine kinase 9 (STK9), is located on chromosome Xp22. Alterations in this gene were originally found to cause early-onset epilepsy and infantile spasms with severe mental retardation (Grosso *et al*., 2007). The observation that mutations in *MECP2* and *CDKL5* cause similar phenotypes in early onset seizure variant of RTT suggested that these genes might participate in the same molecular pathways. Mari *et al*. (2005) showed that *MECP2* and *CDKL5* have an overlapping temporal and spatial expression profile during neuronal maturation and synaptogenesis and that they physically interact. The interaction was shown to require a portion of the C terminal domain of MeCP2, suggesting that mutations in this region might be involved in RTT onset owing to loss of interaction between the two proteins. Furthermore, it was shown that the kinase activity of CDKL5 can cause both autophosphorylation and MeCP2 phosphorylation, and this latter activity is eliminated in pathogenic CDKL5 mutants (Bertani *et al*., 2006). Phosphorylation of MeCP2 has a crucial role in the regulation of its target gene expression (Mari *et al*., 2005).

1.2.7. *MECP2 M*utation Profile

Mutations in the MECP2 gene are associated with several disorders that include Rett syndrome (RTT), Angelman syndrome like phenotype, autism, and even mild forms of

mental retardation (Amir *et al*., 1999; Couvert et a., 2001; Watson *et al*., 2001). *MECP2* mutations can be identified in 70–90 per cent of classical sporadic RTT cases, however, in only 29-45 per cent of atypical RTT and familial cases (Webb and Latif, 2001; Schanen *et al*., 2004, Fukuda *et al*., 2005).

Up to date more than 200 different mutations of *MECP2* have been identified in patients with classical and atypical RTT. Most mutations are *de novo* that arise in the paternal germline and often involve a C to T transition at CpG dinucleotides (Trappe *et al*., 2001; Wan *et al*., 1999). Among 200 different mutations of *MECP2* eight missense and nonsense mutations (p.R106W, p.R133C, p.T158M, p.R168X, p.R255X, p.R270X, p.R294X, and p.R306C) are known to account for almost 70 per cent (RettBASE).

Among those mutations, the great majority (80 per cent) represent single nucleotide changes, with the remainder small-scale deletions (17 per cent) or insertions (3 per cent). Most missense mutations are tightly clustered at the methyl-CpG binding domain (MBD). Deletion/insertion mutations leading to loss of the open reading frame occur throughout the gene, but are clustered in the C-terminal coding region, which contains a poly-histidine repeat (RettBASE).

With the use of quantitative experimental methods in recent years, *MECP2* exon deletions were identified in 2.9-14 per cent of cases with RTT (RettBASE). On the other hand, duplication was reported in only one female patient with PSV variant of RTT who was found to carry three copies of the MECP2 exon 4 (Ariani *et al*., 2004). Regardless of the mechanism, mutations within the *MECP2* lead to loss of function or a protein product with diminished stability.

A wide spectrum of phenotypic variability is observed in patients with *MECP2* mutations and considered with respect to the mutation type, location in the gene, and the X-chromosome inactivation (XCI) pattern. Genotype–phenotype correlations in females with Rett syndrome have yielded conflicting results. In general, female patients with mutations in *MECP2* that truncate the protein towards its C-terminal end (late-truncating mutations) have a milder phenotype, and less typical of classical Rett syndrome when compared to patients who have missense or N-terminal (early truncating) mutations

(Charman *et al*., 2005). Patients with mutations upstream of or within the TRD domain show greater clinical severity (Jian *et al*., 2005). In addition, p.Arg133Cys mutation causes an overall milder phenotype while the p.Arg270X mutation, which is predicted to result in a truncated protein, is associated with increased mortality (Kerr *et al*., 2006; Jian *et al*., 2005).

It has been suggested that genetic background and/or non-random X-chromosome inactivation in the brain influences the biological consequences of mutations in *MECP2*. In females, only one of the two X chromosomes is active in each cell and the choice of which X chromosome is active is usually random, such that half of the cells have the maternal X chromosome and the other half have the paternal X chromosome active. Therefore, a female with a *MECP2* mutation is typically mosaic, whereby half of her cells express the wild-type *MECP2* allele and the other half express the mutant *MECP2* allele. Occasionally, cells expressing the wild-type *MECP2* allele divide faster or survive better than cells expressing the mutant allele, which therefore results in a nonrandom pattern of XCI and amelioration of the RTT neurological phenotypes. Depending on the extent of such favorable skewing, some patients can be mildly affected or are even asymptomatic carriers of *MECP2* mutations (Weaving *et al*., 2005). The best examples for illustrating the dramatic effects of XCI patterns in RTT are monozygotic twins who manifest very different phenotypes (Dragich *et al*., 2000). In addition, skewed XCI patterns occur in brain regions of female mice heterozygous for a mutant *MECP2* allele, where phenotypic severity correlates with the degree of skewing (Young and Zoghbi, 2004).

1.2.8. MeCP2 Function

1.2.8.1. Transcription Regulation and Chromatin Remodeling. Findings of extensive research suggests that MeCP2 acts as a transmitter of epigenetic information by binding to methylated CpG dinucleotides, recruiting complexes that include histone deacetylase and methyltransferase, and leading to local transcriptional repression. The function of MeCP2 as a transcriptional repressor was first suggested based on *in vitro* experiments in which MeCP2 specifically inhibited transcription from methylated promoters (Nan *et al*., 1997). When MeCP2 binds to methylated CpG dinucleotides of target genes via its MBD, its TRD recruits the corepressor Sin3A and histone deacetylases (HDACs) 1 and 2 (Jones *et al*.,

1998; Nan *et al*., 1998). The transcriptional repressor activity of MeCP2 involves compaction of chromatin by promoting nucleosome clustering, either through recruitment of HDAC and histone deacetylation or through direct interaction between its C-terminal domain and chromatin (Figure 1.4) (Nikitina *et al*., 2007).

According to the dominant model of MeCP2 action, target genes are silenced by MeCP2 binding to the promoter. However, combined ChIP–chip promoter and expression profiling analysis reveals that 62.6 per cent of MeCP2-bound promoters (including *BDNF*) are transcriptionally active (Yasui *et al*., 2007). These studies clearly demonstrate that MeCP2 promoter occupancy does not correlate with transcriptional silencing of target genes but rather functions as a modulator of gene expression depending on the physiologic state of the organism. Metaphorically speaking, MeCP2 may be best thought of as the dimmer that regulates the amount of light rather than the switch that turns the lamp on and off (Chahrour and Zoghbi, 2007). Extensive studies of the binding of MeCP2 (or the MBD alone) to DNA *in vitro* have revealed that the affinity for methylated DNA is not strong and is only ~3-fold weaker for unmethylated DNA (Fraga *et al*., 2003).

Transcriptional profiling indicates that MeCP2 is not a general transcriptional repressor *in vivo* but has a more subtle effect involving a subset of genes (Tudor *et al*., 2002; Ballester *et al*., 2005). Also, the finding that MeCP2-induced repression is only partially alleviated by inhibiting HDACs suggests that its activity is not restricted to HDAC recruitment (Yu *et al*., 2000). Furthermore, there is evidence that MeCP2 is responsible for the formation of large chromatin loops (Horike *et al*., 2005) (Figure 1.5). Nikitina *et al*. (2007) has shown that MeCP2 dependent chromatin loop formation occurs in two steps: a methylation-independent interaction between chromatin and the C terminus that is required for the second, methylation-specific, interaction between DNA and the MBD domain. The yellow and blue arrows in Figure 1.5 indicate MeCP2-interacting sequences. When MeCP2 is present, it interacts with sequences that are near the imprinted DLX5 and DLX6 genes and define the boundaries of an 11-kb chromatin loop. This leads to an integration of *DLX5* and *DLX6* into a loop of silent, methylated chromatin, and represses their expression (Figure 1.5a). In neurons that are deficient for MeCP2, the chromatin in this region is structured into a distinct conformation that corresponds to active chromatin loops, which are bordered by sequences (indicated by long purple and orange

arrows) that interact with chromatin factors. Therefore, in MeCP2- deficient neurons, the expression of *DLX5* and *DLX6* is no longer repressed (Figure 1.5b) (Bienvenu and Chelly, 2006).

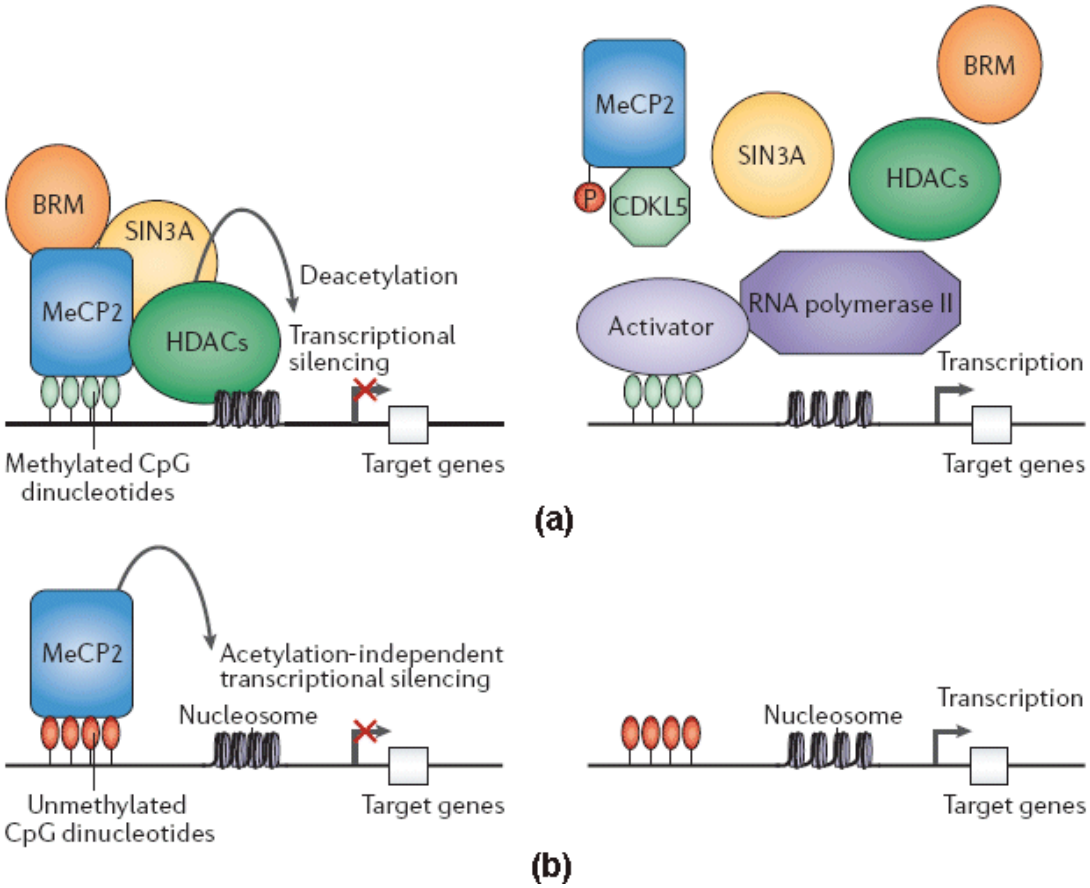

Figure 1.4. Mechanisms of methylation dependent (a) and independent (b) transcription regulation and chromatin remodeling (Bienvenu and Chelly, 2006).

1.2.8.2. RNA Splicing. Recent studies suggest that the function of MeCP2 might be more complex than previously anticipated. For instance, purified recombinant MeCP2 was shown to have a high-affinity RNA binding activity that is mutually exclusive to its methyl-CpG-binding properties and does not require the methyl-CpG-binding domain (Jeffery *et al*., 2004).

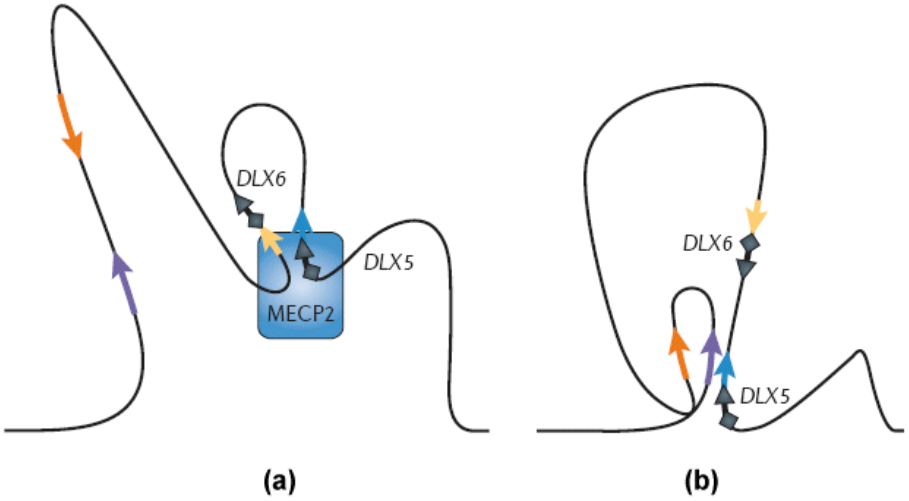

Figure 1.5. Regulation of imprinted regions through formation of a silent chromatin loop. (a) transcriptionally inactive and (b) active conformation (Bienvenu and Chelly, 2006).

Interestingly, although the biological significance of a MeCP2–RNA complex remains to be elucidated, recent data indicated that MeCP2 interacts with the RNA-binding Y box-binding protein 1 (YB1) and regulates splicing of reporter minigenes (Figure 1.6) (Young *et al*., 2005). Importantly, aberrant RNA-splicing patterns of several genes including *Dlx5* were identified in Mecp2 null mice (Young *et al*., 2005). The finding that MeCP2 regulates transcription and splicing of some of its targets suggests the existence of multiple layers of epigenetic regulation (Moretti and Zoghbi, 2006).

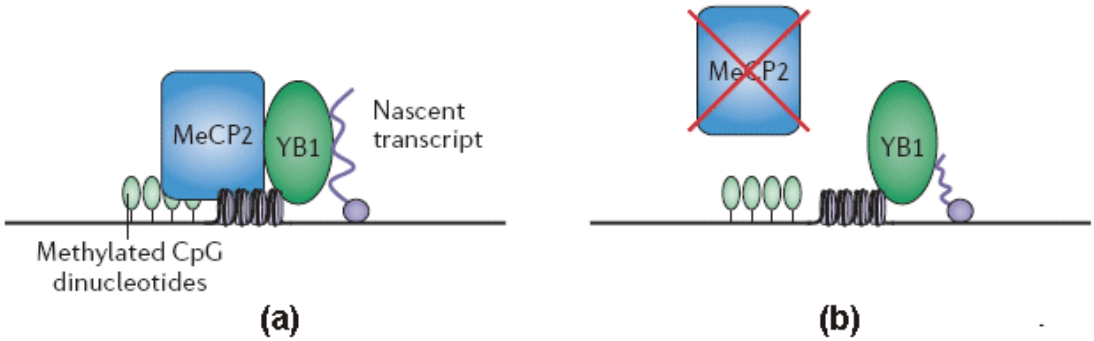

Figure 1.6. Regulation of alternative splicing by MeCP2; a) RNA splicing in the presence of MECP2 and b) aberrant splicing in the absence of MECP2 (Bienvenu and Chelly, 2006).

1.2.9. Mouse Models of RTT

To unravel the molecular changes that underlie RTT, several mouse models with different MECP2 mutations were generated. *Mecp2*-null male ($Mecp2^{-/y}$) and female ($Mecp2^{-/-}$) mice generated via cre/lox recombination have no apparent phenotype until around 6 weeks. There follows a period of rapid regression resulting in reduced spontaneous movement, uncoordinated gait, irregular breathing, hind limb clasping and tremors. Rapid progression of symptoms leads to death at 8 weeks of age (Guy *et al*., 2001; Chen *et al*., 2001). Detailed brain examination revealed that the brains of *Mecp2* null mice are smaller in size and weight than brains of wild type littermates, but have no detectable structural abnormalities, except for smaller, more densely packed neurons (Chen *et al*., 2001). In addition, the olfactory neurons of *Mecp2* null mice demonstrate a transient delay in differentiation, and abnormalities of axonal targeting, suggesting that Mecp2 mediates a crucial function in the final stages of neuronal development (Matarazzo *et al*., 2004). Recently, Pelka *et al*. (2006) reported a null mice with XO background ($Mecp2^{-/0}$) showing similar phenotypes with male $Mecp2^{-/y}$ mice. This finding indicates that the Y-chromosome has no effect on the phenotypic manifestation in *Mecp2* null mice (Pelka *et al*., 2006).

Shahbazian *et al*. (2002) reported another RTT mouse model generated with insertion of a stop codon in the Mecp2 gene at nucleotide position corresponding to amino acid 309. This mutation results in a truncated protein with the MBD, TRD, and NLS domain and a lack of the C-terminal region, which is predicted to have similar effects of p.Arg294X mutation observed in RTT patients. $Mecp2^{308/Y}$ mice display no initial phenotype until 6 weeks of age, and then they develop progressive neurological phenotypes, including motor dysfunction, forepaw stereotypies, hypoactivity, tremor, seizures, kyphosis, social behavior abnormalities, decreased diurnal activity, increased anxiety-related behavior, and learning and memory deficits, reminiscent of the clinical picture in human girls with RTT. Female mice heterozygous for the truncation display milder and more variable features. *In vivo*, the truncated protein maintains normal chromatin localization, but histone H3 is hyperacetylated in the brain, indicating abnormal chromatin architecture (Shahbazian *et al*., 2002; Moretti *et al*., 2005).

Collins *et al*. (2004) has developed a mouse model that transgenically over-expressed *MECP2* under the endogenous human promoter. Initially, *MECP2*^{Tg} mice display increased synaptic plasticity, with enhancement in motor and contextual learning abilities. However, at 20 weeks of age, these mice developed seizures, hypoactivity and spasticity with several other progressive neurological abnormalities.

The conditional inactivation of *MeCP2* in only post-mitotic neurons of the forebrain caused delayed onset of symptoms similar to those shown by *Mecp2* knockout mice. This finding indicates that Mecp2 plays an essential role in post-mitotic neurons (Chen *et al*., 2001). Additionally, the expression of Mecp2 in only post-mitotic neurons of Mecp2-null mice was shown to be sufficient to restore normal neurological function. This finding indicates that Mecp2 deficiency in peripheral tissues does not significantly influence disease manifestations and suggests that Mecp2 plays no essential role in the early stages of brain development (Luikenhuis *et al*., 2004).

1.2.10. MeCP2 Target Genes and Their Relevance with Disease

Although biochemical evidence suggested that MeCP2 functions as a global repressor of gene expression, transcriptional profiling failed to identify profound changes of gene expression in the brain of *Mecp2* knockout mice (Tudor *et al*., 2002). Using the candidate gene approach or CGH analysis of samples from both human and mouse tissues, only a few number of putative MeCP2 targets that might be relevant to the pathogenesis of RTT was identified (Figure 1.7).

The first gene shown to be repressed by MeCP2 was brain-derived neurotrophic factor (*BDNF*), encoding a protein that has essential functions for neuronal plasticity, learning and memory (Chen *et al*., 2003). In basal conditions, BDNF expression is repressed by MeCP2 bound to its promoter; upon membrane depolarization, phosphorylated MeCP2 dissociates from the promoter and BDNF expression is induced by binding of CREB (Moretti *et al*., 2005 and 2006). Conditional deletion of Bdnf in postmitotic neurons of mice mimicked some of the phenotypes observed in Mecp2 null mice, including hind limb clasping, reduced brain weight, and reduced olfactory and hippocampal neuronal sizes. However, Chang and colleagues reported that BDNF protein

levels are decreased rather than increased in brains of symptomatic Mecp2$^{-/Y}$ mice. Since Bdnf is known to be upregulated in response to neuronal activity, the reduced cortical activity in Mecp2 null mice is expected to negatively affect Bdnf expression, hence masking the expected upregulation that would normally result from loss of repression in resting cortical neurons that lack MeCP2 (Chang *et al*., 2006). Consistent with this data, forebrain-specific deletion of Bdnf in Mecp2$^{-/Y}$ mice resulted in earlier onset of locomotor dysfunction and reduced lifespan, while forebrain- specific overexpression of Bdnf in these mice improved locomotor function and extended their lifespan (Chang *et al*., 2006).

Horike *et al*. (2005) reported the loss of imprinting of a maternally expressed gene, distal-less homeobox 5 (DLX5), in both *Mecp2*-null mice and in lymphoblastoid cell lines obtained from RTT patients. MeCP2 was shown to be essential for the formation of a silent chromatin structure at the *Dlx5* locus by histone methylation and through the formation of a chromatin loop. Dlx5 regulates GABA neurotransmission and osteogenesis; therefore, alterations in Dlx5 expression can account for epilepsy, osteoporosis and somatic hypoevolutism observed in RTT girls.

MeCP2 was shown to affect the expression pattern of UBE3A located in PWS/AS imprinted region. *UBE3A* encodes the ubiquitin ligase E3A and imprinted only in the brain. Mutations in the maternal copy of the gene account for about 10 per cent of Angelman Syndrome (AS) cases. *UBE3A* mRNA and protein levels are slightly reduced in human and mouse MeCP2-deficient brains due to the overexpression of anti sense *UBE3A* (Makedonski *et al*., 2005). Since maternal mutations in *UBE3A* (or repression of the maternal allele) give rise to AS, it is speculated that deregulation of UBE3A expression that results from MeCP2 loss of function might contribute to the clinical manifestations of Rett syndrome, such as mental retardation, seizures, muscular hypotonia and acquired microcephaly, that are common to both conditions (Makedonski *et al*., 2005).

Chip analyses revealed that MeCP2 binds to promoter region of the corticotropin-releasing hormone (CRH) gene, glucocorticoid-inducible genes, serum glucocorticoid-inducible kinase 1 (Sgk1) and FK506-binding protein 5 (Fkbp5) in wild type brain. It was shown that these genes are upregulated in Mecp2 null mice (Bale and Vale, 2004; Nuber *et al*., 2005). Since the genes Sgk1, Fkbp5, and Crh are involved in regulation of behavioral

and physiological responses to stress it may be suggested that at least some RTT symptoms arise from the disruption of MeCP2 regulation on stress-responsive genes (Nuber *et al*., 2005).

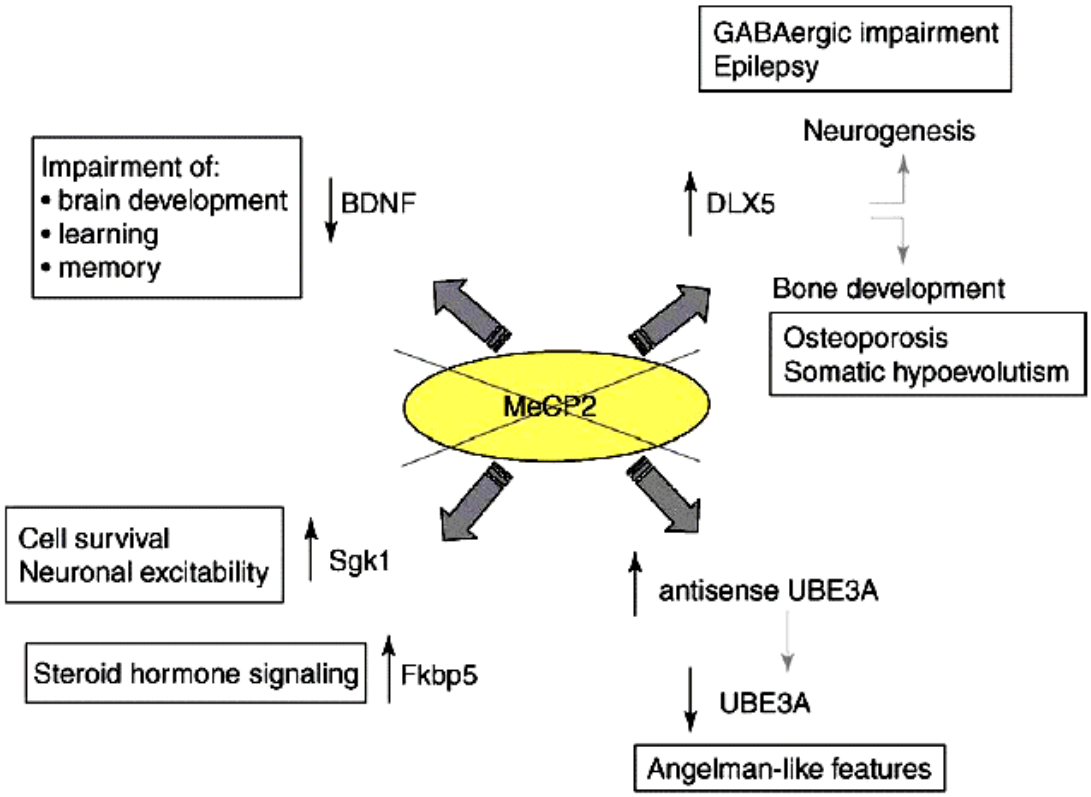

Figure 1.7. MeCP2 target genes and their relevance with the disease. Loss of MeCP2 affects the expression pattern of specific genes: BDNF, DLX5, Sgk1, Fkbp5 and antisense UBE3A (Mari *et al*., 2005).

1.3. Breast Cancer

1.3.1. Breast Tissue

The breast, being an apocrine gland, is composed of glandular, fatty, and fibrous tissues positioned over the pectoral muscles of the chest wall and attached to the chest wall by fibrous strands called Cooper's ligaments. A layer of fatty tissue surrounds the breast glands and extends throughout the breast. The fatty tissue gives the breast a soft

consistency. The glandular tissues of the breast house the lobules (milk producing glands at the ends of the lobes) and the ducts (transporting milk from the milk glands to the nipple). Toward the nipple, each duct widens to form a sac (ampulla) (Figure 1.8). During lactation, the bulbs on the ends of the lobules produce milk. Once milk is produced, it is transferred through the ducts to the nipple.

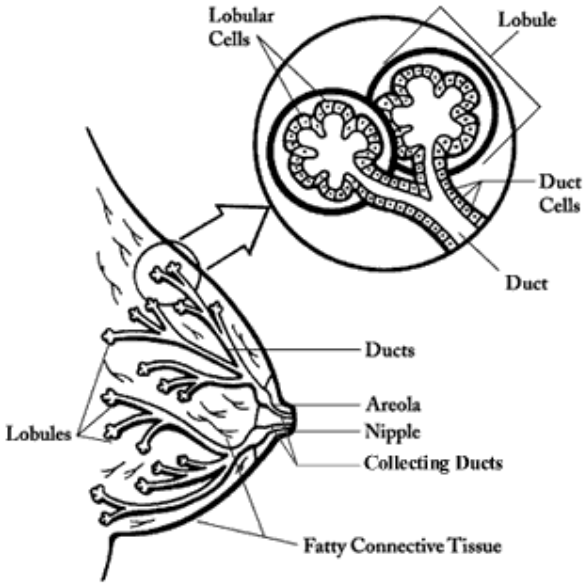

Figure 1.8. A schematic diagram of a normal female breast (www.cancer.org/docroot/CRI/content/CRI_2_4_1X_what_is_breast_cancer_5.asp).

1.3.2. Breast Cancer Risk

Breast cancer is the most common malignancy among women in industrialized countries and diagnosed in 1 x 10^6 women in the world each year. The highest age-adjusted incidence rate is reported for North America, being 86.3 per 100,000 women per year, while the lowest rate, reported in China, is only 11.8. The average incidence is 63.2 for more developed countries and 23.1 for the less developed regions.

Breast carcinomas originate from the epithelial cells lining the ducts or lobules, therefore classified as ductal or lobular carcinomas. Ductal carcinoma is the most common type of breast cancer, accounting for 85 to 90 per cent of the cases. Lobular carcinoma occurs in 10 to 12 per cent of the cases (Feig SA, 2000). Ductal breast malignancies are divided into two categories, pre-invasive and invasive. Pre-invasive ductal cancer is called

ductal carcinoma *in situ* (DCIS). It is a very early stage of breast cancer and is the result of proliferation of the ductal luminal cells which fills the lumen but do not enter the basement membrane and the surrounding stroma. It accounts for 5 per cent of all breast carcinomas. Invasive (infiltrating) ductal carcinoma (IDC) is the most aggressive type with capability of metastasis. Invasive lobular carcinomas (ILC) only account for about 10 per cent of all breast cancers and they tend to be somewhat less aggressive than IDC. Unlike IDC, it is now believed that lobular carcinoma *in situ* (LCIS) is not a precursor of invasive lobular carcinoma. The confusion exists because LCIS, while it has the word carcinoma in its name, does not behave like a cancerous condition. LCIS does not grow, form masses, transform into invasive cancer, or metastasize. Therefore, it does not represent a true malignancy.

The molecular mechanisms underlying the development of breast cancer are not completely understood. However, it is generally believed that the initiation of breast cancer is a consequence of cumulative genetic damages leading to genetic alterations that result in activation of proto-oncogenes and inactivation of tumor suppressor genes. These in turn are followed by uncontrolled cellular proliferation and/or aberrant programmed cell death, or apoptosis. Also, the role of reactive oxygen species (ROS) has been related to the etiology of cancer, as they are known to be mutagenic, and therefore capable of tumor promotion.

The risk of developing breast cancer is increased if a family history of the disease is present. The epidemiological studies have shown that 12 per cent of women with breast cancer had one and one per cent had two or more affected relatives. Therefore the genesis of most breast cancers can not be explained by heritage. Age and the duration of exposure to endogenous or exogenous steroid hormone levels are suggested as the best defined risk factors for breast cancer. Breast cancer is uncommon among women younger than 30 years of age but the incidence increases sharply with age. The rate of increase in breast cancer incidence continues throughout life but slows somewhat between ages 45 and 50 years. This finding strongly suggests the involvement of reproductive hormones in breast cancer etiology, because non-hormone-dependent cancers do not exhibit this change in slope of the incidence curve around the time of menopause (Pike *et al*., 1993). Several reproductive factors that alter estrogen status affect the risk of breast cancer: early age at menarche and

late age at menopause are associated with increased risk of breast cancer. After menopause, adipose tissue is the major source of estrogen, and obese postmenopausal women have both higher levels of endogenous estrogen and a higher risk of breast cancer (Harris *et al*., 1992; Huang *et al*., 1997). Postmenopausal hormone use increases the breast cancer risk depending on the duration of use and whether estrogen alone or estrogen in combination with progestin is taken (Ross *et al*., 2000).

The age might be the driving force for the accumulation of mutational load due to the reactive oxygen species, telomere dysfunction, and increased epigenetic gene silencing. Exposure to growth factors like estrogen increases the likelihood of occurrence of these changes in breast epithelial stem cells as well as the propagation of these changes by enabling the cells to divide.

Hereditary (familial) form of the breast cancer represents 5-10 per cent of all cases. BRCA1, BRCA2, p53, ATM, CHECK2, and PTEN are the major breast cancer susceptibility genes (Marcus *et al*., 1996; Miki *et al*., 1994; Stratton and Wooster, 1995; Hill *et al*., 1997, Bell *et al* 1999, Cantor *et al* 2001). BRCA1, BRCA2 and ATM genes maintain genomic stability and involved in repair of double-strand breaks. BRCA1 and BRCA2 play also role in transcription and cell cycle control acting as a tumor suppressor gene (Venkitaraman, 2002). p53 is known to be involved in cell cycle regulation, DNA damage repair, apoptosis and inhibition of angiogenesis. Therefore, loss of functional protein eliminates the growth arrest in response to DNA damage and allows the replication of mutated DNA. CHECK2, a G2 check point kinase, is involved in the repair of DNA breaks. PTEN is a lipid phosphatase that was identified as a candidate tumor suppressor gene. It is suggested to have an inhibitory role on PKB/Akt that is required for cell growth and survival (Downward J, 1998). It is also found to inhibit integrin-mediated cell migration thus preventing metastasis (Tamura *et al*., 1998).

1.3.3. Breast Carcinogenesis

Breast cancer progression is a multi-step process encompassing progressive changes from normal, to hyperplasia with and without atypia, carcinoma in situ, invasive carcinoma, and metastasis (Figure 1.9) (Simpson *et al*., 2005).

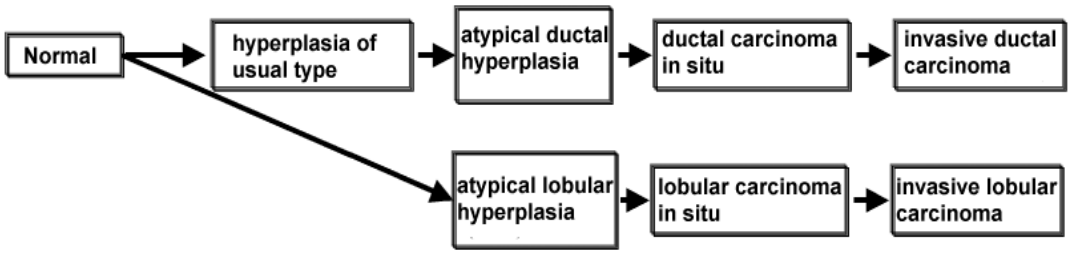

Figure 1.9. Simplified multi-step model of breast cancer progression based on morphological features (Simpson *et al*., 2005).

It has been suggested that a cell has to acquire six features to become malignant (IDC or ILC): (1) limitless replicative potential, (2) self-sufficiency in growth signals, (3) insensitivity to growth-inhibitory signals, (4) evasion of programmed cell death, (5) sustained angiogenesis and (6) tissue invasion and metastasis (Hanahan and Weinberg, 2000). This process requires complex series of stochastic genetic events including gene amplifications, gene deletions, point mutations, loss of heterozygosity, chromosomal rearrangements, and overall aneuploidy. Some of the observed genetic lesions are loss of 16q, 11q, 14q, 8p, 13q, gain of 17q, 8q, 5p, and amplifications on 17q12, 17q22–24, 6q22, 8q22, 11q13, and 20q13. Besides the genetic alterations, epigenetic alterations are among the most common molecular alterations in human neoplasia (Baylin and Herman, 2000; Jones, 1996; Jones and Laird, 1999). Hypermethylation and global hypomethylation of more than 25 genes have been correlated with breast carcinogenesis. Abnormal methylation of each gene enables cells to acquire new capabilities needed for tumorigenesis (Figure 1.10 and Table 1.1).

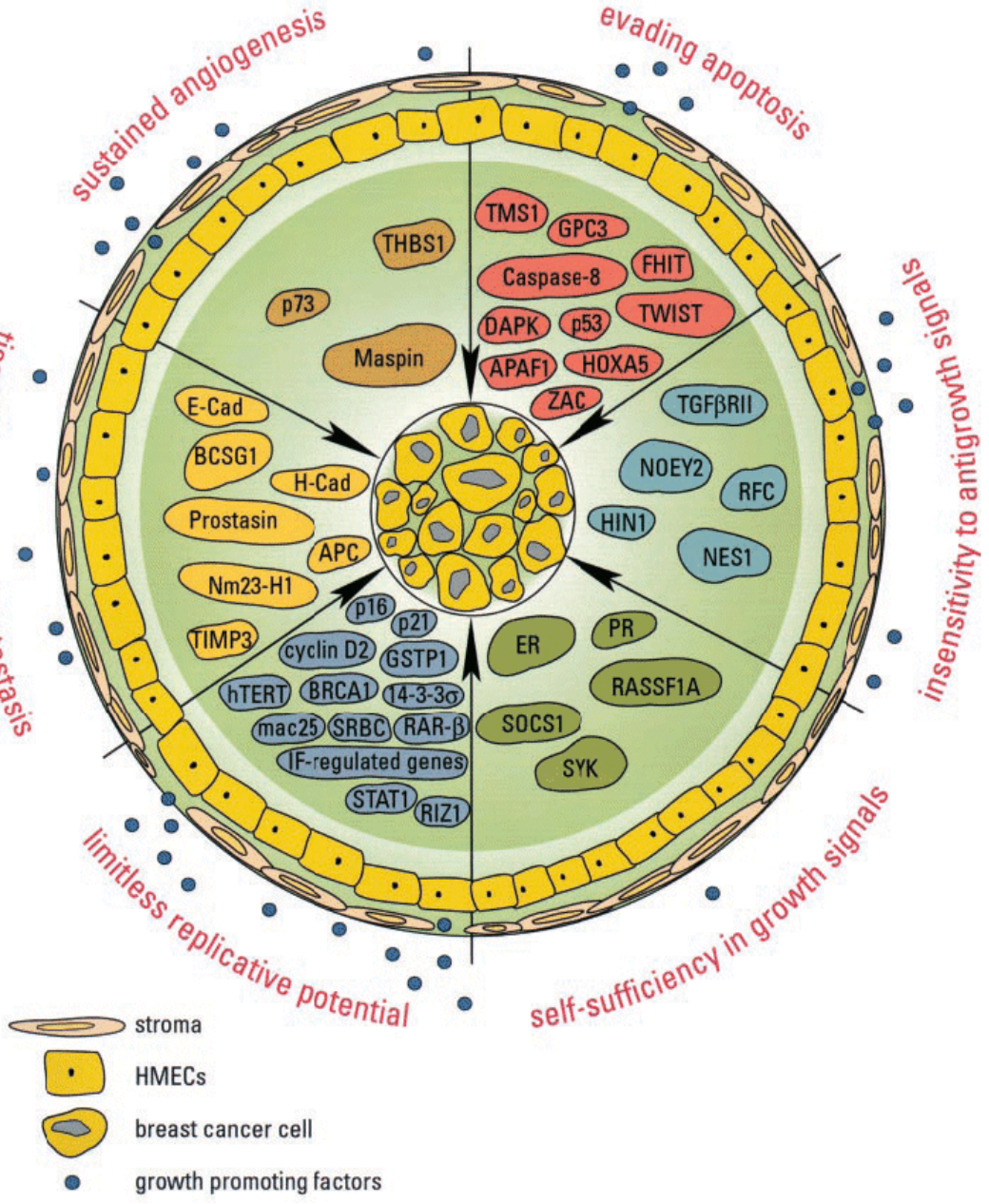

Figure 1.10. View of breast carcinogenesis from a DNA methylation standpoint (Widschwendter and Jones, 2002).

Table 1.1. The list of methylated genes in breast cancer (Widschwendter *et al*., 2002).

Gene	*Alternate gene name*	*Function*
APAF1	Apoptosis Protease-Activating Factor 1	Activation of procaspase-9, results in initiation of a cascade involving the downstream executioners caspase-3, -6, and -7→apoptosis
APC	Adenomatous Polyposis of the Colon	Cell adhesion, signal transduction, stabilization of the cytoskeleton, regulation of cell cycle and apoptosis
BCSG1	Breast Cancer Specific Gene 1; Synuclein-γ	Increases motility and invasiveness
BRCA1	Breast Cancer type 1	Involved in DNA repair, recombination, checkpoint control of the cell cycle and transcription. Interacts with p53, STAT-factors, SRBC, etc.
Caspase-8	Apoptosis-related cysteine protease	apoptosis
CCND2	Cyclin D2	Cell cycle regulation
DAPK	Death-associated protein kinase 1	Mediator of interferon-γ induced apoptosis
E-Cad	E-Cadherin	Epithelial cell–cell adhesion, suppresses invasion and metastasis
ER	Estrogen receptor α and β	Regulation of cell proliferation, predictor of endocrine therapy
FHIT	Fragile histidine triad gene	Controls proliferation and apoptosis, tumor suppressor
GPC3	Glypican 3	apoptosis
GSTP1	Glutathione S-transferase P1	Carcinogen detoxification
H-Cad	H-Cadherin	Cell-cell adhesion
HIN1	High in normal 1	Putative cytokine, inhibits cell growth
HOXA5	Homeo box A5	Upregulates p53, apoptosis
hTERT	Telomere reverse transcriptase	synthesizes the telomere ends of linear chromosomes, implicated in human cell immortalization
IF-regulated genes	Interferon regulated genes	Interleukin 6, ICAM 1, Superoxide dismutase and Elafin are regulated by Interferons and mediate tumorsuppressive functions; involved in senescence
mac25	Insulin-like growth factor binding-related protein 1	Cell cycle regulation, apoptosis, involved in senescence
Maspin	Protease inhibitor 5	Inhibitor of angiogenesis, reduces cells' ability to induce tumors and metastasize
NES1	Kallikrein 10	Inhibition of anchorage-independent growth and tumor formation
Nm23-H1	Metastasis inhibition factor NM23	Metastasis suppressor activity
NOEY2	Ras homolog gene family member I	Suppresses clonogenic growth; regulation of cyclin D1 and p21
p16	Cyclin-dependent kinase inhibitor 2A	Cell cycle regulation, involved in senescence
p21	Cyclin-dependent kinase inhibitor 1A	Cell cycle regulation
p53	Transformation-related protein 53	Apoptosis, cell cycle regulation, inhibition of growth and invasion

Table 1.1. The list of methylated genes in breast cancer (continued).

Gene	*Alternate gene name*	*Function*
p73	P53 related protein p73	Inhibitor of angiogenesis, apoptosis
PR	Progesterone receptor	Growth regulation
Prostasin	Protease serine 8	Suppresion of invasion
RAR-β	Retinoic acid receptor β	Apoptosis, involved in senescence, inhibition of proliferation
RASSF1A	Ras Association domain family protein 1	Reduces colony formation, suppresses anchorage-independent growth, and inhibits tumor formation, apoptosis
RFC	Reduced folate carrier	Cellular uptake of methotrexate
RIZ1	Retinoblastoma protein-binding zinc finger protein	Tumor suppressor
SOCS1	Suppressor of cytokine signaling 1	Suppresses growth rate and anchorage-independent growth, induction of apoptosis, regulation of STAT activation
SRBC	Serum deprivation response factor (sdr)-related gene product that binds to c-kinase	Interaction with BRCA1
STAT1	Signal transducer and activator of transcription	Growth regulation, induction of apoptosis, involved in senescence
SYK	Spleen tyrosine kinase	Inhibits tumor growth and metastasis
TGFβRII	Transforming growth factor β receptor II	Cell cycle regulation
THBS1	Thrombospondin 1	Inhibition of angiogenesis and invasion
TIMP3	Tissue inhibitor of metalloproteinase-3	Suppresses tumor growth, angiogenesis, invasion and metastasis
TMS1	Target of methylation induced silencing 1	apoptosis
TWIST	TWIST	Inhibits oncogene- and p53-dependent cell death
ZAC	Pleomorphic adenoma gene-like	Induction of apoptosis and cell cycle regulation
14-3-3σ	Stratifin	Cell cycle regulation

1.3.4. DNA Methylation and Genetic Instability

The genomic instability is the common feature of all cancer types and DNA methylation might be responsible for these chromosomal instabilities. Methylation leads to instability in several ways. First, 5meCs serve as sites of transition mutations by the hydrolytic deamination of 5meC to thymine. For example, such mutations frequently occur in the tumor suppressor genes p53, Rb, and c-H-ras-1 (Magewu and Jones, 1994; Ghazi *et al*., 1990). Secondly, epigenetic inactivation of certain critical genes in cancer by promoter methylation may predispose to genetic instability (Herman and Baylin, 2000). For instance, methylation of MLH1, a gene involved in mismatch repair, precedes the MIN + phenotype

in sporadic colon, gastric and endometrial cancers (Esteller *et al.* 1999). Furthermore, there is a striking correlation between mismatch repair, genetic instability and methylation capacity in colon cancer cell models (Lengauer *et al.*, 1997, 1998). In addition, promoter CpG island methylation and resulting inactivation of the detoxifying π-class glutathione S-transferase (GST) can lead to accumulation of oxygen radicals and subsequent DNA damage (Lee *et al.*, 1994, Henderson *et al.*, 1998, Matsui *et al.*, 2000). A p53-inducible gene, 14–3–3σ, is methylated and inactivated in many breast cancers. Loss of its expression may also facilitate the accumulation of genetic damages (Ferguson *et al.*, 2000). Apart from regional hypermethylation of some critical tumor suppressor genes, genome-wide hypomethylation is an important feature in cancer and can also contribute to genetic instability (Schmutte and Fishel, 1999).

Genomic integrity, senescence, and evasion of programmed cell death (apoptosis) are thought to be important barriers to the development of malignant lesions. DNA repair proteins have emerged as the key regulators among the multitude of players involved in cell cycle control and apoptosis by inducing apoptosis in stressed or abnormal cells, thereby protecting the organism from cancer development.

1.3.5. DNA Repair System

DNA repair enzymes maintain the integrity of the genetic code by removing damaged DNA segments and minimizing replication errors. DNA damage may be a consequence of normal cellular function (e.g. replication errors, oxidative metabolism, reactive metabolites of hormone synthesis) or of environmental factors such as radiation (UV) or xenobiotic chemicals (Mohrenweiser and Jones, 1998). Cells with damaged DNA may be removed by apoptosis, or programmed cell death. If DNA adducts escape cellular repair mechanisms and persist, they may lead to miscoding, resulting in permanent mutations. If a permanent mutation occurs in a critical region of an oncogene or tumor suppressor gene, it can lead to activation of the oncogene or deactivation of the tumor suppressor gene. Multiple events of this type lead to aberrant cells with loss of normal growth control and ultimately to cancer.

Multiple and complementary DNA repair systems have evolved to protect the genome against the detrimental effects of DNA lesions. DNA repair may take place by one of several pathways, depending on the type of damage, including nucleotide excision repair (NER), base excision repair (BER), mismatch repair, or recombinatorial repair. Nucleotide excision repair (NER) enzymes are responsible for removing 'bulky' DNA damage that distorts the DNA helix such as UV photoproducts (thymine dimers), chemically induced intra-strand crosslinks and bulky chemical adducts (polycyclic aromatic hydrocarbons and aromatic amines). Two distinct sub-pathways are present in the mammalian NER system: i.e., global genome NER (GG-NER) that operates genome wide, and transcription-coupled NER (TC-NER) that is specialized to eliminate transcription-blocking lesions on the DNA strand of active genes (Figure 1.11). The NER pathway includes several steps: (i) DNA damage recognition; (ii) assembly of repair factors; (iii) incision of damaged DNA; (iv) repair synthesis to fill gapped DNA; and (v) DNA ligation. DNA damage is recognized by the Xeroderma Pigmentosum Group C (XPC)–hHR23B complex, followed by recruitment of the transcription factor IIH (TFIIH) complex of proteins. The TFIIH complex is composed of nine subunits, including XPD and XPB (de Boer and Hoeijmakers, 2000). TFIIH unwinds the DNA duplex around the damaged site. Next, XPG binds to the TFIIH complex and DNA, followed by recruitment of the XPF–ERCC1 complex. XPG and XPF–ERCC1 produce dual incisions of 30 and 50 nucleotides at damaged site. After release of the damaged DNA strand, the gap is filled by repair synthesis and ligation (Bradsher *et al*., 2002).

The *in vitro* and *in vivo* experiments suggest that XPC-hHR23B complex is the initial component for detecting DNA damage and plays at least four roles in DNA damage recognition. First, XPC-hHR23B can discriminate between DNA distortions and the Watson-Crick structure. Second, XPC-hHR23B may be the first NER factor to respond to DNA damage in GGR. Third, XPC-hHR23B's presence at sites of DNA damage can induce a further bending of the DNA, which may enhance the binding of other downstream NER proteins to the site of DNA lesions (Sugasawa *et al*., 1998). Finally, XPC-hHR23B has a critical role in the recruitment of TFIIH, which is known to promote the opening of the DNA helix in the vicinity of the lesion, presumably to assist in the assembly of subsequent NER factors for further processing of the lesion (Schaeffer *et al*., 1993; Feaver *et al*., 1993; Drapkin *et al*., 1994).

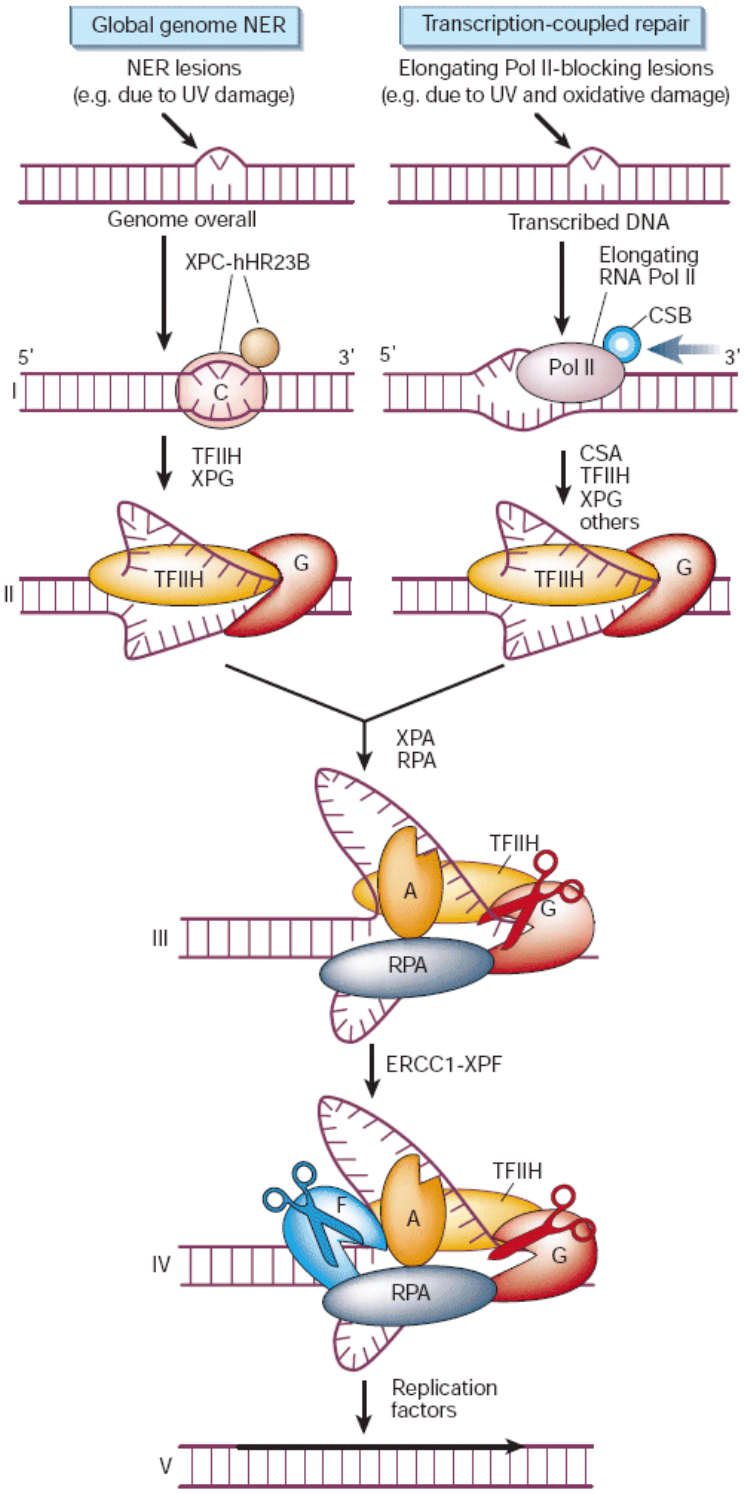

Figure 1.11. Model for mechanism of global genome nucleotide-excision repair and transcription-coupled repair (Hoeijmakers *et al.*, 2001).

1.3.6. hHR23 (RAD23) Genes

Human hHR23A and hHR23B are homologs of Saccharomyces cerevisiae Rad23 and Saccharomyces pombe Rhp23 genes. *hHR23A* and *hHR23B* have been mapped to chromosome 19p13.2 and 9q31.2 encoding 363 and 409 amino acid proteins, respectively. An amino acid sequence comparison of the *Rad23*, *Rhp23*, *hHR23A* and *hHR23B* showed the existence of at least four distinct domains that are well conserved among these proteins (van der Spek *et al*, 1996). First, they contain a novel domain near the N-terminus referred to as UBL (ubiquitin-like) domain which is important for DNA repair. This domain can bind to the 26S proteasome, and the removal of it from the yeast Rad23, prevented interaction with the proteasome and was associated with increased sensitivity to UV light (Watkins *et al*, 1993; Schauber *et al*, 1998). The second and fourth domains from the amino terminus are Ub-associated (UBA) domains, suggesting the involvement of hHR23 in certain pathways of Ub metabolism (Hofmann and Bucher, 1996). The third domain, the stress-induced phosphoprotein (STI1), has been found to be responsible for binding the XP-C protein (Masutani *et al*, 1997) (Figure 1.12).

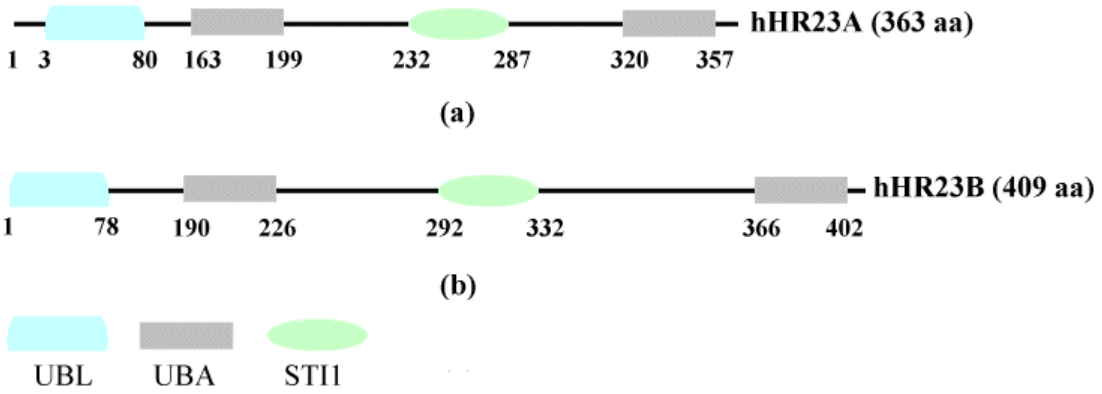

Figure 1.12. Schematic representations of conserved domains in hHR23A (a) and hHR23B (b) proteins.

XPC-hHR23 complex is the initial component for detecting DNA damage in GG-NER pathway. Although both hHR23 proteins can bind to XPC at least *in vitro* (Sugasawa *et al*., 1997), most XPC is complexed with hHR23B *in vivo*, and only a minor fraction of the complex contains hHR23A (Araki *et al*., 2001).

Studies on hHR23A/B knock-out (KO) mice have shown that hHR23A was likely functionally redundant with hHR23B. hHR23B KO mice exhibit moderate UV sensitivity and NER deficiency, whereas hHR23A KO mice do not exhibit any observable defects in DNA repair activity. However, when both hHR23A and hHR23B were deleted, the mice exhibited extremely severe phenotypes, impaired embryonic development and high rates of intrauterine death. Surviving animals displayed retarded growth, male sterility, facial dysmorphology and DNA repair defects (Ng *et al*., 2003). Since these phenotypes were not observed in XPC KO mice, the hHR23A/B KO phenotype was not due to NER deficiency suggesting that hHR23A/B proteins have additional cellular functions. These findings indicate also that the hHR23A does not completely duplicate the function of hHR23B and must have a function of its own. However, mHR23A and mHR23B appeared to have redundant roles in NER. Over expression of hHR23A in the mHR23A/B double knock out cells restored not only the steady-state level and stability of the XPC protein, but also cellular NER activity to near wild-type levels (Okuda *et al*., 2004).

Studies on hHR23A/B knockdown (KD) cell lines have shown that while $hHR23A^{KD}$ cells were not blocked in S phase after UVC irradiation, many $hHR23B^{KD}$ cells were hindered in getting out of S phase. This suggested the presence of unrepaired UVC-induced DNA damage in $hHR23B^{KD}$ cells. Therefore, $hHR23B^{KD}$ cells seemed to behave like XP cells. $hHR23B^{KD}$ cells displayed a significant sensitivity to UVC, in contrast to $hHR23A^{KD}$ cells, which strongly tolerated UVC irradiation (Biard A, 2007). This also suggested that hHR23A and hHR23B displayed diverse biological functions leading cells to different outcomes.

Intriguingly, only a minority of hHR23B and hHR23A is bound to XPC, suggesting that both proteins have additional functions (Sugasawa *et al*., 1996). hHR23 proteins are players for multiple mechanisms including DNA repair and proteasome-mediated protein-degradation and apoptosis (Kim *et al*., 2004; Glockzin *et al*., 2003).

hHR23 proteins connect the NER and ubiquitin/proteasome mediated protein degradation pathways via UBA and UBL domains. The ubiquitin-proteasome pathway plays a key regulatory role in a variety of cellular events, including the removal of misfolded proteins, production of immunocompetent peptides, activation or repression of

transcription, and regulation of cell cycle progression (Schubert *et al*., 2000; Yamaguchi *et al*., 2000). Proteins are ubiquitylated and consequently delivered to the 26S proteasome for degradation. Ubiquitin receptor family can directly connect ubiquitylated proteins to the proteasome via their UBA and UBL domains binding the ubiquitin and proteasome, respectively. However, depending on the levels of UBL/UBA containing proteins they can promote or inhibit the degradation of ubiquitylated substrates. The binding of UBL/UBA containing proteins to the ubiquitylated substrates inhibits the polyubiquitination and prevent proteolysis by proteasomes (Ortolan *et al*., 2000).

hHR23 proteins regulate the induction and stability of XPC via inhibiting the proteolysis by proteasomes. In the absence of hHR23 proteins, XPC is highly unstable since it is ubiquitylated and degraded by 26S proteasome. Under normal conditions, XPC-hHR23 complex results in a significant reduction of XPC proteolysis and consequently in increased steady-state levels of the protein complex. This correlates with proficient GG-NER activity. The protecting role of hHR23 is performed via inhibition of polyubiquitination (Schauber *et al*., 1998; Lommel *et al*., 2002; Ortolan *et al*., 2000). This hypothesis was supported by the observation of presence of XPC-Ub conjugates and increased XPC stability in proteasome inhibitor treated mHR23A/mHR23B KO cells (Ng *et al*., 2003).

In addition to NER, XPC–hHR23B complex is associated with the base excision repair (BER). The XPC protein interacts physically and functionally with the thymine DNA glycosylase, the enzyme that recognizes cyclobutane pyrimidine dimers at the initial step of BER (Shimizu *et al*., 2003). 3-Methyladenine-DNA glycosylase, an initiator of BER also interacts with hHR23A proteins, suggesting that these proteins are involved in BER (Miao *et al*., 2000). Hsieh *et al*. reported that hHR23A^{KD}, but not hHR23B^{KD}, cells, were hypersensitive to the treatment of methylmethane sulfonate, a major substrate for BER (Hsieh *et al*., 2005). This suggests that hHR23A might be a player for the two major DNA repair pathways, BER and NER.

Moreover, multiple engagements between hHR23/Rad23 and cell cycle regulation are present. (1) RAD23 has a partially redundant role with and binds to RPN10 in the G2/M transition (Lambertson *et al*. 1999). (2) RAD23 is involved in spindle assembly and

S-phase checkpoints (Clarke *et al*., 2001). (3) RAD23, together with DSK2, has a role in spindle pole duplication (Biggins *et al*., 1996). The link with spindle pole duplication was recently strengthened by the discovery of the centrosome factor CEN2 as the third component of the XPC/HR23 complex (Araki *et al*., 2001). (4) hHR23 proteins themselves appear to be regulated in a cell-cycle-dependent manner with specific degradation during S- phase (Kumar *et al*., 1999).

The damage-signaling tumor-suppressor protein p53 is partly regulated by hHR23A and hHR23B. hHR23A and a minor amount of hHR23B form a complex with p53. hHR23A and B proteins downregulated the transactivating activity of p53 via inhibition of the CREB (cyclic AMP-responsive element binding) protein, which acts as a coactivator of p53 transcription (Zhu *et al*., 2001). Overexpression of hHR23A and B proteins has led to the accumulation of ubiquitinated p53 and blocked p53 proteasome degradation (Glockzin *et al*., 2003). These paradoxical effects of hHR23 proteins on p53 degradation are consistent with suggestions that the effects of hHR23 on degradation are highly sensitive to stoichiometric variation (Raasi and Pickart, 2003; Verma *et al*., 2004). Additionally, hHR23A and B interact with mouse double minute 2 (MDM2) protein. MDM2 contacts with 20S core particle of the proteasome and functions to antagonize the stabilizing function of hHR23 toward p53, directly promoting p53 recognition and degradation by the proteasome (Brignone *et al*., 2004; Sdek *et al*., 2005).

Kaur *et al*. (2007) has shown that hHR23B was required for genotoxic-specific activation of p53 and apoptosis. After exposure with UV or chemical agents leading to DNA damage, p53–Ub conjugates accumulate in chromatin and hHR23B is required for induction and maintenance of these p53–Ub species. The knockdown of hHR23B blocks p53 stabilization and resulted in significant reduction in apoptosis and increase in viability when compared to hHR23B expressing cells. Robust XPC depletion had no impact on genotoxin-induced apoptosis suggesting that the inhibition of apoptosis due to hHR23B depletion could not be explained by a reduction in DNA repair efficiency. The hHR23B-dependent accumulation of p53–Ub conjugates after DNA damage correlated with p53 stabilization and apoptosis. p53–Ub conjugates could contribute to transcription-dependent functions of p53, which are required for downstream p53 activities (induction of target genes p21 and bax) (Slee *et al*., 2004; Schuler and Green, 2005).

1.4. Congenital Hypothyroidism (CH)

1.4.1. The Thyroid Gland

All vertebrates possess a pair of thyroid glands, located in the anterior neck region. It consists of two lobes: one on either side of the trachea, and a connecting portion called the isthmus, giving the entire gland an H-shaped appearance. The gland varies in size with sexual development, diet and age. The thyroid gland consists of a large number of round or oval follicles surrounded by connective tissue and blood vessels. Each follicle is lined by a cuboidal epithelial cell layer of one-cell thickness. The cavities of the follicles are filled in with viscous protein material called colloid in which the thyroid hormone, thyroxine, is stored.

Normal thyroid function is essential for development, growth and metabolic homeostasis. The primary function of the thyroid is the formation, storage, and secretion of thyroid hormones (Robbins *et al*., 1980; Kohn *et al*., 1993). Thyroid hormone formation involves a coordinated series of steps controlled by hypothalamic-pituitary-thyroid axis (Figure 1.13). The TRH, released from hypothalamus, results in secretion of TSH from the anterior pituitary gland. The TSH stimulates the follicular cells (TFC), via its receptor (TSHr), to release thyroid hormones into the circulation. Thyroid hormone production involves concentrative iodide uptake by the sodium iodide transporter (NIS), as well as iodination of thyroglobulin (TG) by the thyroid peroxidase (TPO) (Robbins *et al*., 1980; Kohn *et al*., 1993).

TG is synthesized as a 12S molecule (330 kDa), post-translationally glycosylated and transported to follicular lumen. The protein contains 70 tyrosine residues that are subject to iodination by TPO. The iodinated TG stored in follicles are degraded by lysosomes to form triiodothyronine (T3) and thyroxine (T4). The major thyroid hormone secreted by the thyroid gland is thyroxine. To exert its effects, T4 is converted to triiodothyronine (T3) by the removal of an iodine atom. This occurs mainly in the liver and in certain tissues where T3 acts, such as in the brain (Robbins *et al*., 1980; Weiss *et al*., 1984; Ekholm, 1990; Kohn *et al*., 1993; Dai *et al*., 1996).

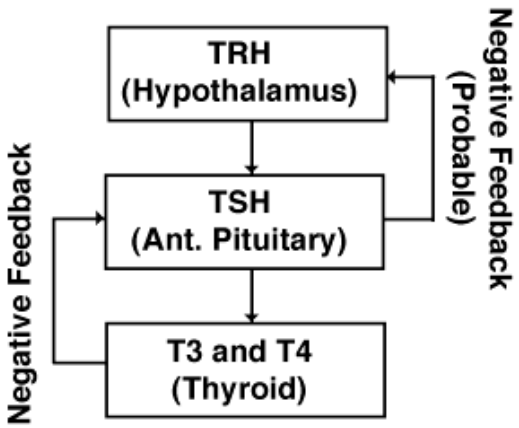

Figure 1.13. Thyroid hormone cascade.

1.4.2. Congenital Hypothyroidism

Any defects in thyroid morphogenesis and hormone synthesis result in Congenital Hypothyroidism (CH), which is a relatively common congenital disorder affecting about 1:3000 to 1:4000 live births (Toublanc, 1992). In about 10 per cent of all cases, CH is the consequence of defects in one of the steps of thyroid hormone synthesis, inborn errors of metabolism referred to as dyshormonogenesis. A heterogeneous group of developmental abnormalities, thyroid dysgenesis, accounts for about 85 per cent of all cases with CH (Gillam and Kopp, 2001). These anomalies include thyroid agenesis, ectopic thyroid tissue, cysts of the thyroglossal duct, and thyroid hypoplasia. In the vast majority of all cases, thyroid dysgenesis is sporadic, but in about 2 per cent it is a familial disorder, an observation supporting the possibility of a genetic etiology (Castanet *et al*., 2000). The higher prevalence of thyroid dysgenesis in Hispanics and Caucasians in comparison to Blacks, the predominance of thyroid dysgenesis in females, and the higher prevalence of associated malformations also suggest the presence of genetic factors in the pathogenesis of CH (Devos *et al*., 1999; Castanet *et al*., 2001). More recently, the data from knockout mice have demonstrated the roles of several genes in thyroid organogenesis; thyroid transcription factors (TTF-1 and TTF-2), paired box homoetic gene 8 (Pax8), and TSH receptor (TSHR). Occasionally mutations in these genes have been reported in CH cases.

Thyroid transcription factor 2 (TTF-2, FKHL15, or Forkhead Box E1 FOXE1) is a member of the forkhead/winged helix-domain protein family, many of which are key regulators of embryonic development. TTF-2 regulates the transcription of target genes such as TG and TPO by binding to specific regulatory DNA sequences in their promoters via its forkhead DNA binding domain. Homozygous recessive mutations (p.S57N and p.A65V) in *TTF-2* result in a syndromic form of thyroid dysgenesis, Bamforth-Lazarus syndrome. This phenotype includes thyroid agenesis, cleft palate, choanal atresia, bifid epiglottis, and spiky hair (Bamforth *et al*., 1989; Clifton-Bligh *et al*., 1998; Castanet *et al*., 2002). Mice homozygous for a disrupted *TTF-2* gene die within 48 hours after birth and are profoundly hypothyroid. They exhibit either small lingual thyroid or have complete thyroid agenesis, and also have severe cleft palates. Hair defects could not be tested since the mice die before hair formation (De Felice *et al*., 1998).

1.4.3. Forkhead Gene Family

Forkhead transcription factors are key regulators of embryogenesis and play important roles in cell differentiation and development. The name derives from two spiked-head structures in embryos of the Drosophila fork head mutant, which are defective in formation of the anterior and posterior gut (Weigel *et al*., 1989). A 110-amino-acid DNA binding domain was evolutionarily conserved between forkhead genes (Figure 1.14). These genes have so far been found in animals, fungi and most of the metazoans. Among the organisms for which the genome sequences are completed, or nearly so, there is indeed a correlation between anatomical complexity and forkhead gene number: four in Saccharomyces and Schizosaccharomyces, 15 in Caenorhabditis, 20 in Drosophila, and 39 in Homo sapiens (Carlsson and Mahlapuu, 2002). X-ray crystallography revealed that the 3D structure of a forkhead domain (FoxA3) resembled the shape of a butterfly and the term "winged helix" was used to describe the structure, which has a helix–turn–helix core of three α-helices, flanked by two loops, or "wings" (Figure 1.15) (Clark *et al*., 1993). The term "Winged helix proteins" is often used synonymously with forkhead proteins. A large proportion of the amino acids in the forkhead domain are invariant or highly conserved (Figure 1.14). Forkhead proteins bind DNA as monomers in contrast to other helix–turn–helix proteins. Hence, the binding sites, which typically span 15–17 bp, are asymmetrical (Pierrou *et al*., 1994).

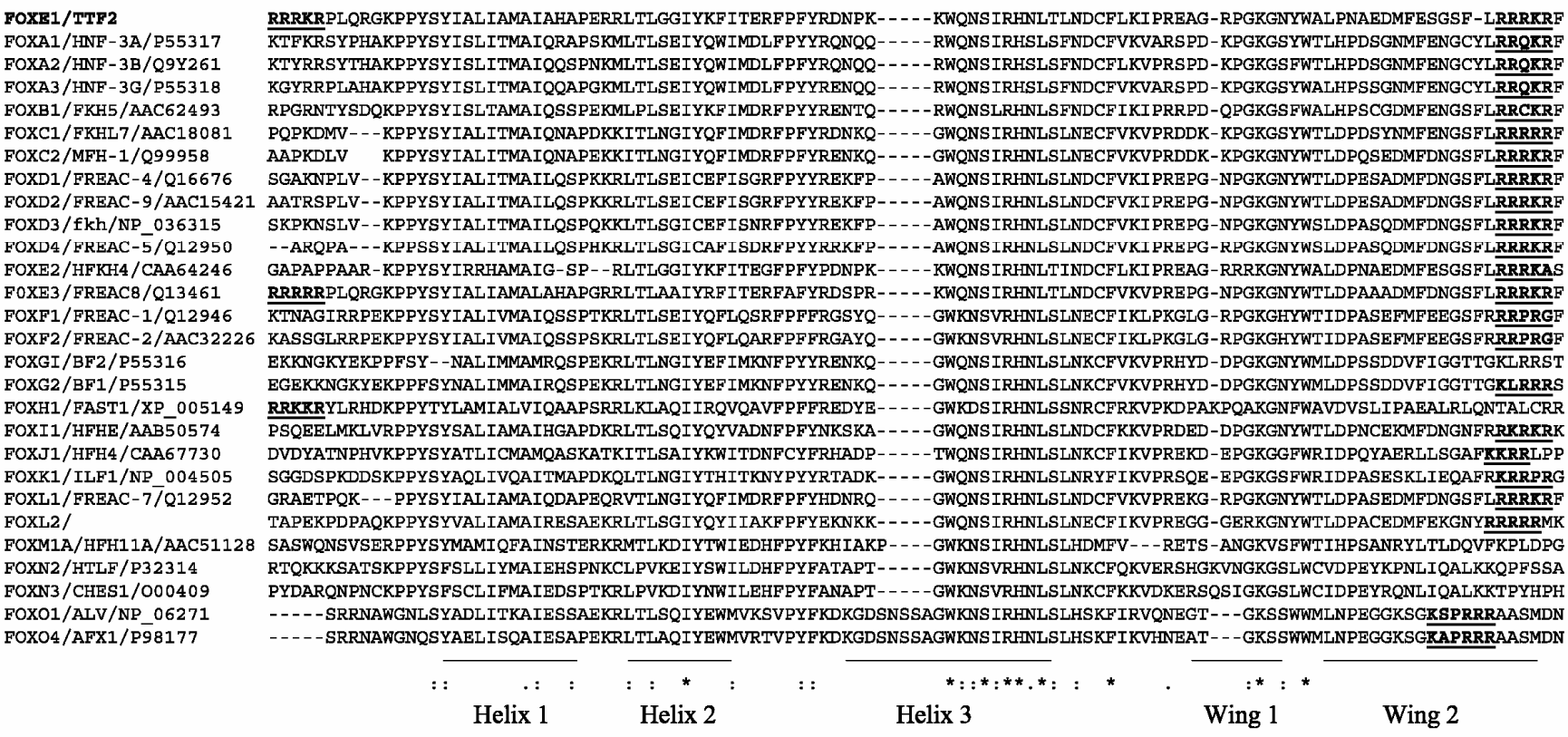

Figure 1.14. Alignment of the TTF2 forkhead DNA-binding domain with selected human FOX representatives. At the bottom, the consensus line indicates; '*' for identical or conserved residues in all sequences; ':' for conserved substitutions; and '.' for semi-conserved substitutions. The positions of predicted 'helix' and 'wing' segments are indicated at the bottom of the panel (Romanelli *et al*., 2003).

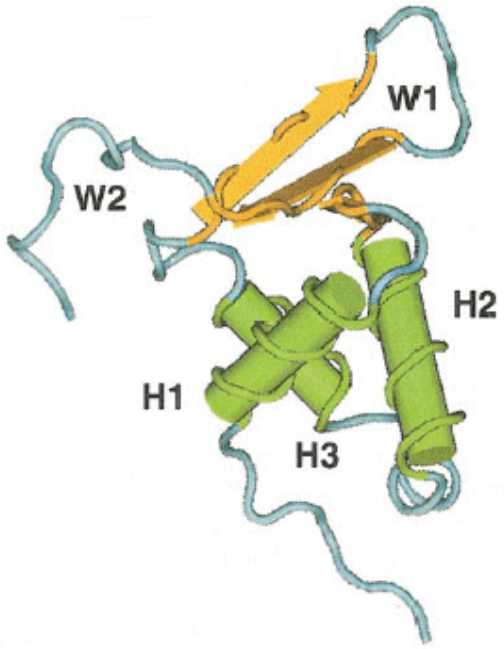

Figure 1.15. Three-dimentional structure of the forkhead domain of FoxC2 (mouse) (van Dongen *et al.*, 2000).

1.4.4. Human *TTF-2* Gene

Human *TTF-2* gene, also known as *FKHL15* or *FOXE1*, has been mapped on chromosome 9q22 (Chadwick *et al.*, 1997). *TTF-2* consists of a single exon encoding for a protein (42 kDa) of 367 amino acids. The gene encodes a forkhead domain, two nuclear localization signals (NLS), a polyalanine tract, and a transcription repression domain (Figure 1.16).

The sequencing of the entire coding region revealed a highly polymorphic polyalanine stretch of 11 to 17 residues, but the most frequent stretch was 14 residues long (Figure 1.16) (Macchia *et al.*, 1999; Hishinuma *et al.*, 2001). Reduced polyalanine tract length (11 and 12 residues) was found only in patients with thyroid dysgenesis (Hishinuma *et al.*, 2001). Similarly, alteration of polyalanine stretch lengths has been found in a homeobox-containing gene, HOX D13, consisting of 15 residues (22-25 residues were reported in normal) in patients with the autosomal dominant disease, synpolydactyly (Akarsu *et al.*, 1996). Functional analysis was performed to reveal whether reduced number of polyalanine tract of TTF-2 is responsible for thyroid dysgenesis. However, the

expression study showed that the transcriptional activities of TTF-2 with reduced polyalanine-tract lengths were equal to that of TTF-2 with an unreduced polyalanine tract. These results suggested that the polymorphism of the polyalanine tract of TTF2 could not be a cause of the developmental defects of the human thyroid gland (Hishinuma *et al*., 2001).

TTF-2 protein contains two short stretches of basic amino acids (RRRKR) at both ends of the forkhead domain (Figure 1.16). Sequence alignments of representative human FOX protein segments show that a stretch of basic amino acids is present in most of the proteins at the C-terminal of DNA-binding domain whereas a basic stretch at the N-terminal of the DNA binding domain is less conserved (Figure 1.14). Previous studies have demonstrated that the basic stretches at the C-terminal of the forkhead domain are *bona fide* NLSs in four FOX proteins (Brownawell *et al*., 2001; Berry *et al*., 2002). Romanelli *et al.* have shown that both stretches are *bona fide* NLSs and required for nuclear import via importin α-dependent pathway (Romanelli *et al*., 2003).

Analysis of the TTF2 amino acid sequence identifies, in addition to the FHD, a second domain rich in alanine and proline residues that has been found in other developmental DNA binding proteins responsible for transcriptional repression activity. The analysis of the activity of the deletion mutants of TTF-2 allowed mapping the repression domain in the region between amino acids 197 and 218 at the carboxyl terminus of the protein (Figure 1.16) (Perrone *et al*., 2000). Comparison of the amino acid sequence of TTF-2 repression domain with the sequences present in the database demonstrates that this region shows 41 per cent of identity with HNF3γ amino terminal. HNF3γ is another member of the forkhead family that plays an important role in the tissue-specific gene expression program both in early development and in the adult (Ang *et al*., 1993).

TTF2 is a promoter-specific transcriptional repressor that displays both promoter and transcriptional activation domain specifity. TTF2 can repress Pax8 activity on TPO promoter, but not on NIS promoter. Additionally, TTF2 is able to repress the C-terminal activation domain of TTF1, while it has no effect on the N-terminal domain (Perrone *et al*., 2000). These observations suggest that it is able to recognize specific promoter architecture and represses only a subset of the genes activated by TTF1 and Pax8, since all these factors

are involved not only in thyroid specific gene expression (Plachov *et al*., 1990; Zannini *et al*., 1992), but also in thyroid development (Kimura *et al*., 1996; Macchia *et al*., 1998; Mansouri *et al*., 1998).

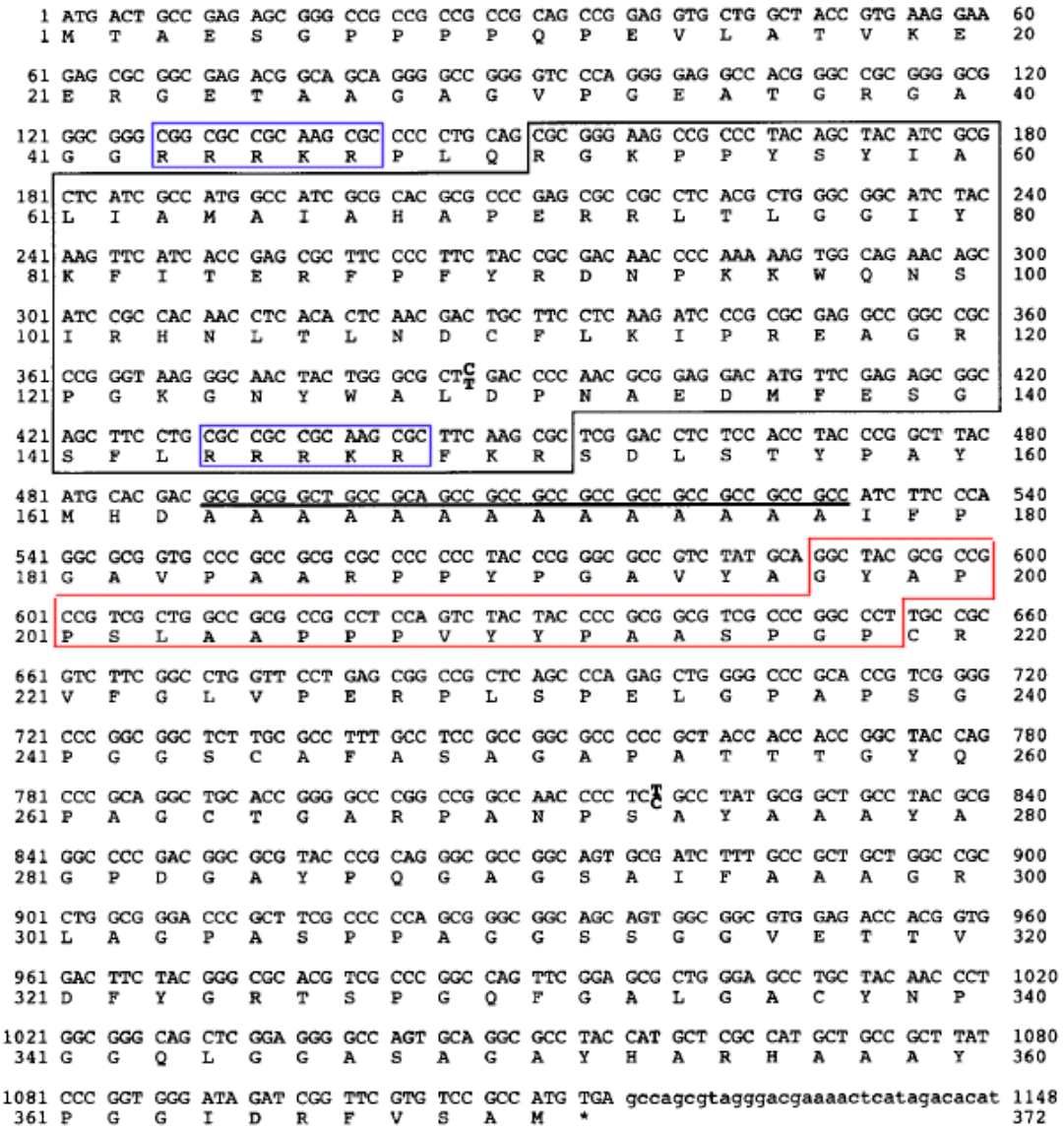

Figure 1.16. Nucleotide sequence of the human TTF2 gene and deduced amino acid sequence. The alanine stretch is underlined. The forkhead, two NLSs and transcription repression domains were boxed with black, blue and red color, respectively (Macchia *et al*., 1999).

1.4.5. Thyroid Development and TTF-2

The mature mammalian thyroid gland evolves from two distinct embryologic structures, the thyroid diverticulum, an endodermal component that gives rise to thyroid follicular cells, and the neuroectodermal ultimobranchial bodies that differentiate into the parafollicular calcitonin-producing C cells. Thyroid follicular cells originate by invagination of pharyngeal endoderm beginning at E8–8.5 of mouse development (Ericson and Frederiksson, 1990). The thyroid primordium migrates downward to reach its final destination in front of the trachea at E13–14. It is only at E15, after completion of the migration process, that thyroid follicular cells differentiate, as measured by expression of several thyroid-specific genes (Tg, TPO and TSHr) (Lazzaro *et al*., 1991). Two transcription factors, TTF-1 and Pax-8, have been proposed to be necessary for thyroid differentiation (Damante and Di Lauro, 1994). These proteins are present in the thyroid at late stage at E8.5, suggesting that an additional, essential event(s) must occur to trigger differentiation of thyroid cells at E13–14 (Lazzaro *et al*., 1991). TTF-2 expression is turned off exactly between E13 and E15 in the developing thyroid. The correlation between the onset of thyroglobulin and thyroperoxidase gene expression and the disappearance of TTF-2 mRNA suggests that in the embryo the role of TTF-2 is to block the activation of thyroid-specific gene expression by TTF-1 and Pax-8. It has been proposed that thyroid cell precursors enter into a determined state at E8.5, which is characterized, and possibly induced, by the presence of TTF-1 and Pax-8. During the next 5 days, thyroid cell precursors undergo a long migration, at the end of which they will express their full-differentiated phenotype. The presence of TTF-2 in the migrating thyroid cell precursors would prevent precocious expression of genes that might have an adverse effect on migration, for example because of changes in the adhesive properties of the cells (Zannini *et al*., 1997). In adult thyroid tissue TTF-2 expression is restored. It also shows a transient expression pattern in the developing pituitary. When Rathke's pouch is completed at E12-12.5, TTF-2 is undetectable in pituitary cells (Hermesz *et al*., 1996).

TTF-2 is expressed in two glands, the thyroid and the pituitary, which are part of a regulatory circuit responsible for homeostatic control of thyroid hormone production. The hypothalamus is also part of this circuit, where TTF-1, another transcription factor of relevance in thyroid cell function and differentiation, is expressed (Kimura *et al*., 1996). It

is inviting to think that recruitment of the same regulatory molecules in functionally related organs in the thyroid–pituitary–hypothalamic axis is advantageous to coordinate development and function.

TTF-2 has a dual function in the development of the thyroid gland (Zannini *et al*., 1997). In the mouse, TTF-2 shows transient expression during the migration of thyroid precursor cells from the invagination of the pharyngeal endoderm to the final destination in front of the trachea. During this period, TTF-2 represses transcriptional activation of the thyroglobulin and thyroperoxidase promoters by TTF-1 and PAX8, respectively. Subsequently, TTF-2 expression is turned off; however, is restored in adult thyroid tissue. In the adult thyroid, TTF-2 functions as a transcriptional activator of thyroglobulin (Sinclair *et al*., 1990) and thyroperoxidase (Francis-Lang *et al*., 1992; Aza-Blanc *et al*., 1993).

1.4.6. *TTF-2* Gene Mutations

Two missense mutations (p.A65V and p.S57N) of human *TTF-2* gene have been reported in two families with CH. In a Welsh family, two male siblings with thyroid agenesis, cleft palate, choanal atresia and bifid epiglottis together with spiky hair were homozygous for a missense mutation (p.A65V) within the forkhead DNA binding domain. Functional studies indicated that the p.A65V mutation is highly deleterious, with the mutant protein exhibiting a complete lack of DNA binding and transcriptional activation. In neither case thyroid tissue was detected by ^{123}I scanning and ultrasonography (Clifton-Bligh *et al*., 1998). In the second family, a homozygous p.S57N missense mutation within the forkhead domain was reported in two probands presented with CH. Both siblings exhibited cleft palate, and the other cervical midline defects (choanal atresia, bifid epiglottis) were absent. When compared directly in functional studies, the p.S57N mutation is less deleterious than the p.A65V mutation, preserving some DNA binding and transcriptional activity. Although p.S57N mutant protein retains 75 per cent of the maximal transcriptional activity, thyroid tissue was absent in both siblings. Unlike the cases described previously, these patients had an incomplete clinical phenotype, which may indicate partial preservation of TTF-2 function *in vivo* (Castanet *et al*., 2002).

1.4.7. Plasma Cholinesterase Deficiency

Patients with CH are candidates for multiple operations due to midline defects (cleft palate and choanal atresia) and their response to administration of muscle relaxants is crucial. Several cases with different disease phenotype showing the prolonged neuromuscular block (paralysis) have been reported following the administration of muscle relaxants such as mivacurium (Kaiser *et al*., 1995; Chung *et al*., 2002). Mivacurium is a short acting non-depolarising neuromuscular blocking agent (Kaiser *et al*., 1995). Deficiency or abnormality of plasma cholinesterase (also called pseudocholinesterase–PChE, butyrylcholinesterase–BChE) may cause prolonged duration of action of mivacurium (Barta *et al*., 2001). Up to date, more than 20 genetic variants of BChE have been described and p.Asp70Gly (A-variant) and Ala539Thr (K-variant) are the most common ones responsible for reduced activity of Butyrylcholinesterase (La Du, 1993).

2. AIM OF THE STUDY

In the context of this study, the aim was to investigate the genetic mechanisms responsible for Rett Syndrome (RTT), Breast Carcinogenesis, and Congenital Hypothyroidism (CH).

To provide further delineation of *MECP2* mutations in RTT patients, we have investigated the mutation profile of the entire coding region of the MECP2 gene and XCI pattern in a cohort of 71 patients with classical or atypical RTT. The analyses in RTT patients were extended:

- to establish quantitative Real Time PCR and quantitative fluorescent multiplex PCR assays to detect the *MECP2* exon rearrangements in mutation negative patients,
- to evaluate the impact of the use of stringent clinical criteria on *MECP2* mutation detection rate,
- to establish XCI analysis using two different reference genes,
- to evaluate the contribution of XCI to RTT clinical phenotype,
- to perform genotype/phenotype correlation based on comparison of severity score of patients with the type and location of the mutation and the XCI pattern.
- to develop a rapid and efficient *MECP2* mutation screening strategy to be used as a preliminary step for genetic diagnosis of RTT. We aimed to design a simpler multiplex ARMS-PCR strategy that allows identification of seven mutations accounting for up to two thirds of pathogenic *MECP2* mutations.
- to analyse the effect of DNA concentration on reliability and reproducibility of Real Time PCR analysis for identification of *MECP2* exon rearrangments.

Aberrant methylation of CpG-rich sites (CpG islands) was identified as an epigenetic mechanism for the transcriptional silencing of repair genes in different types of cancer. In this study, the methylation status of 5' flanking regions (including the CpG islands and putative promoter sequence) of hHR23A and hHR23B genes were investigated in primary breast tumor, tumor adjacent tissues, and normal breast tissues. Since the methylation status of these genes was not investigated before, we aimed;

- to characterize the CpG islands and the putative promoter region in the 5' flanking region of the hHR23 genes using web-based analysis,
- to design primer sequences to investigate the methylation status of CpG di-nucleotides,
- to determine the methylation status of the putative promoter region of hHR23 genes in archival formalin-fixed, paraffin-embedded breast tumor and normal tissues.

The genetic mechanisms leading to congenital hypothyroidism and prolonged paralysis after mivacurium in a patient with Bamforth Syndrome were investigated. For this purpose;

- The patient was screened for the presence of mutations within the TTF2 gene responsible of hypothyroidism. The effect of the identified mutation on DNA binding ability of the TTF2 protein was tested based on a collaborative study.
- Since our CH patient was the first case with Bamforth Syndrome showing plasma cholinesterase deficiency, the patient DNA sample was investigated for the presence of BChE variants responsible for prolonged neuromuscular block (paralysis) after administration of mivacurium as a muscle relaxant.

3. MATERIALS

3.1. Subjects and Samples

Peripheral blood samples of patients with Rett Syndrome were provided with an informed consent by Istanbul University (Department of Neurology, Division of Child Neurology), Marmara University Hospital (Department of Pediatrics, Division of Child Neurology), Health Ministry Tepecik Education Hospital (Child Health and Diseases Clinics), and other centers.

The patient with Congenital Hypothyroidism was referred from Kocaeli University, Faculty of Medicine, Department of Pediatrics.

Archival formalin-fixed, paraffin-embedded tissues were kindly provided by Marmara University Hospital (Department of Pathology) and Nişantaşı Pathology Laboratories (Istanbul, Turkey).

3.2. Chemicals

All solid and liquid chemicals used in this study were purchased from Merck (Germany), Sigma (USA), Riedel de-Häen (Germany), and Carlo Erba (Germany), unless stated otherwise in the text.

3.3. Fine Chemicals

3.3.1. Enzymes

Taq DNA Polymerases were purchased from Fermentas (MBI Fermentas, Lithuania). The restriction enzymes were purchased from Promega (USA), Fermentas (Lithuania), and New England Biolabs (England).

3.3.2. Oligonucleotide Primers

The primers used in the framework of this thesis were synthesized by Integrated DNA Technologies (USA), Alpha DNA (Canada), or Iontek (Istanbul). The sequence and PCR conditions for the primers used throughout the thesis are given in Table 3.1 through Table 3.7.

Table 3.1. Sequence of the primers used for exon amplification of the MECP2 gene.

Ekxon	**Primers (5'→ 3')**	**PCR Product Length (bp)**	**Annealing Temp. (°C)**
Exon 1	Rettex1F: ggacaggaaatctcgccaat Rettex1R: cacggcggtcccactc	340	57
Exon 2	Rett1F: tttctttgttttaggctcca Rett1R: ggccaaaccaggacatatac	190	57
Exon 3	Rett2.3F: gtgatacttacatacttgtt Rett2.3R: ggctcagcagagtggtgggc	172	56
	Rett 2.1F: gagcccgtgcagccatcagc Rett2.2R: ctgtagagataggagttgct	270	62
Exon 4	Rett 3AF: tgtgtctttctgtttgtccc Rett 3AR: gatttgggcttcttaggtgg	182	57
	Rett 3BF: cctcccggcgagagcagaaa Rett 3BR: tgacctgggtggatgtggtg	240	57
	Rett 3CF: tgcctttcaaacttcgcca Rett 3CR: tgaggaggcgctgctgctgc	410	57
	Rett 3CF: tgcctttcaaacttcgcca Rett 3MR: tggcctgagggtcggcctcagctttgc	120	58
	Rett 3DF: gcagcagcagcgcctcctca Rett 3DR: tggcaaccgcgggctgaggca	244	60
	Rett 3EF: tgccccaaggagccagctaa Rett 3ER: gctttgcaatccgctccgtg	200	58

Table 3.2. Primers used in X chromosome inactivation analysis.

Gene	Primers (5'→ 3')	PCR Product Length (bp)	Annealing Temp. (°C)
AR	Xinact F: gctgtgaaggttgctgttcctcat Xinact R: tccagaatctgttccagagcgtgc	280	65
ZNF261	Xinact2 F: atgctaaggaccatccagga Xinact2 R: ggagttttcctccctcacca	280	58

Table 3.3. Sequences and PCR conditions for the primers used in quantitative Real Time PCR analysis.

Gene	Primers (5'→ 3')	PCR Product Length (bp)	Annealing Temp. (°C)
MECP2	Rett_exon2F: tttctttgttttaggctcca Rett_exon2R: ggccaaaccaggacatatac	190	58
	Rett_exon3F: gtgatacttacatacttgtt Rett_exon3R: ggctcagcagagtggtgggc	172	58
	Rett_exon4F: tgtgtctttctgtttgtccc Rett_exon4R: gatttgggcttcttaggtgg	182	58
NDRG1	NDRG1_exon7F: aggctcccgtcactctg NDRG1_exon7R: gtcttccttcatcttaaaatg	175	58
PRX	PRX_exon6F: cgtgcaagtgggcagaacta PRX_exon6R: tgacaagacagagggcaagg	383	58

Table 3.4. Sequence of the primers used in quantitative fluoresent multiplex PCR analysis.

Gene	Primers (5'→ 3')	PCR Product Length (bp)	Annealing Temp. (°C)
MECP2	MeCP2-3Fam: gagcccgtgcagccatcagc MeCp2-3R: cgtgtccagccttcaggcag	180	58
PRNP	PRNP-2Fam: actgcgtcaatatcacaatc PRNP-2R: tccccactatcaggaagatga	227	58

Table 3.5. Sequence of the primers used in methylation analyses of the putative promoter region of hHR23A and hHR23B genes.

Gene	Primers (5'→ 3')	PCR Product Length (bp)	Annealing Temp. (°C)
hHR23A	Rad23A-CF: ttagtataggtatataaaaattttgttaaa Rad23A-CR: aatcttaaaaatctactactacaacatttt	433	50
	Rad23A-CF2: gtgagagtggggatattagagttattttgt Rad23A-CR: aatcttaaaaatctactactacaacatttt	390	54
	Rad23A-F1: gaagaaatataaatgtttgtaattagtatagg Rad23A-R1: ttaaaattctaacctccccgccc	555	50
	Rad23A-CF2: gtgagagtggggatattagagttattttgt Rad23A-R1: ttaaaattctaacctccccgccc	480	54
hHR23B	Rad23B-CF: tttttgttttagggttttgtatttat Rad23B-CR: tcaccaaaacatacccccctc	370	50
	Rad23B-CF2: tttattttgttgggtttttatg Rad23B-CR: tcaccaaaacatacccccctc	349	54
	Rad23B-CN: ttgtgtaattttggtagttgggt Rad23B-CR: tcaccaaaacatacccccctc	304	54

Table 3.6. Sequence of the primers used for exon amplification of the TTF2 gene.

Exon	Primers (5'→ 3')	PCR Product Length (bp)	Annealing Temp. (°C)
Exon 1	TTF2A: agcctgggccgctgggctctccg TTF2D: ttgtggcggatgctgttctgc	463	58
	TTF2C: cggcatctacaagttcatcac TTF2E: cagcagcggcaaagatcg	671	53

Table 3.7. Sequence of the primers used for exon amplification of the BChE gene.

Variant	Primers (5'→ 3')	PCR Product Length (bp)	Annealing Temp. (°C)
A-Variant	M-6: acatactgaagatgacatcata M115: tgttccagtttgaaaaccacca	373	52
K-Variant	AP5: cgaaattatttttcagttaatgaaacagataaaaattt C539: tgctttccactcccattcag	103	60

3.3.3. DNA Size Marker

Size marker used in this study was 100-bp DNA ladder between 100 and 1000 bp (MBI Fermentas, Lithuania).

3.4. Kits

QIAquick PCR Purification Kit was purchased from Qiagen (Germany). SYBR Premix Ex Taq was purchased from TaKaRa (Japan). Methylamp^{TM} DNA Modification Kit was purchased from Epigentek (USA). Deoxyribonucleoside triphosphates (dNTPs) were purchased from Fermentas (MBI Fermentas, Lithuania).

3.5. Buffers and Solutions

3.5.1. DNA Extraction from Peripheral Blood

Cell Lysis Buffer : 155 mM NH_4Cl
10 mM $KHCO_3$
1 mM Na_2EDTA (pH 7.4)

Nuclei Lysis Buffer : 10 mM Tris-HCl (pH 8.0)
400 mM NaCl
2 mM Na_2EDTA (pH 7.4)

Sodiumdodecylsulphate	:	10 per cent SDS (w/v) (pH 7.2)
Proteinase K	:	20 mg/ml
TE Buffer	:	20 mM Tris-HCl (pH 8.0) 0.1 mM Na_2EDTA (pH 8.0)
5 M NaCl solution	:	292.2 g NaCl in 1 l dH_2O

3.5.2. Polymerase Chain Reaction (PCR)

10 X $MgCl_2$ Free Buffer	:	500 mM KCl 100 mM Tris-HCl (pH 9.0) 1 per cent Triton X-100 (Promega, USA)
10 X PCR Buffer	:	100 mM Tris-HCl (pH 8.8 at 25 °C) 500 mM KCl 0.8 per cent Nonidet P40 (Fermentas, Lithuania)
10 X PCR Buffer with $(NH_4)_2SO_4$	:	750 mM Tris-HCl (pH 8.8 at 25 °C) 200 mM $(NH_4)_2SO_4$ 0.1 per cent Tween 20 (Fermentas, Lithuania)
$MgCl_2$	:	25 mM $MgCl_2$ (Fermentas, Lithuania and Promega, USA)

3.5.3. Agarose Gel Electrophoresis

10 X Tris-Borate-EDTA Buffer	:	0.89 M Tris-Base 0.89 M Boric Acid 20 mM Na_2EDTA (pH 8.3)
1, 2 or 3 per cent Agarose Gel	:	1, 2 or 3 per cent (w/v) Agarose in 0.5 X

TBE Buffer

Ethidium Bromide	:	10 mg/ml
10 X Loading Buffer	:	2.5 mg/ml Bromophenol Blue 1 per cent SDS in 2 ml glycerol

3.5.4. Polyacrylamide Gel Electrophoresis

10 X TBE Buffer	:	0.89 M Tris-Base 0.89 M Boric Acid 20 mM Na_2EDTA (pH 8.3)
30 per cent Acrylamide Stock: (29:1)		29 per cent Acrylamide 1 per cent N, N'-methylenebisacrylamide
8 per cent Denaturing Gel	:	8 per cent Acrylamide Stock (19:1) 8.3 M Urea 1X TBE Buffer (pH 8.3)
Ammoniumpersulfate	:	10 per cent APS (w/v)
10X Denaturing Buffer	:	95 per cent Formamid 20 mM EDTA 0.05 per cent Xylene Cyanol 0.05 per cent Bromophenol Blue

3.5.5. Silver Staining

Buffer A	:	10 per cent Ethanol 0.5 per cent Glacial Acetic Acid
Buffer B	:	0.1 per cent $AgNO_3$ in dH_2O

Buffer C	:	1.5 per cent NaOH 0.01 per cent $NaBH_4$ 0.015 per cent Formaldehyde
Buffer D	:	0.75 per cent Na_2CO_3

3.6. Equipments

Automated DNA Sequencing and Quantitative Fluorescent Multiplex PCR analyses were perfomed using ABI 3100 and 3130 PRISM (Applied Biosystems) in Iontek and Burc Laboratories (Istanbul, Turkey), respectively. Other experiments were performed using facilities of the Department of Molecular Biology and Genetics at Boğaziçi University (Istanbul, Turkey). The equipments used were as follows:

Autoclave	:	Model MAC-601 (Eyela, Japan)
Balances	:	Electronic Balance Model VA124 (Gec Avery, UK) Electronic Balance Model CC081 (Gec Avery, UK)
Centrifuges	:	Centrifuge 5415C (Eppendorf, Germany) Universal 16R (Hettich, Germany)
Deep Freezers	:	-20°C (Bosch, Germany) -70°C (GFL, Germany)
Documentation System	:	GelDoc Documentation System (Bio-Rad, USA)
Electrophoretic Equipments	:	Horizon 58, Model 200 (BRL, USA) Sequi-Gen Sequencing Cell (Bio-Rad,USA) DGGE System Model # DGGE-200 (C.B.S. Scientific Co., USA) Horizon 1020, Model H1 (BRL, USA)

		PROTEAN Vertical electrophoresis System (Bio-Rad, USA)
Incubators	:	Shake'n'Stack (Hybaid, UK) Oven EN400 (Nuve, Turkey)
Magnetic Stirrer	:	Chiltern Hotplate Magnetic Stirrer, HS31 (UK)
Ovens	:	Microwave Oven (Vestel, Turkey)
Power Supplies	:	Power Pac Model 3000 (Bio-Rad, USA) PSU 400/200 (Scie-Plus, UK)
Refrigerator	:	+4°C (Arçelik, Turkey)
Spectrophotometers	:	NanoDrop ND-1000 (NanoDrop, USA) CE 5502 Scanning Double Beam 5000 Series (CECIL Elegant Technology, UK)
Thermal Cyclers	:	Icycler (Bio-Rad, USA) Mycycler (Bio-Rad, USA) Light-Cycler 1.5 (Roche, Germany)
Vortex	:	Nuvemix (Nuve, Turkey)
Water Purification System	:	WA-TECH Ultra Pure water Purification System (WA-TECH, Germany)

4. METHODS

4.1. Molecular Basis of Rett Syndrome (RTT)

4.1.1. DNA Extraction from Peripheral Blood

Genomic DNA was extracted from peripheral blood by using a modified version of salting-out method described by Miller *et al*. (1988). Peripheral blood samples were collected from individuals into vacutainer tubes containing K_3EDTA. Thirty ml ice-cold red blood cell (RBC) lysis buffer is added to 10 ml blood sample and mixed thoroughly. The samples are then left at +4 ˚C for 15 minutes (min) to allow lysis of erythrocyte membranes. Leukocyte nuclei were collected after centrifugation of lysed solution at 5000 revolution per minute (rpm), +4 ˚C for 10 min. The supernatant was discarded and the nuclei were resuspended in 10 ml RBC lysis buffer by vortexing. Resuspension was centrifuged again at 5000 rpm, +4 ˚C for 10 min. After discarding the supernatant, the nuclear pellet was resuspended in three ml nuclei lysis buffer by vortexing. Thirty µl of Proteinase K and 40µl of 10 per cent SDS were added and the mixture was incubated at 37 ˚C overnight or at 56 ˚C for three hours. Afterwards ten ml of 2.5 M NaCl were added to mixture and centrifuged at 5000 rpm at room temperature for 20 min. The supernatant was transferred into a new 50 ml falcon tube. The DNA was precipitated with addition of two volumes of absolute ethanol. The DNA was transferred in to a 1.5 ml Eppendorf tube containing 200-500 µl of Tris-EDTA (TE) buffer, and left overnight at room temperature to dissolve completely.

4.1.2. Quantitative Analysis of the Extracted DNA

The concentration of the isolated DNA was calculated measuring the optical density at 260 nm. The formula below was used, which is based on the fact that 50 µg of double stranded DNA has an absorbance of 1.0 at 260 nm.

4.1.3. Mutation Analysis of MECP2 Gene

The RTT patients were screened for mutations within the MECP2 gene using PCR-RFLP, SSCP and subsequent DNA sequencing.

4.1.3.1. Restriction Endonuclease Analysis. The most common mutations p.R106W, p.T158M, p.R168X, p.R255X, p.R270X, and p.R306C were screened in each patient using PCR-RFLP as a preliminary step. The region containing the mutation site was amplified using the primers given in Table 1. PCR reaction was performed in a total volume of 25 µl containing approximately 100 ng DNA, 2.5 µl of 10X polymerase buffer, 2.0 mmol/l $MgCl_2$, 0.2 mmol/L dNTPs, 0.4 µmol/l of each primer and 1 U of *Taq* polymerase (Fermentas). The PCR program on Icycler™ (BioRad) thermal cycler was as follows: an initial denaturation step at 94 ºC for 4 min, followed by 33 cycles of 45 sec at 94 ºC, 30 sec at annealing temperature, 45 sec at 72 ºC, and a final extension step of 8 min at 72 ºC. Five µl from the PCR product was run on two per cent agarose gel to check for any nonspecific bands. A total of ten µl of the PCR product was digested with 3U of the appropriate restriction enzyme (Fermentas) and 2 µl of its 10X reaction buffer in a 20 µl reaction volume (Table 4.1). The mixture was incubated at 37 ºC for 4 hours. The digested products were electrophoresed on three per cent agarose gel at 100 V for 30 min. The gel and running buffers were 0.5X TBE. The fragments were visualized by ethidium bromide under UV light. The genotyping was performed according to restriction fragment profiles (Table 4.1).

4.1.3.2. Single Strand Conformation Polymorphism. Patients were further screened for the presence of point mutations by Single Strand Conformation Polymorphism (SSCP) analysis. The four coding exons and the flanking intronic regions were amplified in ten overlapping fragments by use of primers listed in Table 1.1.1. The primers designed by Bienvenu *et al*. (2000) were used, except for the exon 1. The sequences of the exon 1 primers were 5'-ggacaggaaatctcgccaat-3' (forward) and 5'-cacggcggtcccactc-3' (reverse). PCR reactions were carried out in a total volume of 50 µl containing approximately 200 ng DNA, 5 µl of 10X polymerase buffer, 2.0 mmol/l $MgCl_2$, 0.2 mmol/L dNTPs, 0.4 µmol/l of each primer and 2 U of *Taq* polymerase (Fermentas). The PCR program on Icycler™ (BioRad) thermal cycler was as follows: an initial denaturation step at 94 ºC for 4 min,

followed by 33 cycles of 45 sec at 94 ºC, 30 sec at annealing temperature, 45 sec at 72 ºC, and a final extension step of 8 min at 72 ºC. Five µl from the PCR product was run on a two per cent agarose gel to check for any nonspecific bands.

Table 4.1. The list of the MECP2 gene mutations analyzed by PCR-RFLP method.

Exon	**Mutation**	**Restriction Enzyme**	**Primers**	**PCR product**	**RFLP Results**
Exon 3	p.R106W (c.316 C>T)	*Nla*III	Rett 2.1F Rett 2.2R	277 bp	Wt: 124 + 153 bp Mt: 34 + 90 + 153 bp
Exon 4	p.T158M (c.473 C>T)	*Nla*III	Rett 3AF Rett 3AR	182 bp	Wt: 182 bp Mt: 120 + 62 bp
Exon 4	p.R168X (c.502 C>T)	*Hph*I	Rett 3AF Rett 3AR	182 bp	Wt: 182 bp Mt: 150 + 32 bp
Exon 4	p.R255X (c.763 C>T)	*Hha*I	Rett 3CF Rett 3MR	120 bp	Wt: 90 + 30 bp Mt: 120 bp
Exon 4	p.R270X (c.808 C>T)	*Nla*IV	Rett 3CF Rett 3CR	410 bp	Wt: 140+ 270 bp Mt: 410 bp
Exon 4	p.R306C (c.916 C>T)	*Hha*I	Rett 3CF Rett 3CR	410 bp	Wt: 250 + 160 bp Mt: 410 bp

4.1.3.3. Preparation of SSCP Gels. The amplification products were run on eight per cent acrylamide gels with or without four per cent glycerol. The glass plates of 180 mm x 200 mm were cleaned with alcohol to remove any dust and oily fingerprints. Then, 0.7 mm thick spacers were placed on the two edges of the glass plates and the plates were tightened with clamps. The eight per cent acrylamide solution was prepared as follows: 350 µl of ammonium per sulfate (10 per cent) and 35 µl of TEMED were added in 9.3 ml of 30 per cent stock acrylamide solution (29:1 acrylamide to N, N'-methlene-bis-acrylamide). The mixture volume was adjusted to 35 ml with dH_20 and poured between two plates. A 20-well comb was inserted between the two plates and the gel was allowed to polymerize for at least one hour.

4.1.3.4. SSCP Electrophoresis. An aliquot of 15 µl of the PCR product was mixed with 15 µl of denaturing loading dye (95 per cent form amid, 0.05 per cent bromophenol blue, 0.05 per cent xylene cyanol). Just before loading, they were denatured at 94°C for five min, and chilled on ice for five min. Thirteen µl of the denatured sample was loaded on the gel. Electrophoresis of the samples was carried out in 0.6 X TBE buffer at 150-250 V for 16 hours.

4.1.3.5. Silver-Staining. The alleles, separated on gels, were visualized by silver-staining. The gel was incubated with buffer A for five min to fix the DNA fragment. Buffer A was replaced with buffer B, which is a silver nitrate solution, and the gel was left for 10-15 min. After a short wash with dH_2O, the gel was immersed in freshly prepared buffer C until the bands appeared (approximately 10 min). After color development, Buffer D is used to terminate the color reaction for five min. The gel was then transferred to a transparent folder, and was sealed on all four sides for preservation.

4.1.4. DNA Sequence Analysis

When a single strand conformation polymorphism was observed, genomic DNA was amplified using the same primer pairs used for SSCP and both forward and reverse strands were sequenced. Patient and control PCR products were purified using Qiagen PCR purification kit (Qiagen) and sequenced with automated sequencer ABI 3700 PRISM (Applied Biosystems) in Iontek (Istanbul, Turkey). The resulting sequences were aligned with the CLUSTAL W program.

4.1.5. Quantitative Real Time PCR

The real time PCR was performed in a total volume of 20 µl, containing 10 µl 2X SYBR Green PCR Master Mix (TaKaRa, Japan), 5 pmol of each primer per reaction, 4 µl of the genomic DNA (5 ng/µl) and distilled water. The PCR protocol on Light Cycler (LC) (Roche Diagnostics, Mannheim, Germany) was as follows: an initial denaturation step (95°C for 2 min) followed by amplification and quantification steps repeated for 30 cycles (95°C for 5 sec, 58°C for 10 sec, 72°C for 20 sec, with a single fluorescence measurement

at the end of the elongation step at 72°C), a melting curve program (65–98°C with a heating rate of 0.2°C per second and a continuous fluorescence measurement) and terminated by cooling to 40°C. Each sample was amplified with the MECP2 and reference gene primer pairs. The coding exons of the MECP2 was amplified using the following primers designed by Bienvenu *et al*. (2000); Rett_exon2F: tttctttgttttaggctcca; Rett_exon2R: ggccaaaccaggacatatac; Rett_exon3F: gtgatacttacatacttgtt; Rett_exon3R: ggctcagcagagtggtgggc; Rett_exon4F: tgtgtctttctgtttgtccc; and Rett_exon4R: gatttgggcttcttaggtgg. The reference NDRG1 gene was amplified using NDRG1_exon7F: aggctcccgtcactctg and NDRG1_exon7R: gtcttccttcatcttaaaatg primers. Within each PCR batch three aliquots of wild type control DNA in decreasing concentrations (20, 10, and 5 ng) from a healthy female were included to construct a standard curve. Melting point analysis was conducted on all PCR products to check for any nonspecific amplicons. Using the Fit Points Method, the DNA was quantified relative to the standard curve for each exon. Subsequently, the ratios between target (MECP2) and reference (NDRG1) exon were calculated for each individual. The ratio was 1.0 for normal individuals, a ratio of 0.5 was accepted as a heterozygous deletion, and 1.5 as a heterozygous duplication.

4.1.6. Quantitative Fluorescent Multiplex PCR Assay

Quantitative fluorescent multiplex PCR (QF-PCR) assay was used to detect the MeCP2 exon 3 rearrangments. Multiplex QF-PCR assay was set up to amplify exon 3 of MeCP2 gene and exon 2 of Prion Protein (PRNP) gene simultaneously. The following primers were used: 6-FAM labeled MeCP2-3F: gagcccgtgcagccatcagc, MeCp2-3R: cgtgtccagccttcaggcag, 6-FAM labeled PRNP-2F: actgcgtcaatatcacaatc, and PRNP-2R: tccccactatcaggaagatga (Bienvenu *et al*., 2000). Primers were at first tested in equimolar amounts and their concentrations were then changed to obtain equal fluorescent peak area for both MeCP2 and PRNP gene. PCR was performed in a total volume of 20 µl containing 30 ng genomic DNA, 10 µl 2X SYBR Green PCR Master Mix (TaKaRa, Japan), 5 pmol (for MeCP2) and 7.5 pmol (for PRNP) of each primer. The PCR protocol on Light Cycler (LC) (Roche Diagnostics, Mannheim, Germany) was as follows: an initial denaturation step (95°C for 2 min) followed by amplification steps repeated for 25 cycles of 95°C for 5 sec, 58°C for 10 sec, 72°C for 20 sec and a melting curve program (65–98°C with a heating rate of 0.2°C per second). Melting point analysis and agarose gel

electrophoresis were performed to check for any nonspecific amplicons. Fragments were then electrophoresed on ABI prism 3100 Genetic analyzer and areas under the curve were calculated by GeneMapper software package (Applied Biosystem, Foster City, CA) in Burç laboratory, Istanbul.

4.1.7. X Chromosome Inactivation

X Chromosome Inactivation (XCI) was assessed by the method described by Allen *et al*. (1992) and Beever *et al*. (2003). Initially, two µg genomic DNA of the each patient and mother was digested with 10U of *Hha*I restriction enzyme (MBI Fermentas) in a volume of 20 µl. The mixture was incubated at 37 ºC for overnight.

The *Hha*I digested and undigested genomic DNAs from the patients were amplified by primers flanking the CAG repeat region in the Androgen Receptor (AR) or ZNF261 genes (Table 3.2). PCR reaction was performed in a total volume of 25 µl containing approximately 100 ng DNA, 2.5 µl of 10X polymerase buffer, 1.0 mM $MgCl_2$, 10 per cent dimethyl sulfoxide (DMSO), 200 µM dNTPs, 0.4 µlM of each primer, and 1 U of Taq polymerase (Fermentas). The following PCR program was used: 94ºC for 4 min, followed by 35 cycles of 45 sec at 94 ºC, 30 sec at annealing temperature (65ºC for AR-F/R, 58ºC for ZNF261-F/R), 1 min at 72ºC, and a final extension step of 8 min at 72ºC.

4.1.7.1. Preparation of Denaturing Polyacrlamide Gels. The PCR products were analyzed on eight per cent denaturing acrylamide gel. The gel was cast in a 40 cm long sequencing apparatus that was assembled using 0.35 mm spacers. Four hundred µl of APS (10 per cent) and 40 µl of TEMED were added in 40 ml of denaturing stock acrylamide solution and poured between the glass plates. A 24-well shark's tooth comb was inserted in an inverted orientation and the gel was allowed to polymerize for at least one hour.

4.1.7.2. Electrophoresis of PCR Products on Denaturing Polyacrlamide Gels. The gel was initially pre-run with hot 1X TBE buffer at constant power of 40 Watts for 15-20 min to allow the temperature to rise to 45 ºC. Then, ten µl of the PCR product was mixed with ten µl of denaturing loading dye, denatured at 94°C for five min, and chilled on ice for five min. After the comb was re-oriented, three µl of the denatured sample was loaded. The

gels were run at 30W constant power for three hours, then silver-stained and sealed for documentation.

4.1.8. Clinical Severity Score Analysis

4.1.8.1. Clinical Severity Score. Patients were evaluated by a scoring system with respect to: hand function, eye contact and gait function. The scoring was performed as follow: Hand function: (1) can hold a glass, can use a spoon or fork; (2) can sometimes grasp an object; (3) does never use her hands purposefully. Eye contact: (1) intense, use eye pointing; (2) direct eye contact possible to obtain; (3) eye contact very difficult to obtain. Gait function: (1) walks independently; (2) has lost gait function; (3) has never walked (Cheadle *et al*., 2000).

4.1.8.2. Huppke Scoring. Patients were scored with respect to the following criteria: Normal prenatal and perinatal period (1); Normal psychomotor development during the first 6 months (1); Normal head circumference at birth (1); Deceleration of head growth (1); Never good hand skills (1); Loss of hand skills (2); Stereotypic hand movements (1); Communication dysfunction and social withdraw (1); Never acquired language (1); Loss of acquired language (2); Severe psychomotor retardation (1); Impaired or absent locomotion (1) (Huppke *et al*., 2003).

4.1.8.3. Statistical Analyses. The non-parametric Wilcoxon Mann–Whitney test with a significance level of 95 per cent was used for comparing total severity score values of samples with respect to the presence, type and location of the mutation in the MECP2 gene, and the XCI status. Severity score for specific clinical features of patients were compared by Fisher exact test. All statistical analyses were performed by using SPSS v 15.0 software (SPSS Inc., Chicago, IL, USA).

4.1.9. Multiplexed ARMS-PCR Approach for the Detection of Common *MECP2* Mutations

4.1.9.1. Primer Design. The multiplex amplification refractory mutation system (ARMS) - PCR procedure was established to identify seven of the most common MECP2 gene

mutations. Primers were designed according to *MECP2* sequence (GenBank accession NT_004992) using web-based software Primer 3.0. The specificity of the primers were confirmed using the 'BLAST'' program at http://www.ncbi.nlm.nih.gov/blast. The primer nucleotide sequences are given in Table 1. To increase the specificity of the reaction for p.R168X and p.T158M mutations a mismatch is introduced at the 3′ end of the corresponding allele-specific primers. Each primer is designed to amplify fragments of different sizes to resolve the products easily on agarose gel electrophoresis (Figure 4.1). Panel 1 can screen for four of the mutations and the corresponding wild type alleles (p.R133C, p.R168X, p.R255X and p.R294X) whereas Panel 2 detects mutant/wild type alleles for p.T158M, p.R270X and p.R306C mutations.

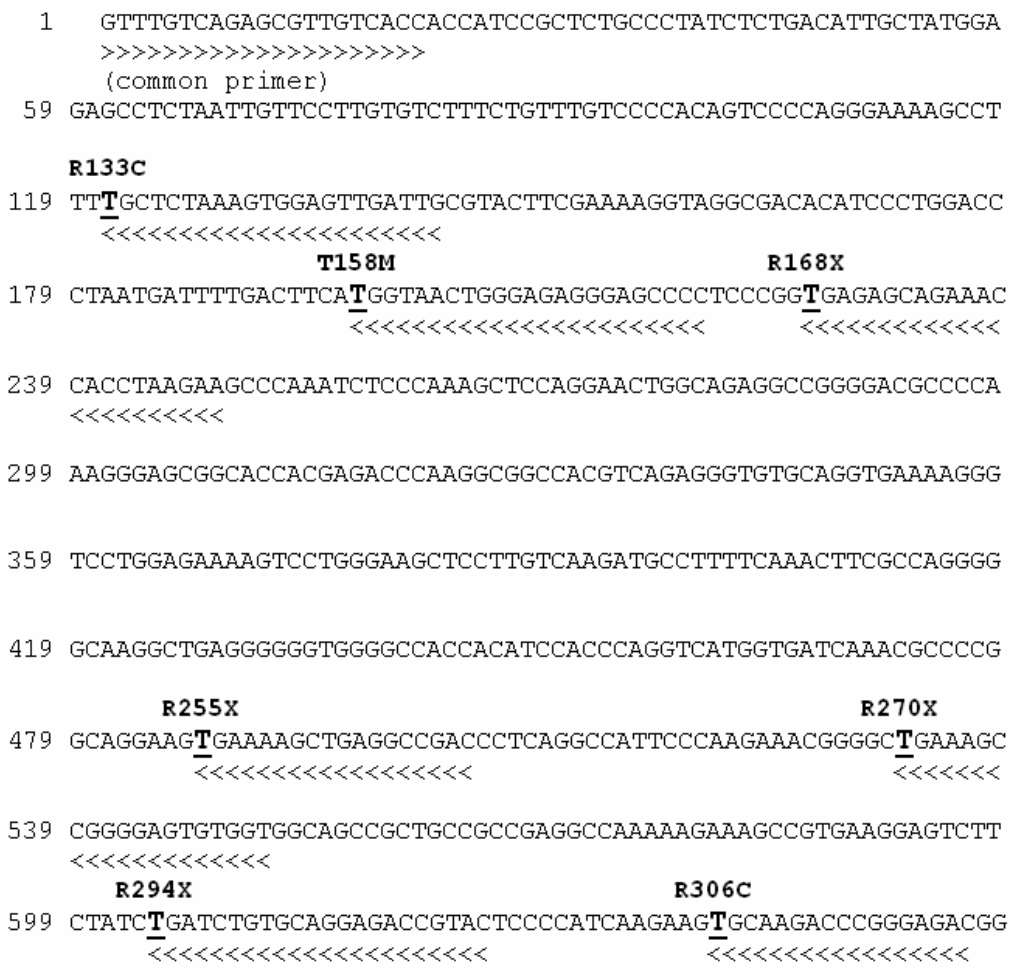

Figure 4.1. Schematic representation of primer positions on MECP2 gene nucleotide sequence.

4.1.9.2. PCR conditions. PCR was performed in a total volume of 25µl containing approximately 60 ng genomic DNA, 2.5 µl of 10X buffer, 2.5 mM $MgCl_2$, 0.2 mM dNTPs, and 1.5U of Taq polymerase (MBI Fermentas, Hanover, MD). The concentrations of primers used are given in Table 4.2. The PCR program on the thermal cycler (icycler™, BioRad) was as follows: an initial denaturation step at 94 ºC for 5 min, a 10 cycles of touchdown PCR consists of 30 sec at 94 ºC, 45 sec at 63 ºC with 0.4 ºC decrement in each cycle and 1 min at 72 ºC followed by 35 cycles of 25 sec at 94 ºC, 45 sec at 59 ºC, 1 min at 72 ºC, and a final extension step of 10 min at 72 ºC.

A total of 15 µl from the PCR product were run on two per cent standard agarose gels at 100 V for 15 min. The fragments were visualized by ethidium bromide on a UV transilluminator.

Table 4.2. Primer sequences and concentrations used in the two panels for multiplexed ARMS-PCR assay.

Mutation	**[conc.]**	**wildtype Primer**	**mutant primer**	**[conc.]**	**PCR product size**
		Panel 1-wt	Panel 1-mut		
R133C	5 pmol	caatcaactccactttagagcG	caatcaactccactttagagcA	20 pmol	141bp
R168X	3 pmol	atcttaggtggtttctgctctcG	atcttaggtggtttctgctcacA	10 pmol	247bp
R255X	15 pmol	gtcggcctcagcttttcG	gtcggcctcagcttttcA	5 pmol	504bp
R294X	20 pmol	gtacggtctcctgcacagatcG	gtacggtctcctgcacagatcA	10 pmol	625bp
Forward	10 pmol	GTTTGTCAGAGCGTTGTCACC		10 pmol	
		Panel 2-wt	Panel 2-mut		
T158M	10 pmol	ggggctccctctcccagttaccG	ggggctccctctcccagttaacA	5 pmol	220bp
R270X	10 pmol	accacactccccggctttcG	accacactccccggctttcA	10 pmol	551bp
R306C	10 pmol	gtctcccgggtcttgcG	gtctcccgggtcttgcA	10 pmol	656bp
Forward	10 pmol	GTTTGTCAGAGCGTTGTCACC		10 pmol	

4.1.9.3. p.R106W mutation detection. The c.316 C>T (p.R106W) mutation was also investigated by ARMS-PCR using the following primers: wild-type R106W-R: 5'-ctgcctgaaggctggacac -3', mutant R106W-W: 5'- ctgcctgaaggctggacat -3'and common R106W-C: 5'- gccctgtagagataggagttgc -3'. Using the above cycling conditions with 10 pmol primers, a 112 bp long product was produced.

4.1.9.4. PCR-RFLP and DNA Sequencing. The mutations p.R106W (+NlaIII), p.T158M (+NlaIII), p.R168X (+HphI), p.R270X (-NlaIV), and p.R306C (-HhaI) were screened using PCR-RFLP whereas mutations p.R133C, p.R255X and p.R294X were investigated by DNA sequencing as described in sections 4.1.3.1 and 4.1.4.

4.1.10. The Effect of DNA Concentration on Reliability and Reproducibility of SYBR Green Dye-based Real Time PCR Analysis to Detect the Exon Rearrangements

4.1.10.1. Preparation of DNA Samples. Photometric measurement of the stock DNA and the dilutions of 200 ng/µl were performed on an ND-1000 spectrophotometer (NanoDrop Technologies). DNA was diluted first to 200 ng/µl, stored at 37 ℃ overnight, and then diluted to final concentration of 0.025 ng/µl. Six dilutions at concentrations of 0.025, 0.25, 1.25, 12.5, 25, and 50 ng/µl were prepared from the patient R23 with MECP2 exon 3 deletion, patient R19 with MECP2 exon 3 duplication, and two healthy females and one male. Standards (1.25, 2.5, and 5 ng/µl) were prepared by dilution of a healthy female genomic DNA. All dilutions were prepared in a volume of 200 µl.

4.1.10.2. Quantitative Real Time PCR Conditions. The real time PCR was performed in a total volume of 20 µl, containing 10 µl 2X SYBR Green PCR Master Mix (TaKaRa, Japan), 1 µl of each primer per reaction, 4 µl of the genomic DNA dilution and distilled water. The PCR protocol on Light Cycler (LC) (Roche Diagnostics, Mannheim, Germany) was as follows: an initial denaturation step (95°C for 2 min) followed by amplification and quantification steps repeated for 40-50 cycles (95°C for 5 sec, 59°C for 10 sec, 72°C for 20 sec, with a single fluorescence measurement at the end of the elongation step at 72°C), a melting curve program (65–98°C with a heating rate of 0.2°C per second and a continuous fluorescence measurement) and terminated by cooling to 40°C. Each sample was amplified with the MeCP2 and reference gene primer pairs. The coding exon 3 of the MeCP2 was

amplified using the following primers designed by Bienvenu *et al*. (2000); Rett_exon3F: gtgatacttacatacttgtt; Rett_exon3R: ggctcagcagagtggtgggc. The reference NDRG1 gene was amplified using primers NDRG1_exon7F: aggctcccgtcactctg; NDRG1_exon7R: gtcttccttcatcttaaaatg (Kalaydjieva *et al*., 2000).

Each target and reference gene assay included: 1) a standard curve of three dilution points of healthy female DNA (20, 10, and 5 ng), 2) 20 ng of calibrator healthy female DNA, and 3) test sample DNAs. Melting point analysis was conducted on all PCR products to check for any nonspecific amplicons.

4.1.10.3. Quantification. Quantification was performed using both the standard curve method and the comparative Ct method. Within each PCR batch three aliquots of wild type control DNA in decreasing concentrations (20, 10, and 5 ng) from a healthy female were included to construct a standard curve and the copy numbers of the exons in each sample were interpolated. Since two different standard curves were constructed for the target and reference genes, the copy numbers of MECP2 exon 3 were normalized against a calibrator DNA sample. After normalization to the calibrator, the copy number of MECP2 exon was calculated by dividing these normalized values by the copy number of the reference gene.

Instead of interpolating unknown samples from a standard curve, it is also possible to calculate the copy number based on the observed Ct values as follows:

$$2^{-\Delta\Delta CT} = (1+E)^{-\Delta C_{T\text{targetgene}} + \Delta C_{T\text{referencegene}}} \quad (4.1)$$

Where E is the efficiency of the PCR reaction (set at default value 0.95), $\Delta C_{T\text{targetgene}}$ is the difference in threshold cycle value between test sample and calibrator sample for the gene under investigation (test gene), and $\Delta C_{T\text{referencegene}}$ is the difference in threshold cycle value between test sample and calibrator sample for reference gene.

4.1.10.4. Statistical Analysis. The results were evaluated by a paired sample *t*-test and Pearson correlation coefficient using SPSS v 15.0 software (SPSS Inc., Chicago, IL, USA).

4.2. Methylation Analyses of the Putative Promoter Region of hHR23 Genes in Breast Tumor Tissues

4.2.1. Non-heating DNA Extraction Protocol

Genomic DNA was extracted from archival formalin-fixed, paraffin-embedded human primary breast tumors and normal breast tissues by using a modified version of non-heating DNA extraction protocol described by Shi *et al*. (2002). Two sections (10 µm thick) were obtained from each archival tissue. Sections were deparaffinized by adding 1 ml of xylene to the eppendorf tube for 30 min for two changes, followed by 100 per cent and 75 per cent ethanol for 15 min with three changes. After a washing step with PBS for 15 min in two changes, 500 µl of tissue lysis buffer was added and incubated at 50 ºC for 48-72 hours until the whole tissue were dissolved completely. The mixture was centrifuged at 13,000 rpm for 5 min and the supernatant fluid was transferred to a clean eppendorf tube. Five hundred µl of phenol:chloroform:isopropanol solution (25:24:1) was added, vortexed and centrifuged at 13,000 rpm for 10 min. The upper aqueous layer was carefully transferred to a clean tube, 0.1 volume of 3M sodium acetate and 1 volume of isopropanol were added, mixed by vortexing, and incubated at – 20 ºC for 10 min. The DNA was precipitated by centrifugation at 13,000 rpm at 4 ºC. The supernatant fluid was discarded and the precipitate washed once with 75 per cent ethanol. The DNA pellet was dissolved in 50 µl of distilled H_2O. The concentration of the isolated DNA was calculated after measuring the optical density at 260 nm on ND-1000 spectrophotometer (NanoDrop Technologies).

4.2.2. Promoter Region Analyses and Primer Design

The web-based PROSCAN program (Prestridge, 1995) was used to predict the putative eukaryotic Pol II promoter sequences in primary sequence data of hHR23A and hHR 23B genes. MATCH and PROSCAN programs were used to identify high scoring transcription factor (TF) binding sites. MethPrimer program (Li and Dahiya, 2002) was used to identify the CpG islands and design the primers using the standard criteria, i.e., sequence was considered as a CpG island if there was a minimum G+C content of 50 per

cent with a minimum CpG (obs)/CpG (exp) of 0.6 in a 200-bp window length, and the sequence length was at least 500-bp.

4.2.3. Bisulfite Modification

Genomic DNA was modified by Methylamp^{TM} DNA Modification Kit (Epigentek, NY, USA) according to the manufacturer's protocol. Briefly, 0.25-1 µg of DNA in a volume of 24 µl was denatured by adding 1 µl of denaturing buffer for 10 min at 37°C. Bisulfite-Conversion buffer (125 µl) was added and mixed, and samples were incubated at 65 °C for 2 h. Modified DNA samples were applied to columns, washed, and then eluted with 20 µl of elution buffer.

4.2.4. Amplification and Sequencing of the Bisulfite Modified DNA

Semi-nested PCR strategy was used to investigate the methylation status of the putative promoter region of hHR23 genes (Figure 4.2). Several primer combinations were used to get successful amplification product. The primer combinations were shown in Figure 4.2. In general, 2.5 µl of the modified DNA was used in subsequent PCR reactions. First-round PCR reactions were performed in a total volume of 25 µl containing 2.5 µl of modified DNA, 2.5 µl of 10X polymerase buffer, 2.5 mM $MgCl_2$, 2.5 µl of dimethyl sulfoxide (DMSO), 200 µM dNTPs, 0.4 µM of each primer, and 2 U of Taq polymerase (Fermentas). The following PCR program was used: 94ºC for 4 min, followed by 40 cycles of 45 sec at 94 ºC, 45 sec at annealing temperature, 1 min at 72ºC, and a final extension step of 8 min at 72ºC. One micro liter of the first-round PCR product was then used as a template in the second round of PCR with a mixture that contains 2.5 µl of 10X polymerase buffer, 2.0 mM MgCl2, 200 µM dNTPs, 0.4 µM of each primer, and 1 U of Taq polymerase (Fermentas). The cycling condition was as follow: denaturation at 94°C for 5 min was followed by 35 cycles of amplification: 94°C for 30 sec, 30 sec at annealing temperature, and extension at 72°C for 30 sec. After the last cycle, an 8-min extension at 72°C was performed.

Five µl from the PCR product was run on two per cent agarose gel to check for the quality of amplification. PCR products were purified using QIAQuick PCR purification kit

(QIAGEN) and sequenced with automated sequencer ABI 3130 PRISM (Applied Biosystems) in Burç Laboratory (Istanbul, Turkey).

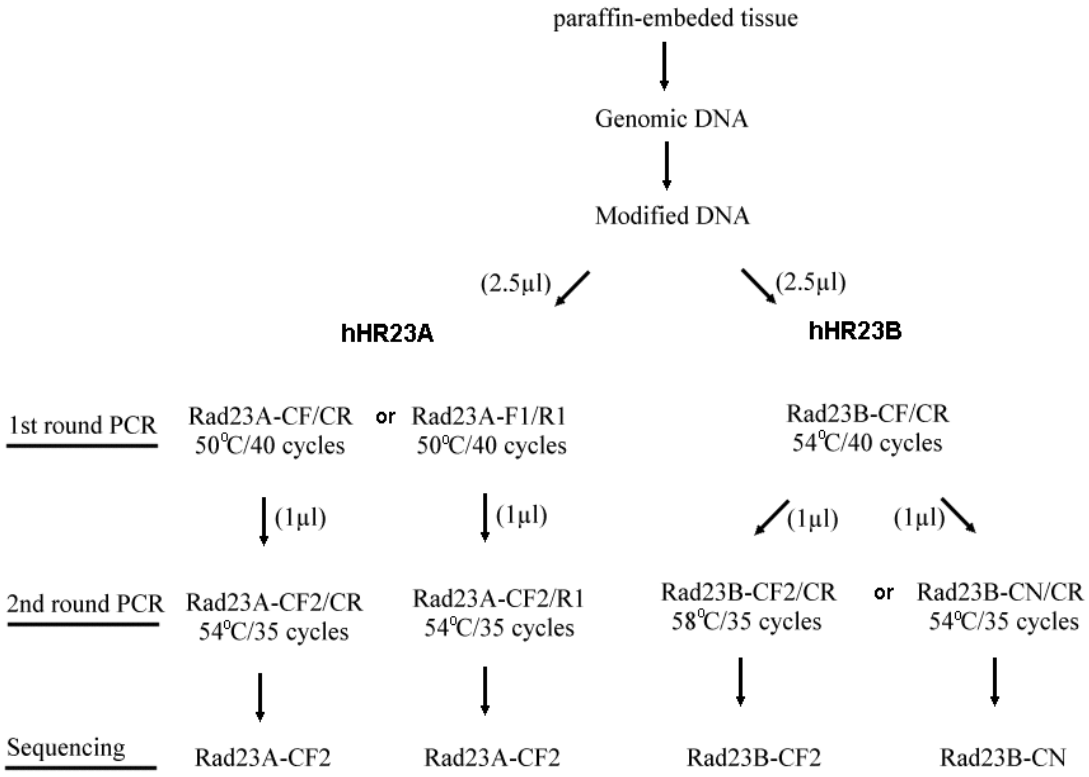

Figure 4.2. Semi-nested PCR strategy showing the primers and PCR cycling conditions used to investigate the methylation status of hHR23 genes.

4.3. Molecular Basis of Congenital Hypothyroidism (CH)

4.3.1. Mutation Analysis of the TTF2 Gene

Genomic DNA was isolated from peripheral blood sample of the patient with CH, her consanguineous parents and unaffected brother using salting out method as described in section 4.1.1.

4.3.1.1. Direct DNA Sequencing Analysis. The entire coding region of TTF2 gene (accession no. NM_004473) was amplified in two overlapping fragments using the primers

designed by Castanet *et al* (2002). PCR reaction was performed in a total volume of 25 µl containing approximately 100 ng DNA, 2.5 µl of 10X polymerase buffer, 2.0 mM MgCl2, 10 per cent dimethyl sulfoxide (DMSO), 200 µM dNTPs, 0.4 µM of each primer, and 1 U of Taq polymerase (Fermentas,). The following PCR program was used: 94ºC for 4 min, followed by 35 cycles of 45 sec at 94 ºC, 30 sec at annealing temperature (58ºC for TTF2A-D, 53ºC for TTF2C-E), 1 min at 72ºC, and a final extension step of 8 min at 72ºC (Table 1.1.1). The PCR products were purified and bi-directionally sequenced using the primers TTF2A and TTF2C as described in section 4.1.4.

4.3.1.2. *AlwN*I Digestion. The PCR products from the patient, her parents, unaffected brother and 100 control chromosomes were subjected to *AlwN*I digestion. Genomic DNA was amplified using the primers TTF2C/TTF2E as described in section 4.2.1.1. A total of ten µl of the PCR product was digested with 3U of *AlwN*I restriction enzyme (Fermentas) and 2 µl of 10X reaction buffer in a 20 µl reaction volume. The mixture was incubated at 37 ºC for 4 hours. The digested products were electrophoresed on two per cent agarose gel at 100 V for 30 min. The c. 304 C>T (p.R102C) mutation creates a new restriction site resulting in 72 bp and 599 bp fragments whereas wild type allele remains undigested.

4.3.2. Functional Characterization of p.R102C Mutant TTF2

Functional analyses were performed by Dr. Chatterjee's laboratory in University of Cambridge, UK. The DNA binding and transcriptional properties of the mutant and wild type TTF2 have been investigated as described by Clifton-Bligh *et al.* (1998). Detailed information was given in Appendix A.

4.3.3. Mutation Analysis of Butyrylcholinesterase (BChE) Gene

The DNA samples of the patient with CH and her family members were analyzed for the presence of two most common BChE variants; p.Asp70Gly (A-variant) and p.Ala539Thr (K-variant) according to Asanuma *et al*. (1999) and Maekawa *et al*. (1995), respectively. PCR reaction was performed in a total volume of 25 µl containing approximately 100 ng DNA, 2.5 µl of 10X polymerase buffer, 2.0 mmol/l $MgCl_2$, 0.2 mmol/L dNTPs, 0.4 µmol/l of each primer, and 1 U of *Taq* polymerase (MBI Fermentas).

The PCR program on Icycler™ thermal cycler was as follows: an initial denaturation step at 94 ºC for 4 min, followed by 33 cycles of 30 sec at 94 ºC, 30 sec at annealing temperature (52 ºC for M6/M115, 60 ºC for AP5/C539), 30 sec at 72 ºC, and a final extension step of 8 min at 72 ºC.

The 373 bp region containing the p.Asp70Gly mutation site was amplified using the primers M6/M115 and digested with the 3U of the *Sau3A*I restriction enzyme (MBI Fermentas). The PCR product was digested to 214 and 135 bp fragments from the wild type allele and remained undigested from the mutant allele. Similarly, 103 bp product harboring the p.Ala539Thr mutation site was amplified using primers AP5/C539. The mutation abolishes *Alu*I restriction recognition site resulting in an undigested 103 bp product for mutant allele whereas wild type allele digested into two fragments of 83 and 20 bp. The digested products were electrophoresed on three per cent agarose gels at 100 V for 30 min. The fragments were visualized by ethidium bromide staining under UV light.

5. RESULTS

5.1. Molecular Basis of Rett Syndrome

5.1.1. Patients

The molecular basis of Rett Syndrome (RTT) in our population was investigated in a total of 71 isolated RTT cases (68 female and 3 male). A detailed clinical data were available for 47 patients (44 females and 3 males). Huppke clinical scoring (Huppke *et al*., 2003) was also available for 33 of these cases. The clinical features of these patients analyzed in this study are summarized in Table 5.1. Twenty-four female patients had been referred to our laboratory for differential diagnosis but the clinical data were not available. All patients were screened for MECP2 gene mutations but quantitative PCR and XCI analyses were performed only for the first group of 47 patients.

5.1.2. Mutation Analysis of MECP2 Gene

All patients were initially screened for the six recurrent *MECP2* mutations (p.R106W, p.T158M, p.R168X, p.R255X, p.R270X, and p.R306C) since these mutations are known to account for up to two thirds of pathogenic mutations in RTT cases (RettBASE). The PCR-RFLP based analyses detected mutation in 15 patients: four patients (R6, R18, R22, and R28) with p.R106W, three patients (R25, R29, and R47) with p.T158M, two patients (R15 and R17) with p.R168X, four patients (R9, R13, R24, and R39) with p.R255X, patient R34 with p.R270X, and patient R16 with p.R306C mutation (Figure 5.1). Patients tested negative for the recurrent mutations were further analyzed for the four coding exons of the MECP2 gene using SSCP analysis. Subsequent DNA sequencing of patients showing altered SSCP pattern revealed ten different pathogenic mutations: c.1156-1192del36 (p.Leu386Hisdel12), c.856delA (p.Leu286fsX288), c.397C>T (p.Arg133Cys), c.1034_1042insGCGGATTGC (p.Lys345fs), c.455C>G (p.Pro152Arg), c.964C>G (p.Pro322Ala), c.880C>T (p.Arg294X), c.744delG (p.Ser194fsX208), and c.826-829delGTGG (p.Val276fsX288) mutations in R2 and R42, R3, R4, R8, R18, R31, R36, R46, and R49, respectively.

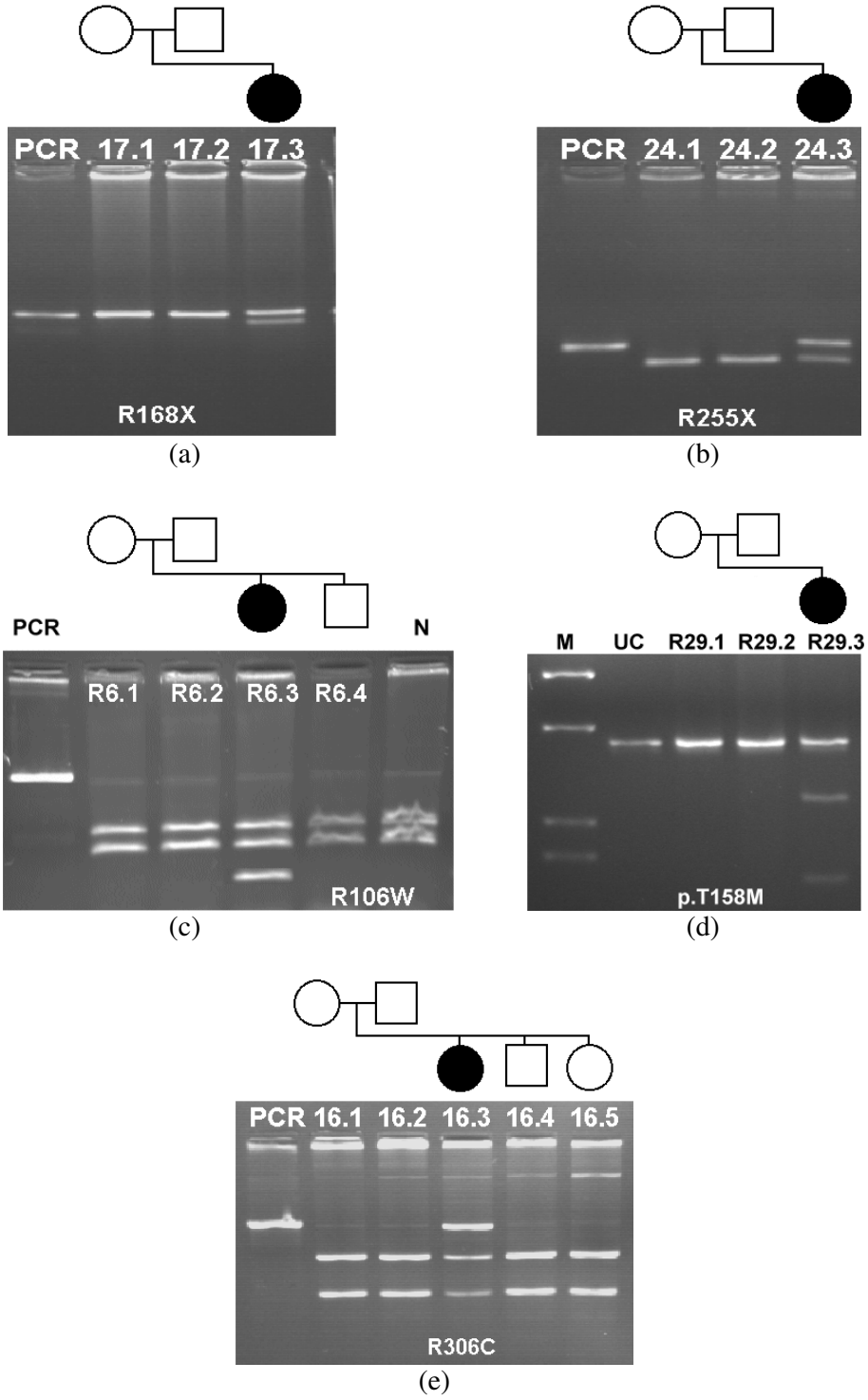

Figure 5.1. PCR-RFLP analysis for the detection of the common *MECP2* mutations in patients R17 (a), R24 (b), R6 (c), R29 (d), and R16 (e).

The molecular analysis revealed 18 different *MECP2* mutations in 30 of 44 (68.2 per cent) female patients in the first group of classical/atypical RTT cases with detailed clinical data (Figure 5.2). Of the 30 patients with mutations, 10 had a missense, eight had a nonsense mutation, six had small nucleotide deletion/insertions. The p.R255X and p. R106W were the most common mutations with an equal frequency of 8.9 per cent in our cohort of patients. Five mutations were novel to this study: p.Ser194fsX208 (c.744delG), p.Val276fsX288 (c.826-829delGTGG), p.Leu286fsX288 (c.856delA), p.Leu386Hisdel12 (c.1156-1192del36) and p.Lys345fs (c.1034_1042insGCGGATTGC) (Figure 5.3 and 5.4). Eighty percent (20 of 25) of the small deletion/insertion or point mutations were detected in the exon 4 of the MECP2 gene. The rest of the mutations (20 per cent) were located within exon 3. Exons 1 and 2 were free of sequence variations. All patients reported were heterozygous for the identified mutations except patient R18 that was found to be a compound heterozygote for p.R106W and p.P152R mutations. All available family members were tested negative for the identified variations implicating *de novo* nature of the mutations. MECP2 gene mutations could not be identified in any of the three male patients.

MECP2 mutations could be detected in three of the 24 patients in the second group that were referred for differential diagnosis. One of these mutations was a complex small insertion in patient R60 and the others were p.R106W and p.R255X identified in patients R68 and R69, respectively.

5.1.3. Quantitative PCR Analyses

We have developed a quantitative real time PCR strategy to screen for *MECP2* exon rearrangements in 23 samples (20 females and 3 males) that were negative for *MECP2* point mutations. Each sample was amplified with the MECP2 and reference NDRG1 gene primer pairs. The amplification products were analyzed using the Light Cycler analysis software (version 4.0) (Figure 5.5). Using the Fit Points Method, the DNA was quantified relative to the standard curve for each exon. Subsequently, the ratios between target (*MECP2*) and reference (*NDRG1*) exon were calculated for each test person.

The observed mean ratios are 0.52±0.12 for deletion carriers (expected value: 0.5) and 1.56±0.18 for duplication carriers (expected value: 1.5) vs. 1.022±0.17 for control individual (expected value: 1.0). *MECP2* exon rearrangements were identified in seven female patients; four with exon 2-4 duplications (R14, R19, R20, and R33), one with exon 3 deletion (R23), one with exon 4 deletion (R30), and one with exon 3-4 deletions (R5) (Table 5.2, Figure 5.6).

QF-PCR assay was used to verify the results obtained by quantitative real time PCR analysis (Figure 5.7). The observed ratios of *MECP2* exon 3/*PRNP* exon 2 were 1.02±0.09, 0.47±0.04, and 1.69±0.21 for the control individuals, exon 3 deletion carriers and exon 3 duplication carriers, respectively (Table 5.2, Figure 5.6). QF-PCR confirmed the presence of exon rearrangements except the MECP2 gene duplication observed in patient R33 (Figure 5.8).

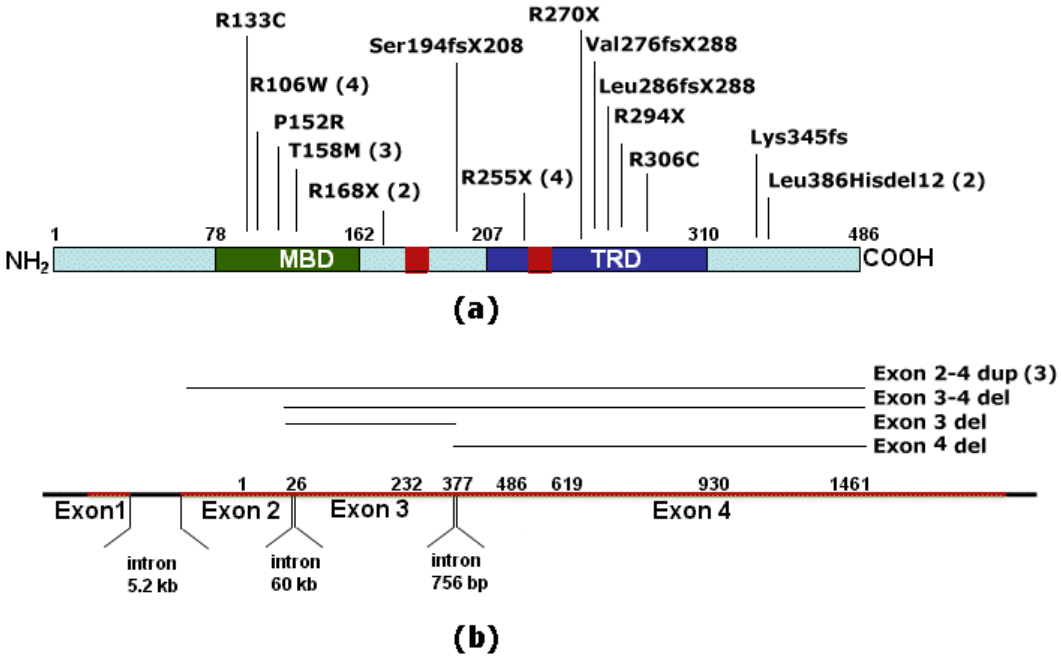

Figure 5.2. Schematic representation of the MeCP2 (a) and MECP2 gene (b) showing the position of the mutations identified in this study. Numbers in brackets represent the number of the patients with the same mutation.

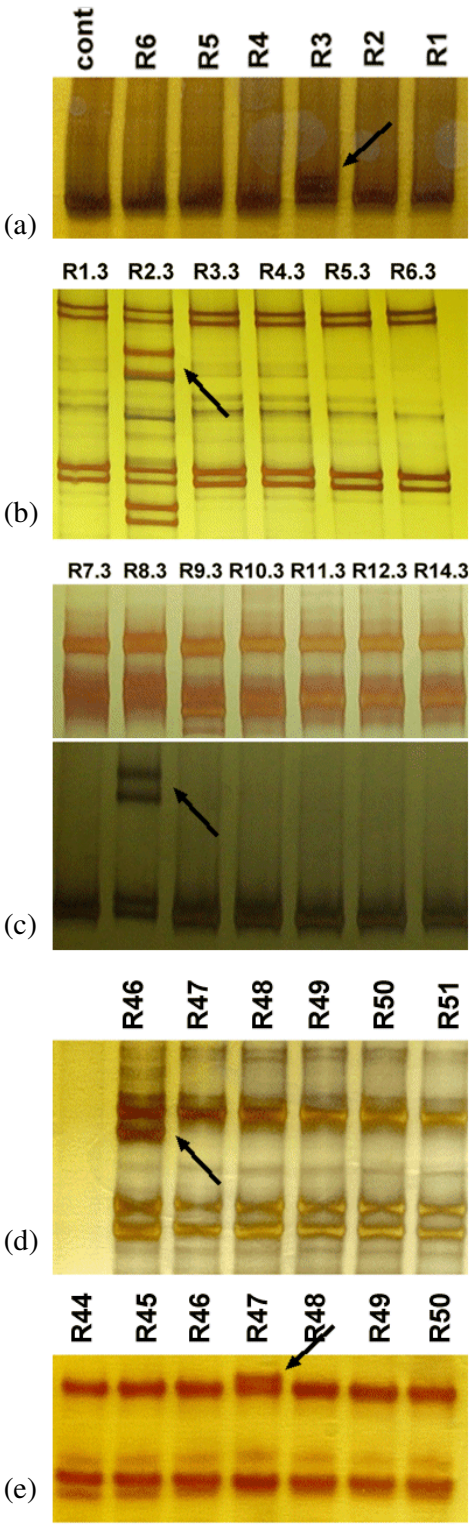

Figure 5.3. SSCP gels showing altered migration patterns for patients R3 (a), R2 (b), R8 (c), R46 (d), and R47 (e) with novel MECP2 gene mutations.

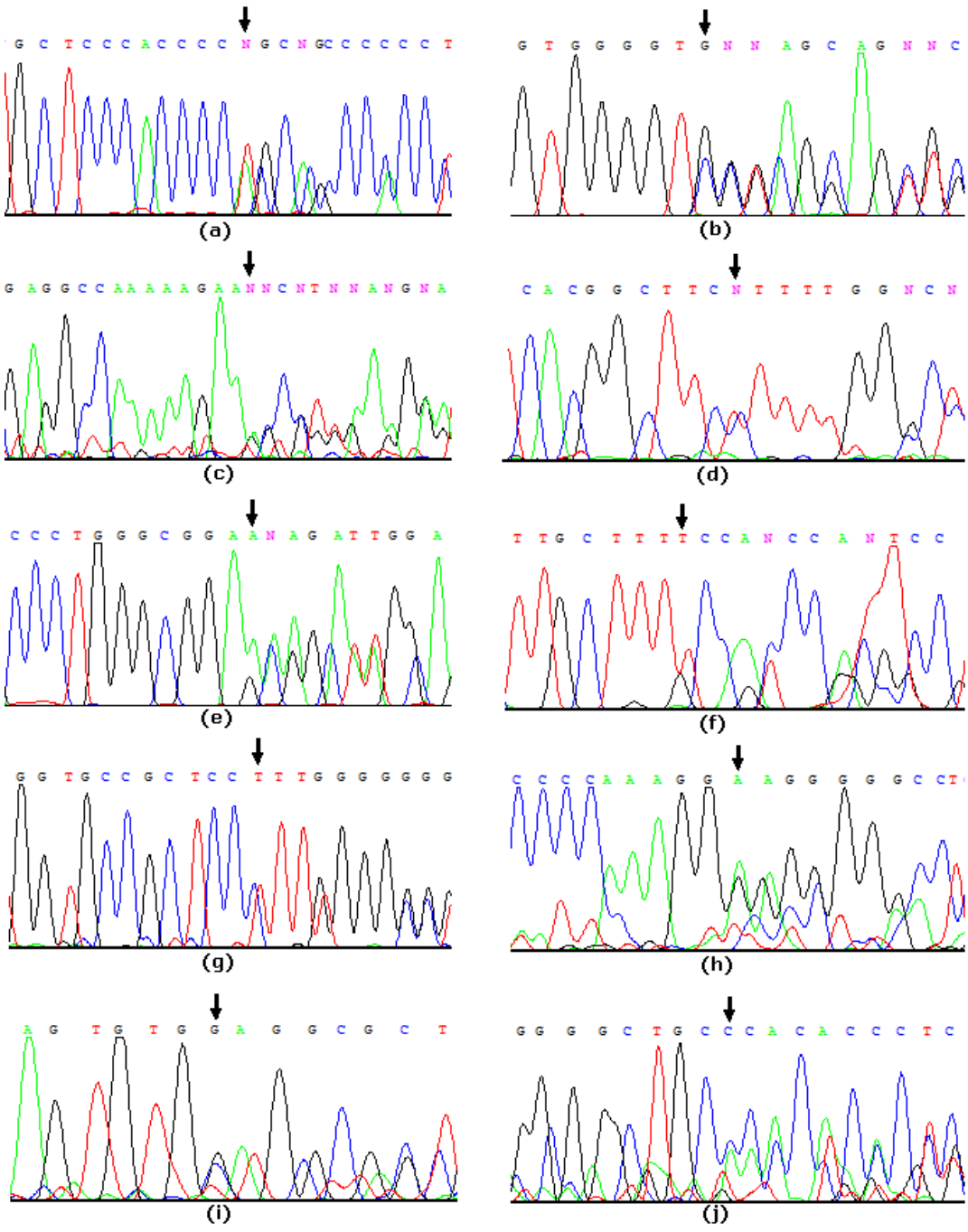

Figure 5.4. Chromatograms showing sequencing profiles of sense (left panel) and antisense (right panel) strands of MECP2 gene for the novel mutations identified in the present study. (a, b) Patient R2 with c.1156-1192del36; (c, d) patient R3 with c.856delA; (e, f) patient R8 with c.1034_1042insGCGGATTGC; (g, h) patient R46 with c.744delG; and (i, j) patient R47 with c.826-829delGTGG. Arrows show the site of the mutations.

Table 5.1. The age, gender, and clinical and genetic features of the first group of 47 patients.

No	Age	RTT type	Mutation	XCI Pattern	Hand Fnc.	Eye Fnc	Gait Fnc	total	Breath. Abnormality	Epilepsy (age at first seizure)	Normal Develop. Period	Scoliosis	Huppke Clinical score
R1	11	Male	-	-	2	3	1	6					
R2	8	Classic	Leu386Hisdel12	SKEWED	3	3	1	7	-	+ (3.5 years)	18 months	+	9
R3	4	Classic	Leu286fsX288	SKEWED	3	3	3	9	-	+ (1 years)	6 months	+	10
R4	4	Classic	R133C	Random	3	3	2	8	+	+ (6 years)	18 months	-	11
R5	13	Classic	exon 3-4 deletion	NI	3	3	3	9	+	+ (1 years)	12months	+	11
R6	7	Classic	R106W	NI	2	2	1	5	-	+ (4 years)	18 months	+	8
R7	16	Forme fruste	-	SKEWED	1	2	1	4	+	+ (7 years)	12 months	+	6
R8	9	Classic	Lys345fs	SKEWED	2	2	3	7	+	+ (5 years)	ND	+	11
R9	13	Classic	R255X	Random	2	2	3	7	+	+ (2 years)	ND	-	10
R10	12	Classic	-	Random	2	3	1	6	+	-	18 months	-	12
R11	13	Early seizure	-	SKEWED	2	3	1	6	+	+ (3 months)	6 months	-	9
R12	8	-	-	Random	3	3	3	9	ND	ND	ND	ND	ND
R13	9	-	R255X	SKEWED	3	2	3	8	ND	ND	ND	ND	ND
R14	7	Early seizure	Exon2-4 duplication	Random	2	3	3	8	-	+ (2 months)	7 months	-	8
R15	13	-	R168X	SKEWED	3	3	2	8	+	+ (8 months)	8 months	-	9
R16	20	Classic	R306C	SKEWED	2	2	1	5	-	+ (17 years)	18 months	+	10
R17	6	Classic	R168X	Random	3	3	2	8	-	+ (1 years)	6 months	-	11
R18	6	Classic	R106W-P152R	NI	3	2	1	6	+	-	15 months	-	9
R19	7	Early seizure	Exon2-4 duplication	Random	2	3	3	8	-	+ (2 months)	9 months	-	7
R20	10	Congenital	Exon2-4 duplication	SKEWED	2	3	1	6	+	+ (6 years)	absent	+	5
R21	11	Male	-	-	3	3	1	7					
R22	9	Forme fruste	R106W	Random	1	2	1	4	-	-	18 months	-	6
R23	8	Classic	exon 3 deletion	Random	3	2	3	8	+	+ (3.5 years)	18 months	+	11
R24	4	-	R255X	NI	2	2	3	7	ND	ND	ND	ND	ND
R25	7	-	T158M	Random	3	2	3	8	ND	ND	ND	ND	ND

Table 5.1. The age, gender, and clinical and genetic features of the first group of 47 patients (continued).

No	Age	RTT type	Mutation	XCI Pattern	Hand Fnc.	Eye Fnc	Gait Fnc	total	Breath. Abnormality	Epilepsy (age at first seizure)	Normal Develop. Period	Scoliosis	Huppke Clinical score
R26	9	Classic	-	Random	2	3	2	7	+	+ (8 years)	10 months	-	9
R28	7	-	R106W	Random	3	2	3	8	ND	ND	ND	ND	ND
R29	6	Classic	T158M	Random	2	3	3	8	+	+ (2.5 years)	6 months	-	12
R30	4	Classic	exon 4 deletion	Random	2	3	3	8	-	-	6 months	-	10
R31	9	Classic	P322A	Random	2	2	3	7		-(subclincal discharges)	18 months	-	12
R33	8	Hanefeld	**Exon2-4 duplication?	SKEWED	3	3	2	8	+	+ (neonatal)	12 months	-	6
R34	13	-	R270X	SKEWED	3	3	3	9	ND	ND	ND	ND	ND
R35	6	Hanefeld	-	Random	3	3	3	9	ND	ND	ND	ND	ND
R36	5	-	R294X	Random	3	3	3	9	ND	ND	ND	ND	ND
R37	12	Male+	-		2	3	1	6	-	-	ND	-	9-10
R39		-	R255X	SKEWED					ND	ND	ND	ND	ND
R40	15	-	-	Random					ND	ND	ND	ND	ND
R41	7	variant	-	Random	1	1	1	3	-	+ (9 months)	12 months	-	8
R42	7	variant	Leu386Hisdel12	NI	2	3	1	6	+	no but EEG abnormality	ND	ND	8
R43	4	Hanefeld	-	Random	2	2	3	7	-	-	ND	-	7
R44	5	Hanefeld	-	Random	3	3	3	9	+	+ (6 months)	6 months	-	9
R45	5	-	-	SKEWED	2	2	3	7	ND	ND	ND	ND	ND
R46	4	-	Ser194fsX208	SKEWED	3	2	3	8	ND	ND	ND	ND	ND
R47	4	Classic	Val276fsX288	SKEWED	3	2	3	8	+	+ (2.5 years)	9 months	+	12
R48		Hanefeld	-	Random					ND	ND	ND	ND	ND
R49		-	T158M	NI					ND	ND	ND	ND	11
R50		-	-	Random					ND	ND	ND	ND	ND

*ND: no data; NI: not-informative; **The duplication identified in this patient by Real Time PCR could not be reproduced with QF-PCR

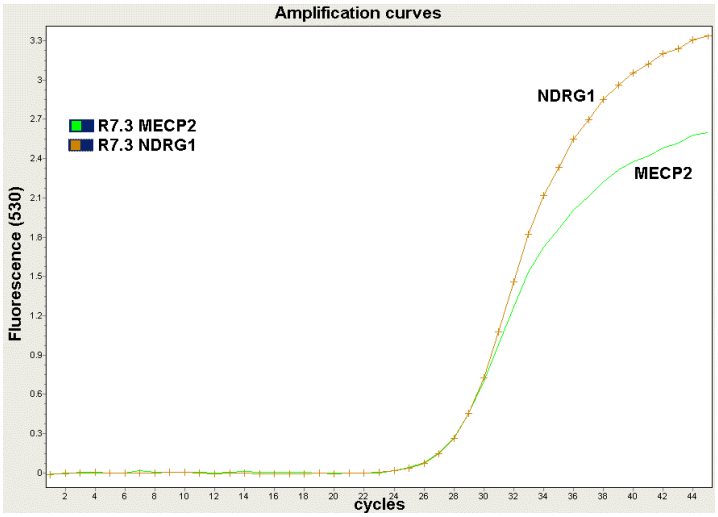

(a)

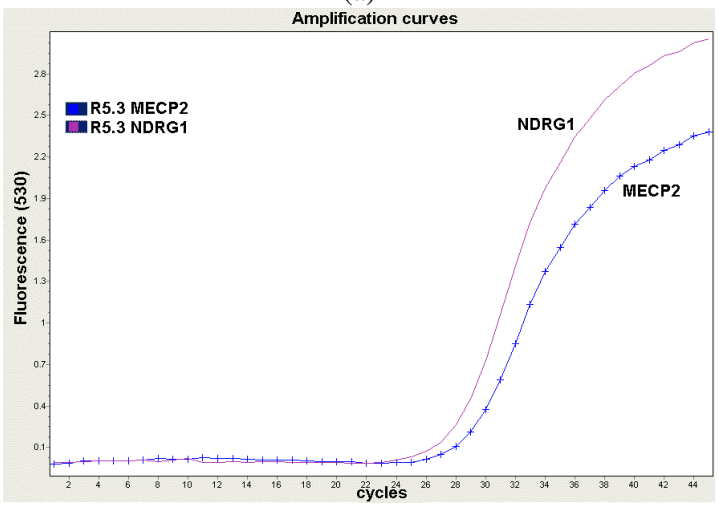

(b)

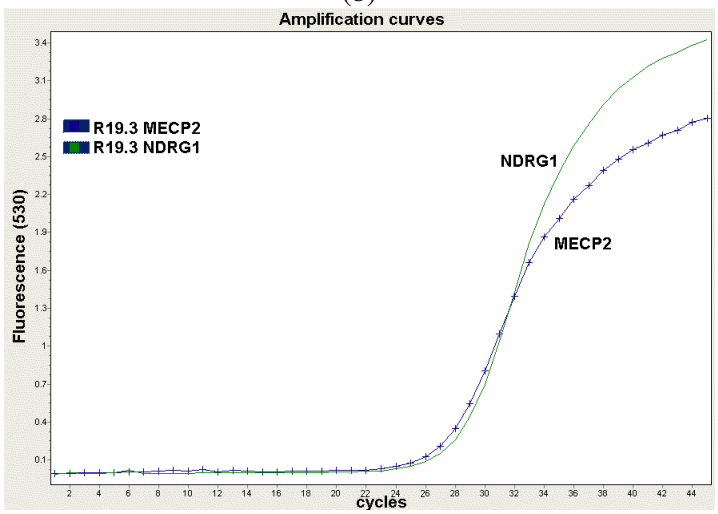

(c)

Figure 5.5. A representative Real Time analysis for a healthy female (a), R5 with exon 3 deletion (b), and R19 with exon 3 duplication (c), respectively.

Table 5.2. Quantitative Real Time PCR and QF-PCR analyses result.

	Quantitative Real Time PCR		QF-PCR
Samples	Exon 3 (MECP2/NDRG1)	Exon 4 (MECP2/NDRG1)	Exon 3 (MECP2/PRNP)
male control	0.51 ±0.05	0.49 ±0.09	0.46 ±0.09
female control	0.99 ±0.07	1.01 ±0.08	1.02 ±0.09
R1 (male)	0.53	0.63	-
R21 (male)	0.51	0.53	-
R37 (male)	0.53	0.53	-
R5	0.50	0.54	0.50
R23	0.46	1.04	0.51
R30	0.95	0.63	1.18
R7	0.98	1.06	0.95
R10	0.88	1.09	1.10
R11	1.00	1.14	0.80
R12	0.87	1.05	1.04
R26	1.02	1.02	1.05
R32	0.91	1.02	0.95
R35	1.10	1.13	0.81
R40	0.77	0.76	0.96
R41	0.87	0.95	0.93
R43	0.85	0.96	1.08
R44	0.85	0.8	0.92
R45	1.00	0.95	0.88
R48	1.00	0.94	1.00
R50	0.83	0.83	1.00
R14	1.44	1.35	1.40
R19	1.85	1.62	1.74
R20	1.41	1.38	1.40
R33	1.45	1.33	0.98

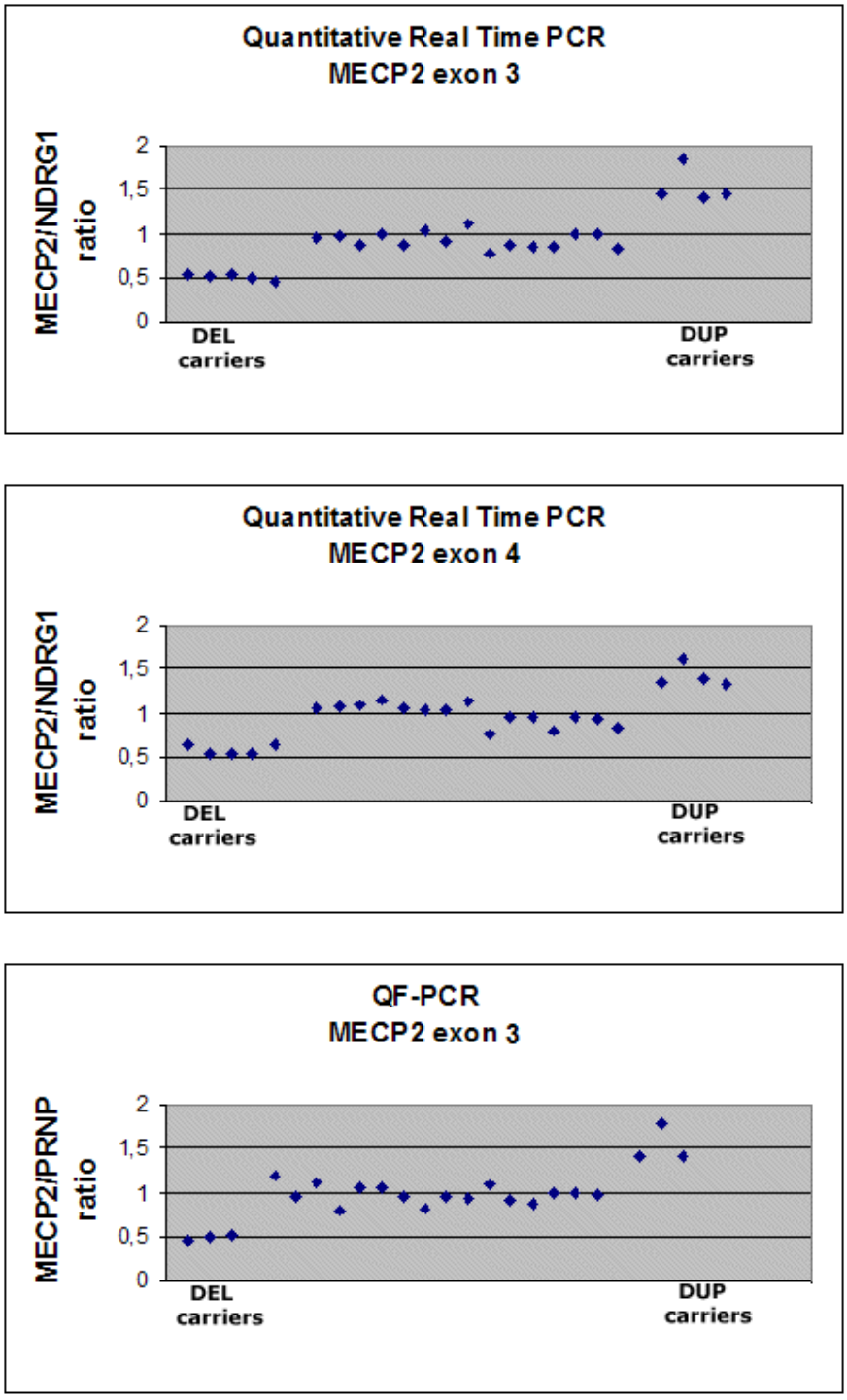

Figure 5.6. The plots of quantitative Real Time PCR and QF-PCR analyses results.

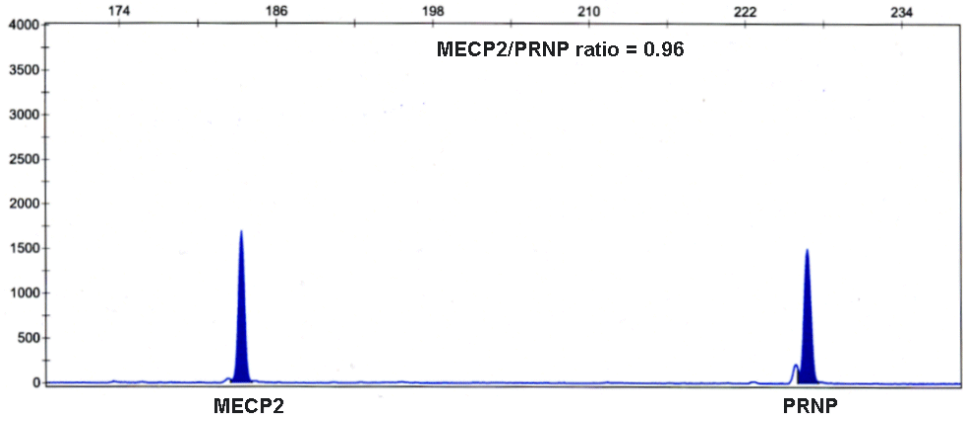

(a)

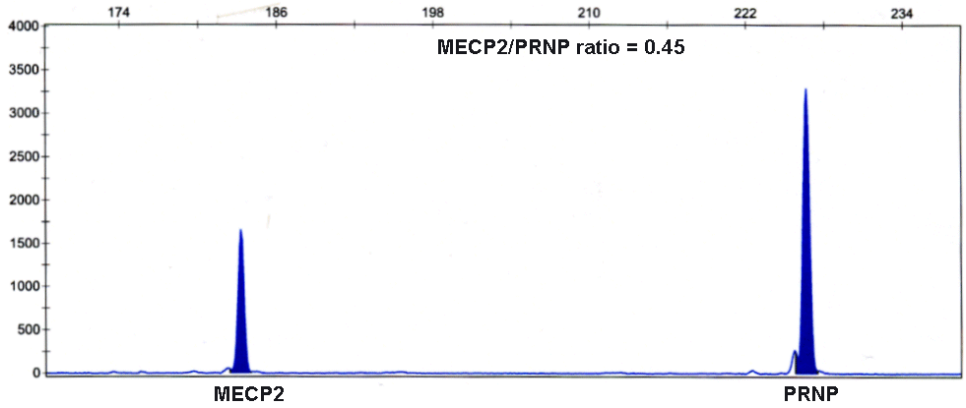

(b)

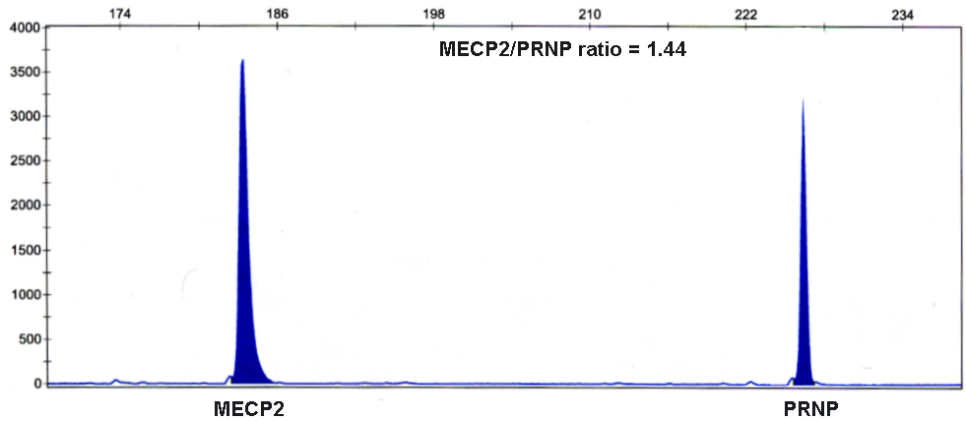

(c)

Figure 5.7. A representative QF-PCR analysis for a healthy female (a), R5 with exon 3 deletion (b), and R19 with exon 3 duplication (c), respectively.

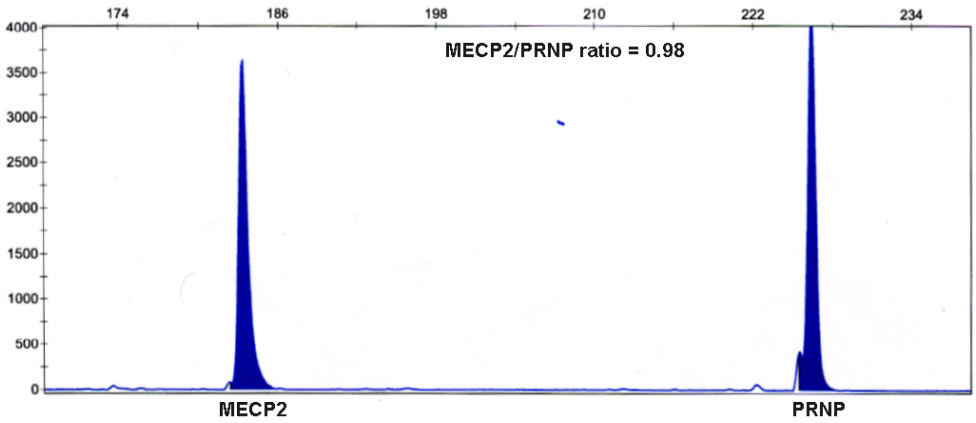

Figure 5.8. QF-PCR analysis of patient R33.

5.1.4. X Chromosome Inactivation Status

X chromosome inactivation analysis was performed for 44 female patients; however, the status of six patients (13.6 per cent) could not be identified because of homozygousity for both *AR* and *ZNF261* loci. X-inactivation was random in 23 (61.5 per cent) and skewed in 15 (39.5 per cent) of 38 informative patients (Table 5.1). The paternal X chromosome was active in one patient and eight patients showed preferential activation of the maternal X chromosome. The origin of the active allele could not be determined in six patients because of unavailability of the maternal sample. A representative XCI analysis of patients with skewed, random, and non-informative XCI status is shown in Figure 5.9.

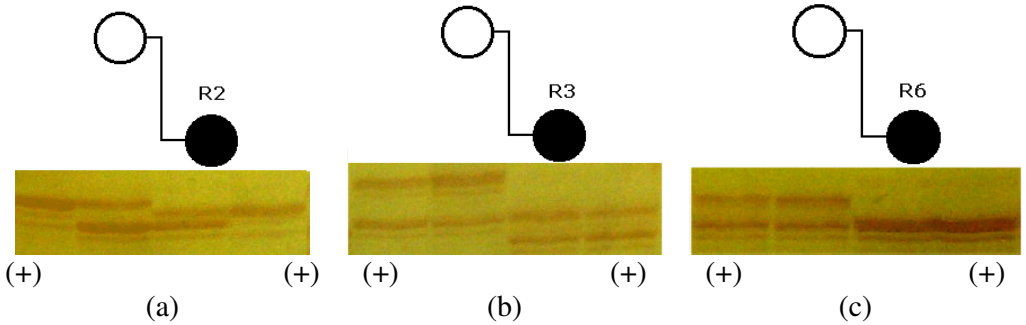

Figure 5.9. X chromosome inactivation analysis of patients with skewed (a), random (b), and non-informative (c) XCI pattern, respectively. (+) represents the PCR products from HhaI digested DNA.

5.1.5. Genotype–Phenotype Correlations

The clinical severity scores of the patients were given in Table 5.1. High scores (maximum score 9) indicate more severe disease phenotype. A statistically significant correlation could not be identified between the mean severity score of patients and the presence, type and location of mutation, and the XCI pattern (Table 5.3). However, the patients with exon deletions were found to have higher clinical severity scores than all other mutation-positive patients (8.33±0.58 vs 6.70±1.57, p=0.066). When site of mutation is considered alone, we observed that the patients with affected TRD domain had more severe phenotype than the patients with affected MBD domain (7.80±1.23 vs 6.88±1.64, respectively). Mutation negative patients and patients with skewed XCI patterns had slightly milder phenotypes when compared to mutation positive patients and patients with random XCI, respectively.

When we performed statistical analysis of severity scores for specific clinical features, we obtained a significant difference in the fields of ‘‘gait function’’ and “eye contact”. None of the patients with *MECP2* exon deletions have ever walked (p=0.019). Eye contact is very difficult to obtain in patients with exon duplications when compared to that of patients with missense mutation (p=0.016). Although the differences were not significant, mutation positive patients had severe problems in their ability in purposeful hand movement and walking skills when compared to mutation negative patients.

5.1.6. Prenatal Diagnosis

Upon request, prenatal diagnosis was performed in the families of the patient R29 with p.T158M, patient R42 with p.L386Hdel12, and patient R69 with p.R255X mutations. Chorionic biopsy specimens were tested and found to be negative for index patient’s mutation (Figure 5.10).

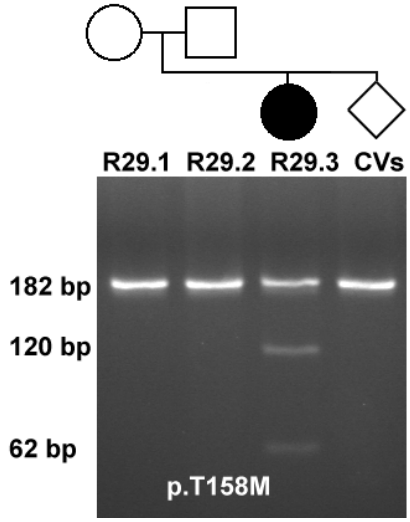

(a)

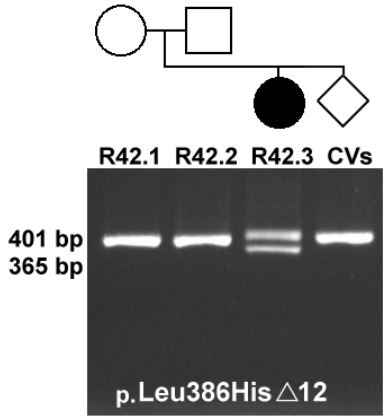

(b)

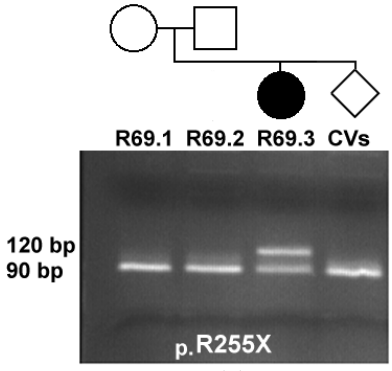

(c)

Figure 5.10. Agarose gel electrophoresis showing the prenatal diagnosis performed in the families of the patient R29 with p.T158M (a), patient R42 with p.L386Hdel12 (b), and patient R69 with p.R255X mutations (c).

Table 5.3. Mean Phenotypic Severity Scores of female patients of first group.

	Mutation		mutation type				affected MECP2 domain			XCI status	
Severity score	present	absent	missense	nonsense	exon-del	exon-dup	MBD	TRD	WDR	random	Skewed
Hand	2.50 (±0.58)	2.18 (±0.75)	2.40 (±0.70)	2.70 (±0.48)	2.67 (±0.58)	2.00 (±0.00)	2.50 (±0.76)	2.70 (±0.48)	2.33 (±0.58)	2.35 (±0.67)	2.50 (±0.65)
Eye	2.50 (±0.51)	2.55 (±0.69)	2.20 (±0.42)	2.50 (±0.53)	2.67 (±0.58)	3.00* (±0.00)	2.25 (±0.46)	2.50 (±0.53)	2.67 (±0.58)	2.55 (±0.61)	2.50 (±0.52)
Gait	2.39 (±0.88)	2.09 (±0.94)	2.10 (±0.99)	2.80 (±0.42)	3.00** (±0.00)	2.33 (±1.55)	2.13 (±0.99)	2.60 (±0.70)	1.67 (±1.16)	2.55 (±0.76)	2.14 (±0.95)
Combined	7.39 (±1.29)	6.83 (±1.99)	6.70 (±1.57)	8.00 (±0.82)	8.33*** (±0.58)	7.33 (±1.16)	6.88 (±1.64)	7.80 (±1.23)	6.67 (±0.58)	7.45 (±1.57)	7.14 (±1.46)

* (P=0.016); **(p=0.019); *** (p=0.066)

5.1.7. Multiplexed ARMS-PCR Approach for the Detection of Common *MECP2* Mutations

In the present study, we have established a multiplex multiplex amplification refractory mutation system (ARMS) - PCR assay to detect the seven common *MECP2* mutations p.R106W, p.R133C, p.T158M, p.R168X, p.R255X, p.R270X, p.R294X, and p.R306C. Each primer set was tested and optimized using mutation positive DNA samples, and then multiplexed (Figure 5.11). A representative multiplex ARMS-PCR assay analysis is shown in Figure 5.12.

5.1.7.1. Assay optimization. Several factors, including the concentration of primers, $MgCl_2$ and Taq polymerase, and PCR cycling conditions that can affect PCR specificity and efficiency were optimized. The concentration of Taq polymerase and $MgCl_2$ both had pronounced effects on the specificity and relative yield of the PCR products. Although high $MgCl_2$ concentration increased the intensity of our desired bands, it resulted in non-specific backgrounds. The optimum amount of $MgCl_2$ was found to be 2.5 mM to ensure specificity of the multiplex PCR assay. A range of Taq polymerase concentration was also tested and PCR specificity was found to be highest with 1.5 U of Taq Polymerase. To improve the specificity and the sensitivity of the amplification, we have used a touchdown PCR strategy with stepwise decrease of the annealing temperature from 63 to 59 C. Different concentrations for each set of primers were tested until maximum sensitivity and specificity were obtained (Table 4.3).

5.1.7.2. Validation of the assay. To evaluate the assay, we tested 14 patients with RTT for whom we had previously determined the genotypes by PCR followed by restriction enzyme digestion or DNA sequencing. We observed complete concordance between the traditional and Multiplex-ARMS methods (Figure 5.13).

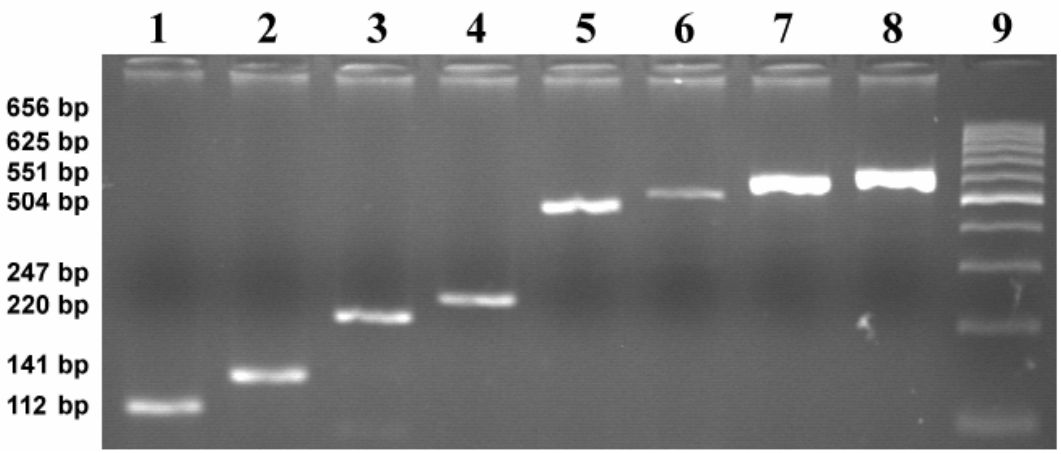

Figure 5.11. Agarose gel electrophoresis of the multiplex ARMS PCR assay products. Each mutant ARMS primer was evaluated with corresponding mutation positive DNA samples. Lane 1-8: Allele specific amplification of mutations p.R106W, p.R133C, p.T158M, p.R168X, p.R255X, p.R270X, p.R294X, and p.R306C, respectively. Lane 9: 100 bp DNA ladder (MBI Fermentas). An aliquot of 10 µl of each PCR product was loaded onto the gel.

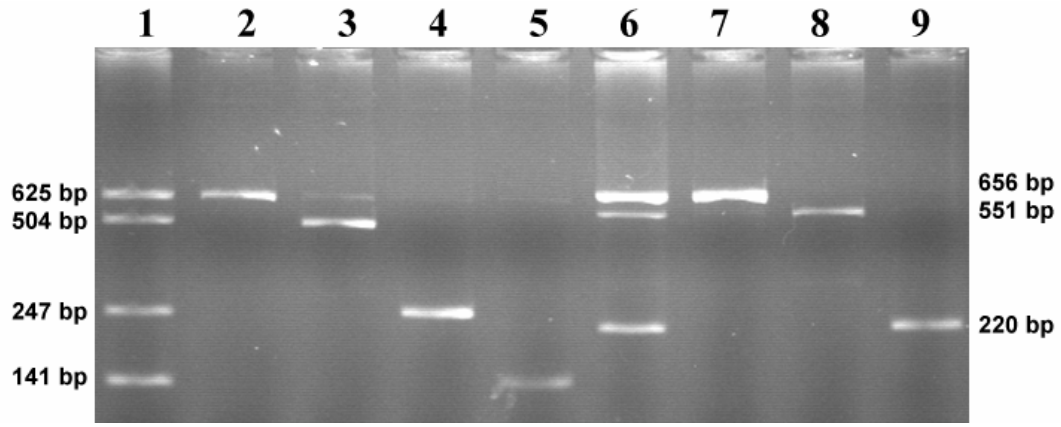

Figure 5.12. A representative multiplex ARMS-PCR assay analysis. Lane 1: PCR with wild-type primers of Panel 1; Lane 2-5: PCR with mutant primers of Panel 1 using samples with p.R294X, p.R255X, p.R168X, and p.R133C mutations, respectively; Lane 6: PCR with wild-type primers of Panel 2; Lane 7-9: PCR with mutant primers of Panel 2 using samples with mutations p.R306C, p.R270X, and p.T158M, respectively. An aliquot of 15 µl of each PCR product was loaded on the gel.

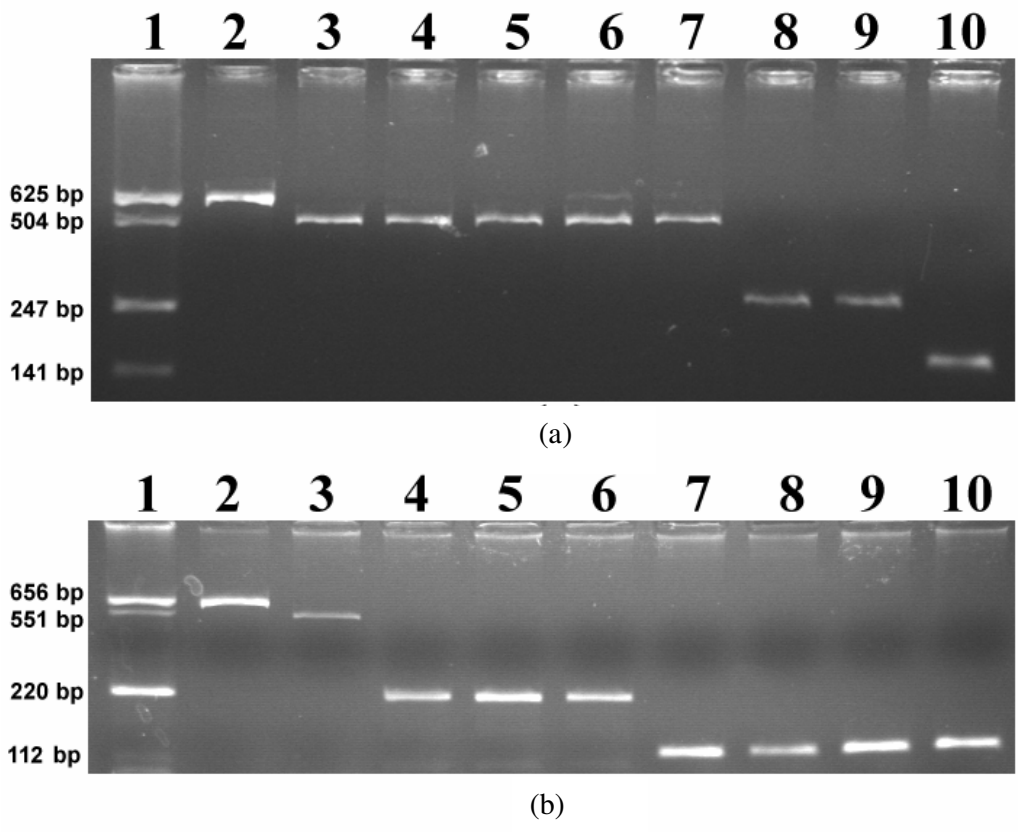

Figure 5.13. Evaluation of the multiplexed ARMS-PCR assay using RTT patient samples with known mutations. (a) Panel 1. Lane 1: PCR with wild type primers; Lane 2: patient with p.R294X; Lane 3-7: patients with p.R255X; Lane 8-9: patients with p.R168X; Lane 10: patient with p.R133C. (b) Panel 2. Lane 1: PCR with wild type primers; Lane 2: patient with p.R306C; Lane 3: patient with p.R270X; Lane 4-6: patients with p.T158M; Lane 7-10: Analysis of patients with p.R106W using ARMS assay. An aliquot of 15 µl of each PCR product was loaded onto the gel.

5.1.8. The Effect of DNA Concentration on Reliability and Reproducibility of SYBR Green Dye-based Real Time PCR Analysis to Detect the Exon Rearrangements

In this part of the study, we have investigated the effect of DNA concentration on reliability and reproducibility of Real Time PCR to detect the exon rearrangements. SYBR

Green dye-based Real Time PCR analysis was performed to detect the *MECP2* exon 3 rearrangements in five samples with previously determined genotypes.

Through optimization of reaction conditions, the optimal concentration of primers was found to be 5 and 10 pmol for *NDRG1* (reference gene) and *MECP2*, respectively. The melting curves of the all PCR products showed a single peak with identical melting temperature (Tm), indicating that there was no non-specific amplification. The specificity of the real-time PCR was further confirmed by analysis of the PCR products on an agarose gel which showed the expected amplification products of 172 and 175-bp for *MECP2* exon 3 and *NDRG1*, respectively.

5.1.8.1. Comparison of Quantification Methods. Two methods for determination of the *MECP2* exon 3 copy numbers from the raw data of Real-Time PCR reaction are available. The relative kinetic method is based on interpolated data from a standard curve, whereas the comparative Ct method transforms a difference in Ct values (between the test sample and the calibrator sample) into a copy number ratio. The relative kinetic method takes in account the actual efficiency of the reaction. The comparative Ct method does not require standard curves and 0.95 was used as default amplification efficiency in quantification. For all samples the *MECP2* exon 3 copy number was calculated using both methods. A paired sample *t*-test showed that the obtained results by both methods were significantly similar ($P = 0.451 > 0.05$). In addition, the Pearson correlation coefficient of 0.996 ($P = 1E\text{-}6 < 0.01$) demonstrated the equivalence of both methods.

5.1.8.2. Quantification. Using the control DNA samples (20 ng) for whom we had previously determined the genotypes, the mean ratios were observed as 0.52±0.12 for deletion carriers (expected value: 0.5) and 1.56±0.18 for duplication carriers (expected value: 1.5) vs. 1.022±0.17 for non-carriers (expected value: 1.0). The differences between the three groups were highly significant ($p<0.001$) (ANOVA).

Triplicate measurements were performed on six DNA concentrations of 0.1, 1, 5, 50, 100, and 200 ng of the patient R23 with *MECP2* exon 3 deletion, patient R19 with *MECP2* exon 3 duplication, and two healthy females and one male (Table 5.4). The expected copy number ratio was obtained in all cases when 1 ng, 5 ng, and 50 ng DNA used. However,

using 0.1 ng DNA, the ratio was out of expected range (± 2SD) in six of 15 measurements resulting in misgenotyping for R5, R19 and female 2 samples. In case of 100 ng DNA, expected ratio could not be obtained in four of 15 measurements leading to misgenotyping of R19 and two female samples. We did not get any expected copy number while using 200 ng DNA (Figure 5.14).

The effect of the DNA concentration on the amplification efficiency and specifity could be observed in amplification curve and melting curve analysis. Use of the high DNA concentrations (100–200 ng) resulted in inhibition of the amplification and/or nonspecific product formation in some cases (Figure 5.15 and 5.16).

Table 5.4. Ct values obtained from Real Time PCR analysis on different amounts of DNA.

Sample	DNA conc.	Ct of MeCP2	Ct of NDRG1	ratio of MeCP2/NDRG1 gene
Female 1	0.1 ng	35.00	32.64	1.20
		37.00	37.00	1.15
		27.76	26.67	1.00
	1 ng	32.50	30.37	1.11
		30.60	29.76	0.89
		31.82	31.58	0.97
	5 ng	29.61	27.84	1.06
		28.16	27.50	1.17
		25.70	24.98	1.00
	50 ng	26.38	25.00	1.00
		26.21	25.79	0.95
		26.21	25.93	0.95
	100 ng	24.88	23.26	0.80
		26.05	23.98	0.27
		26.17	24.98	0.87
	200 ng	23.95	21.83	0.58
		25.60	23.06	0.20
		21.50	21.62	1.42

Table 5.4. Ct values obtained from Real Time PCR analysis on different amounts of DNA (continued).

Sample	DNA conc.	Ct of MeCP2	Ct of NDRG1	ratio of MeCP2/NDRG1 gene
Female 2	0.1 ng	35.00	35.00	4.74
		38.00	38.00	1.09
		31.68	31.21	0.83
	1 ng	32.55	30.13	0.89
		30.79	29.93	0.97
		32.66	32.27	0.83
	5 ng	30.25	27.98	0.98
		29.33	28.85	0.82
		28.33	28.90	1.21
	50 ng	27.57	25.32	1.00
		26.88	26.55	0.86
		26.94	25.53	1.20
	100 ng	28.11	24.26	0.33
		26.30	24.65	0.35
		26.14	25.06	0.93
	200 ng	28.42	23.53	0.16
		28.74	23.14	0.10
Male	0.1 ng	32.28	30.90	0.45
		32.21	30.08	0.29
		35.00	35.00	0.27
	1 ng	31.01	28.92	0.50
		30.96	29.24	0.62
		28.35	26.93	0.66
	5 ng	29.54	27.69	0.46
		29.89	27.65	0.34
		30.15	29.49	0.43
	50 ng	27.71	26.52	0.49
		28.66	25.98	0.50
		29.12	26.09	0.39
	100 ng	27.33	25.18	0.49
		27.1	24.69	0.42
		28.13	25.64	0.22
	200 ng	28.49	24.25	0.08

Table 5.4. Ct values obtained from Real Time PCR analysis on different amounts of DNA (continued).

Sample	DNA conc.	Ct of MeCP2	Ct of NDRG1	ratio of MeCP2/NDRG1 gene
Patient R5 with exon 3 deletion	0.1 ng	37.00	37.00	1.98
		37.00	35.27	0.51
		37.00	37.00	1.98
	1 ng	31.50	29.24	0.47
		31.10	29.24	0.44
		29.92	27.83	0.37
	5 ng	30.27	27.92	0.30
		29.78	27.49	0.32
		28.14	26.81	0.53
	50 ng	27.71	26.52	0.49
		28.66	25.98	0.50
		29.12	26.09	0.39
	100 ng	26.59	24.82	0.48
		27.66	25.98	0.51
		27.98	26.65	0.55
	200 ng	30.57	22.28	0.03
Patient R19 with exon 3 duplication	0.1 ng	35.00	35.00	1.06
		29.21	29.48	1.82
		30.95	30.79	1.10
	1 ng	31.87	32.55	1.70
		30.61	30.51	1.46
		30.20	30.19	1.68
	5 ng	27.90	27.55	1.39
		29.11	29.62	1.52
	50 ng	27.17	27.38	1.51
		27.53	27.98	1.31
	100 ng	28.22	25.56	0.17
		26.17	25.85	1.42
		26.22	25.84	1.38
	200 ng	28.47	24.87	0.09

	DNA Conc.	Female 1	Female 2	Male	R5.3 with exon del	R19.3 with exon dup
MECP2/ NDRG1	0.1 ng	1,12 ±0.10		0,34 ±0.10		
	1 ng	0,99 ±0.11	0,89 ±0.07	0,59 ±0.08	0,43 ±0.05	1,61 ±0.13
	10 ng	1,08 ±0.09	1,01 ±0.20	0,41 ±0.06	0,38 ±0.13	1,46 ±0.09
	50 ng	0,97 ±0.03	1,02 ±0.17	0,46 ±0.06	0,46 ±0.06	1,41 ±0.14
	100 ng			0,38 ±0.01	0,51 ±0.04	
	200 ng					

Figure 5.14. The summary of the Real Time analysis of *MECP2* exon 3 rearrangements using 0.1 – 200 ng DNA. Gray shaded boxes indicate the results in out of range.

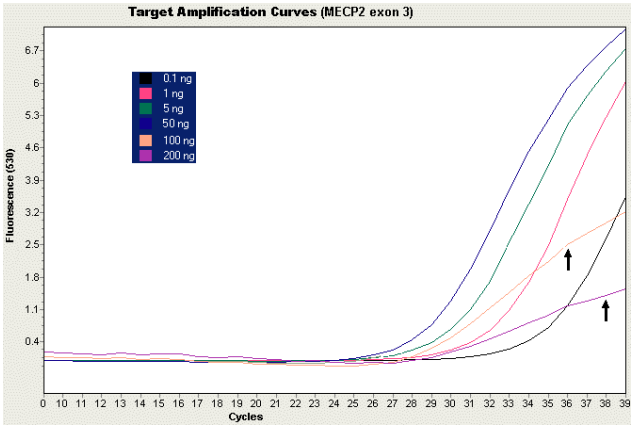

Figure 5.15. The profile of the amplification products of sample R5 with different concentrations of template DNA. Arrows show the unexpected amplification curves.

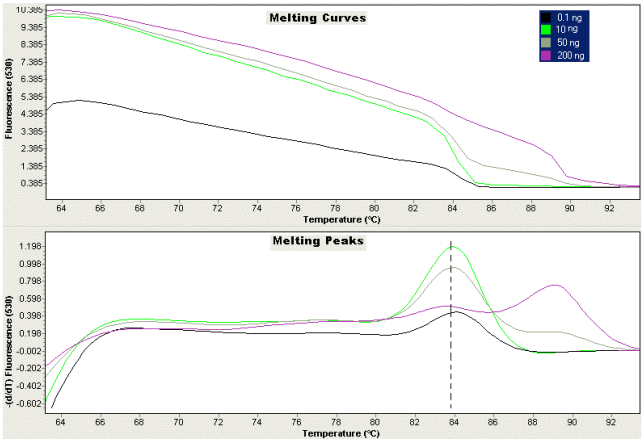

Figure 5.16. Melting curve analysis for PCR products of sample R5 using 0.1, 10, 50, 200 ng DNA. The line shows the expected Tm value for *MECP2* exon 3 products.

5.2. Methylation Analyses of the Putative Promoter Region of Rad23 Genes in Breast Tumor Tissues

In this study, the methylation status of 5' flanking regions (including the CpG islands and putative promoter sequence) of hHR23A and hHR23B genes was investigated in primary breast tumor, tumor adjacent tissues, and normal breast tissues.

5.2.1. Characterization of the 5' flanking region of the hHR23 Genes

5.2.1.1. hHR23A Gene. A part of 5' flanking region (1450-bp upstream and 180-bp downstream sequence, relative to the translation start site (+1 ATG)) of hHR23A gene (GenBank accession NT_011295.10) was analyzed to predict the putative eukaryotic Pol II promoter. Web-based MethPrimer software revealed two CpG islands in the upstream region (Figure 5.17). The first CpG island was 127 bp long and between nucleotide (nt) positions -580 and -454.. A 287 bp long second island is located between nucleotides -341 and -55. PROSCAN program predicted a putative eukaryotic Pol II promoter region within the second CpG island (position -48 to -298 nts) with a score of 98.79 (Promoter Cutoff score = 53.000000). The promoter region lacks the CCAAT and TATA-like elements, a common feature of the house-keeping genes. The analysis revealed potential binding sites for the transcription factor Sp1 (-243/-231 and -233/-241 nts) as inverted overlapping sites, overlapping ATF and CREB sites (-303/-294 nts), and an Elk-1 site (-113/-99 nts). The primers were designed to investigate the methylation status of CpG di-nucleotides within the -310/+140 nts, a region covering the putative promoter sequence and 59 CpG di-nucleotides.

5.2.1.2. hHR23B Gene. Peng *et al*. (2005) has shown that the CpG di-nucleotides in the upstream region (from -338 to -64 nts, relative to the transcription start site) of the hHR23B gene (GenBank accession NW_924539) were methylated in Interleukin-6-responsive Multiple Myeloma KAS-6/1 cell lines. This region was analyzed to characterize the putative promoter sequence. PROSCAN software revealed a CCAAT and TATA- box lacking putative Pol II promoter sequence in between nucleotide positions -14 to -264 with a score of 217.35 (Promoter Cutoff score = 53.000000). Four Sp1 binding sites were identified in positions -286/-279, -270/-261, -134/-127, and -118/-110. Using MethPrimer,

the primers were designed to cover the putative promoter region and 40 CpG di-nucleotides between nucleotides -328 to -19 (Figure 5.18).

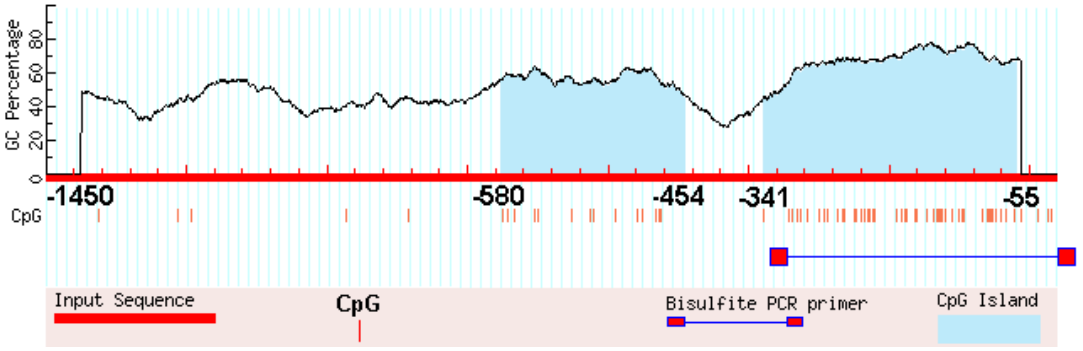

Figure 5.17. MethPrimer program output showing the CpG islands and the investigated region at 5' of the hHR23A gene.

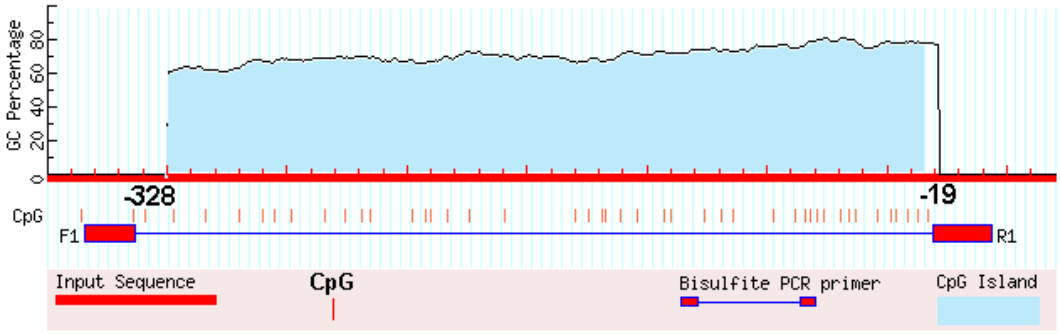

Figure 5.18. MethPrimer program output showing the CpG island and the investigated sequence in 5' flanking region of hHR23B gene.

5.2.2. Bisulfite Sequencing of hHR23A and hHR23B in paraffin-embedded tissues

Sixty-one archival formalin-fixed, paraffin-embedded tissues consisting of 50 primary breast tumors (diagnosed as Invasive Ductal Carcinoma), nine tumor adjacent tissues and four normal breast tissues were included in this study (Table 5.5). Genomic DNA was extracted from tissues by using a modified version of non-heating DNA extraction protocol described by Shi *et al*. (2002). Tissues were incubated with lysis buffer at 50 ºC for 48-72 hours instead of overnight at 45 ºC recommended by Shi *et al*. (2002).

DNA isolation was successful in all samples with concentrations ranging from 3 to 470 ng/µl (Figure 5.19).

The methylation status of the CpG islands was investigated by bisulfite-sequencing method. Semi-nested PCR strategy was used to amplify the bisulfite modified DNA samples. PCR fragments could be produced in 38 samples for hHR23A gene and 58 samples for hHR23B gene out of 61 samples tested. The methylation status of hHR23A and hHR23B genes could be determined in 35 of 38 and 51 of 58 samples, respectively.

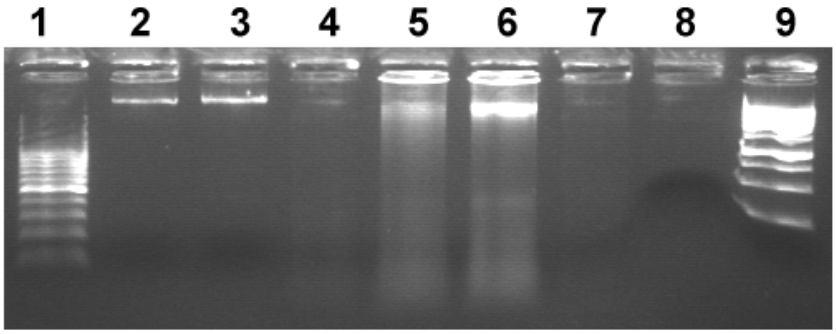

Figure 5.19. Agarose gel electrophoresis showing the quality of the genomic DNAs isolated from paraffin embedded tissues. Lane 1: 100-bp DNA ladder (MBI Fermentas); Lane 2 and 3: DNA isolated from peripheral blood samples, Lane 4-6: DNA isolated from paraffin embedded tissues, Lane 7 and 8: bisulfite treated DNA samples, Lane 9: 1-kb DNA ladder (MBI Fermentas). Approximately 200-400 ng DNA was loaded onto the slots.

5.2.2.1. hHR23A. Methylation analysis of 5' flanking region of hHR23A gene revealed cytosine methylation in 12 tumor and 2 tumor adjacent tissues. The results are summarized in Table 5.5 and Figure 5.20. Hypermethylation was observed in four tumors (from patients Rad21, 27T, 31T, and 32T) and one tumor adjacent tissue sample (Rad31N). The region between nucleotide positions +6/+117 was hypermethylated in tumor adjacent tissue Rad31N whereas hypermethylation spread to the region between -249/+117 nts in tumor tissue of the same sample (Rad31T) (Figure 5.21 and 5.22). Patient Rad29 has CpC methylation at position -114/-113 in tumor adjacent tissue (Rad29N) whereas CpT and CpA di-nucleotides were methylated at positions -133/-132 and +11/+12 in the tumor tissue (Rad29T). Seven patients (Rad4, 6, 15, 29T, 29N, 33T, and 48) have only non-CpG methylation. Bisulfite sequencing revealed no methylation in 21 tissue samples.

Table 5.5. Methylation analysis results for the 5' flanking region of *hHR23A*.

Sample	Cytosine methylation
Rad4	*CpC at -165/-164, *CpA at +15/+16
Rad6	*CpA at -171/-170, *CpC at -2/-1
Rad15	*CpC at +80/+81
Rad17	*CpG at -116/-115
Rad21	Hypermethylation between -249/-27
Rad27T	Hypermethylation between -226/+117
Rad28T	*CpG at -191/-190
Rad29T	*CpT at -133/-132, *CpA at +11/+12
Rad29N	*CpC at -114/-113
Rad31T	Hypermethylation between -249/+117
Rad31N	Hypermethylation between +6/+117
Rad32T	Hypermethylation between -121/+117
Rad33T	*CpCCC at -305/-302, *CpC at -190/-189
Rad48	*CpC +84/+85
*CpN indicates methylated cytosine.	

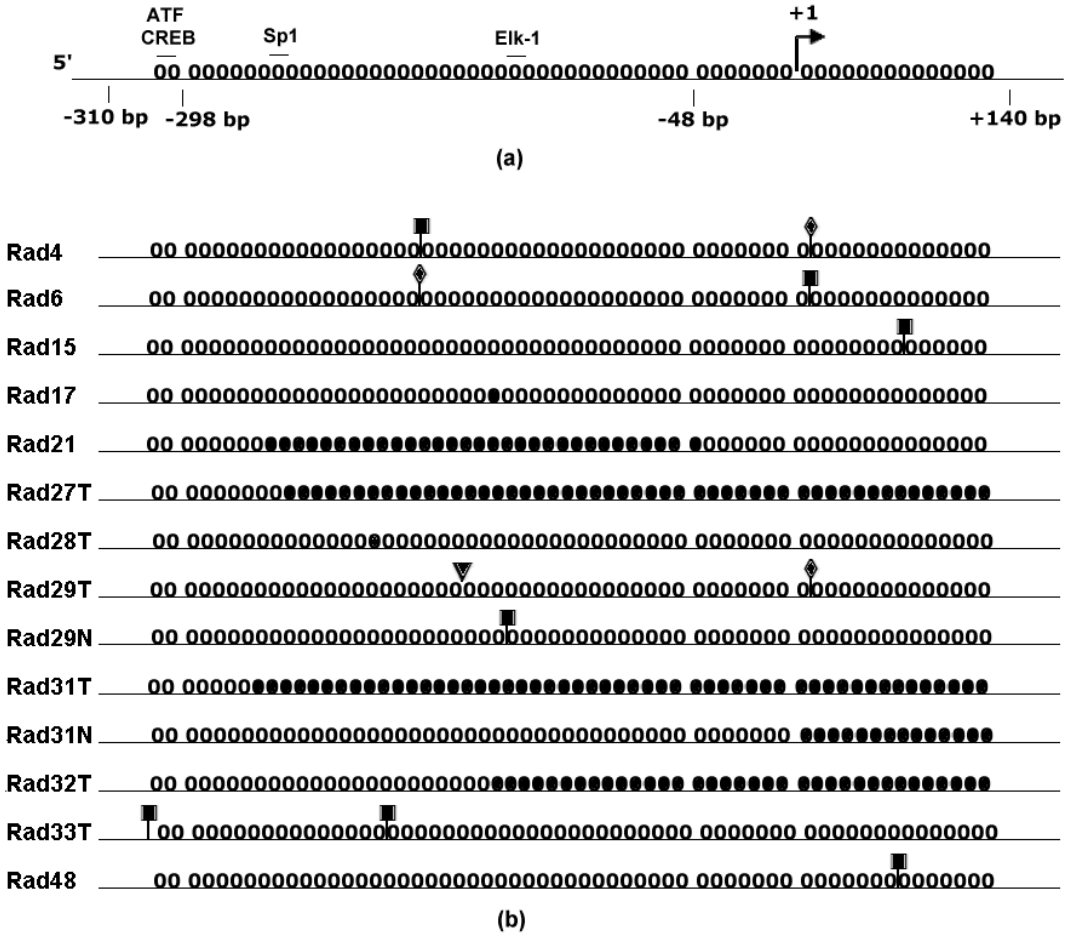

Figure 5.20. Methylation analysis of 5' flanking region of the hHR23A gene. (a) The distribution of CpG di-nucleotides in 5' flanking region (-310 to +140) of hHR23A gene are depicted schematically. Methylation analysis was performed on a region covering the putative promoter sequence and 59 CpG di-nucleotides. (b) The results of methylation analysis of samples. Open circles indicate unmethylated CpGs, and filled circles methylated CpGs. ▼, ◆, and ■ represent the methylated CpA, CpT, and CpC di-nucleotides, respectively.

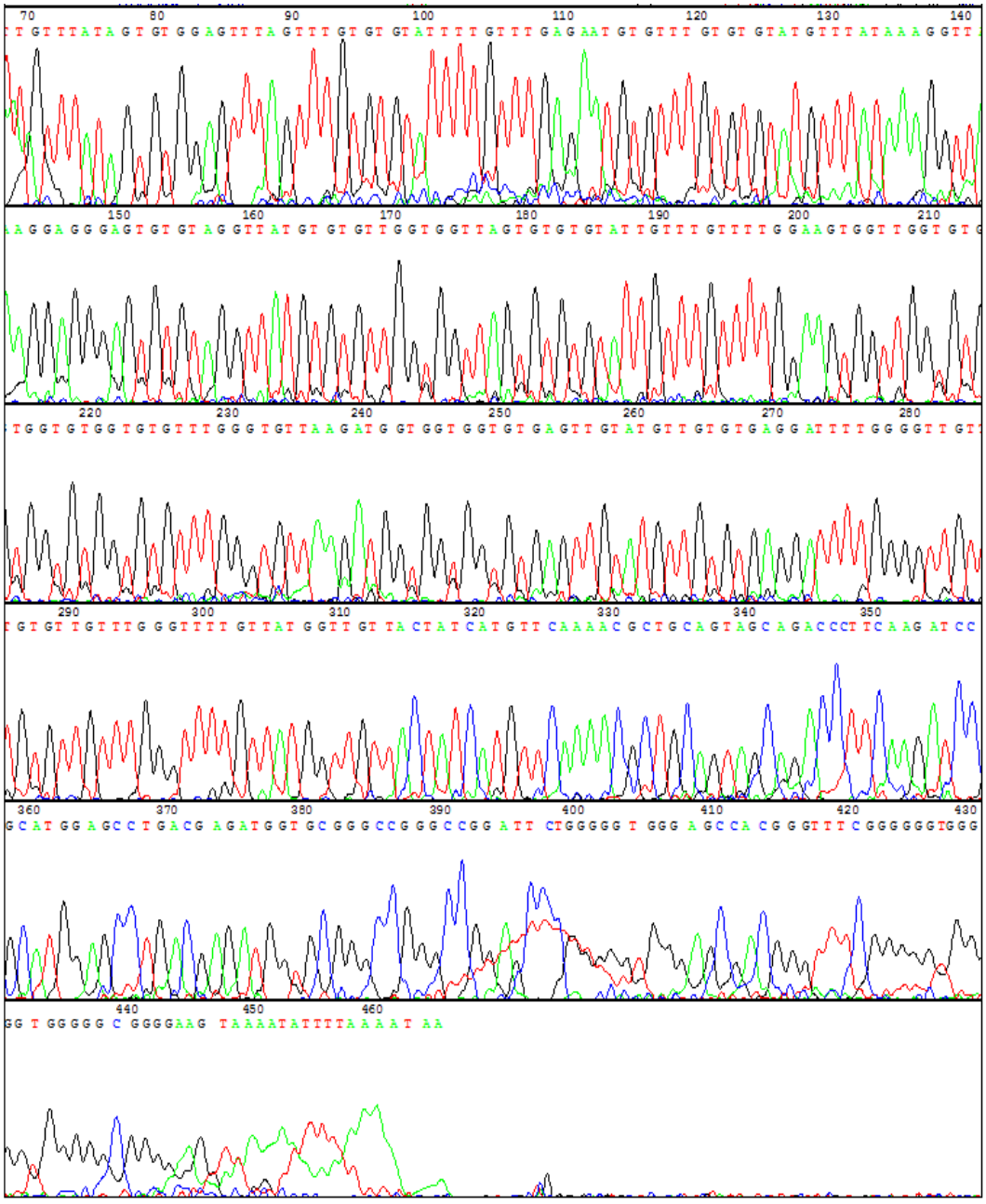

Figure 5.21. Bisulfite sequencing of 5'flanking region of hHR23A gene in tumor adjacent tissue of patient Rad31.

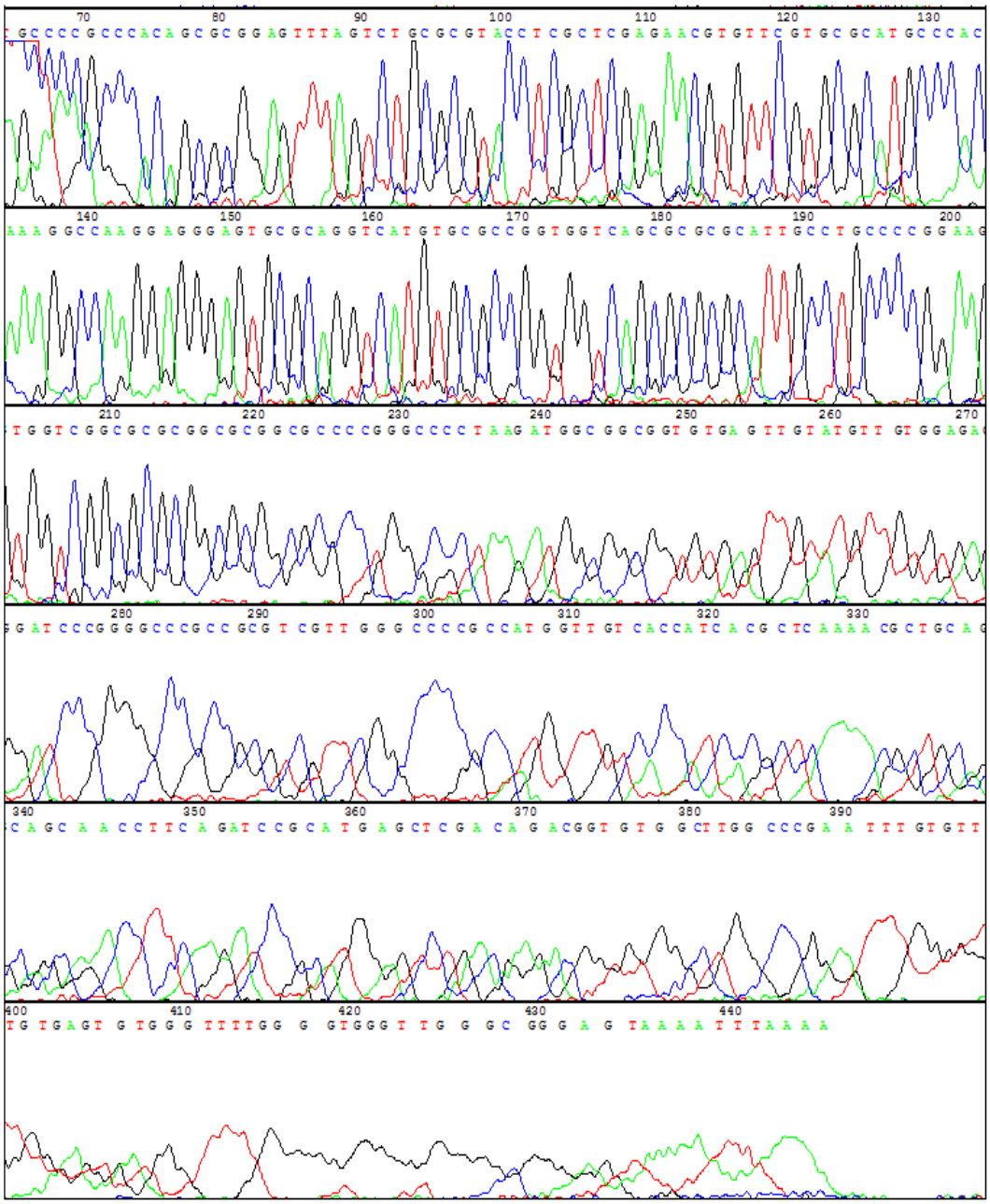

Figure 5.22. Bisulfite sequencing of 5'flanking region of hHR23A gene in tumor tissue of patient Rad31.

5.2.2.2. hHR23B. Cytosine methylation (CpG and non-CpG) in the upstream of hHR23B gene was observed in 15 tumor tissues. A representative result for bisulfite sequencing analysis of hHR23B gene is given in Figure 5.23. Detailed results are given in Table 5.6 and Figure 5.24. CpG methylation was observed in six patients (Rad9, 13, 16, 20, 22, and 27T) and non-CpG methylation was also present in three of them (Rad9, 20, and 22). Nine patients have only non-CpG methylation. The methylated cytosine residues were within the Sp1 binding sites in patients Rad9, 17, 22, 27T, and 32T. C*CpWGG motif was present in four samples (Rad2, 9, 25T, and 30T).

Bisulfite sequencing revealed that three tumor samples (Rad17, 27T, and 32T) have cytosine methylations in both hHR23A and hHR23B genes. The sample Rad27T showed hypermethylated region (between nts -226/+117) in hHR23A and methylated cytosine residue within the Sp1 binding site (-270/-261) in hHR23B gene. Similarly, upstream region (between -121/+117 nts) of hHR23A gene was hypermethylated and cytosine residue within the Sp1 binding site (-135/-126) in hHR23B gene in patient sample Rad32T. Sample Rad17 has CpC methylation at position -116/-115 and methylated cytosine residue within the Sp1 binding site (-135/-126) in hHR23A and hHR23B genes, respectively. The summary of the methylation status and the histopathology of the samples analyzed in this study are listed Table 5.7.

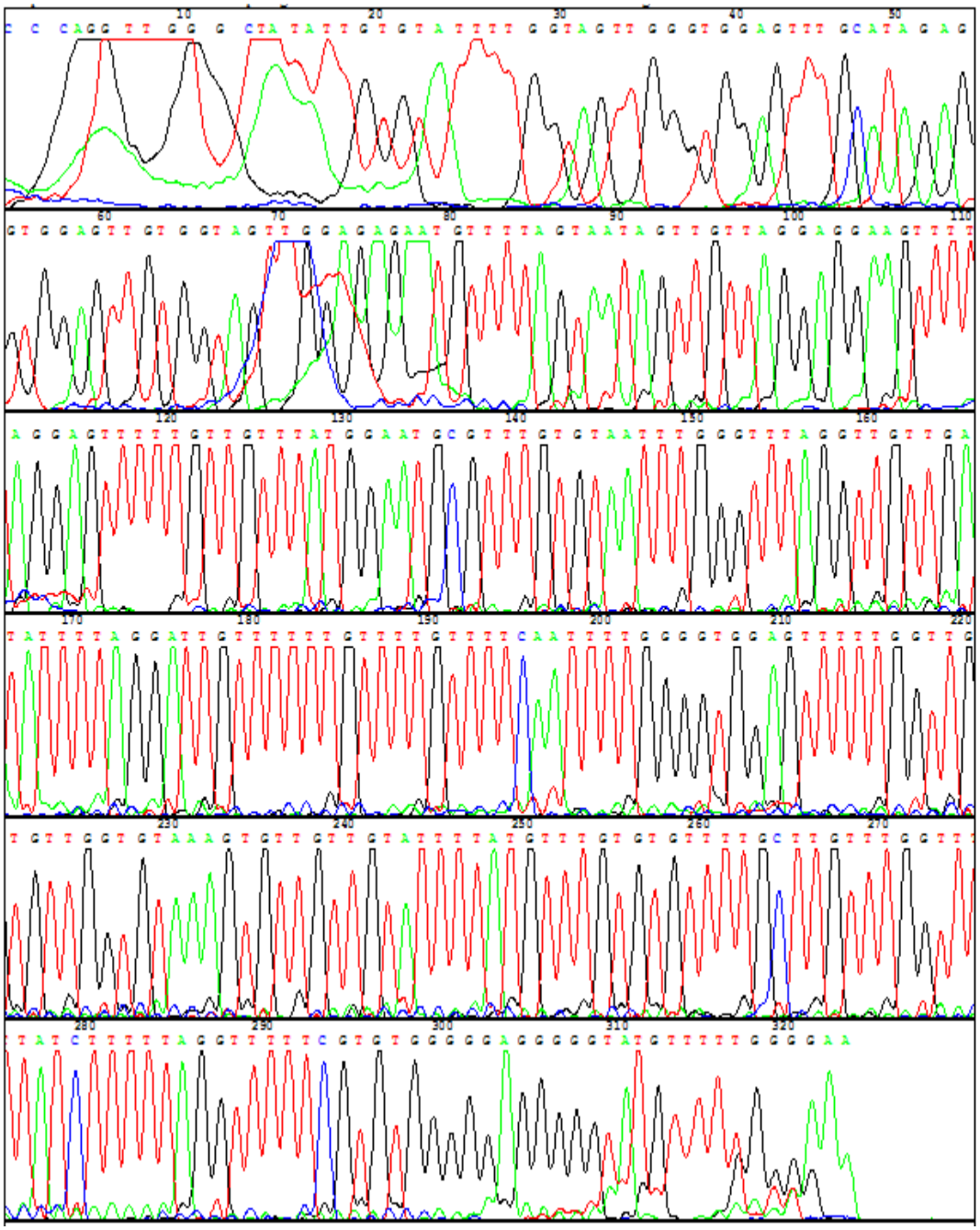

Figure 5.23. Chromatogram showing the bisulfite sequencing of 5'flanking region of hHR23B gene in the tumor tissue of patient Rad22.

Table 5.6. Results of methylation analysis for 5' flanking region of *hHR23B*.

Sample	Cytosine methylation
Rad2	C*CpAGG at -212/-208
Rad9	C*CpAGG at -151/-147, GC*CpCCGCCCC (Sp1) at -135/-126, *CpG at -84/-83
Rad13	*CpG at -172/-171
Rad14	G*CpCC at -205/-202
Rad16	*CpG at -172/-171
Rad17	GC*CpCCGCCCC (Sp1) at -135/-126
Rad20	*CpG at -144/-143, C*CpCCA at -78/-73
Rad22	G*CAC at -78/-75, *CpG at -185/-184, GCCCCGCCC*CpA (Sp1) at -135/-126, GC*CpC at -58/-55, T*CpCCC at -43/-39, *CpG at -28/-27
Rad25T	C*CpAGG at -151/-147
Rad27T	GCCC*CpGCCCC (Sp1) at -270/-261
Rad30T	C*CpAGG at -212/-208
Rad32T	GCCCCGCC*CpC (Sp1) at -135/-126
Rad46	A*CpCCC at -78/-73
Rad50	GCCCCGCC*CpC (Sp1) at -135/-126
Rad51	G*CpAA at -235/-232
*CpN indicates methylated cytosine.	

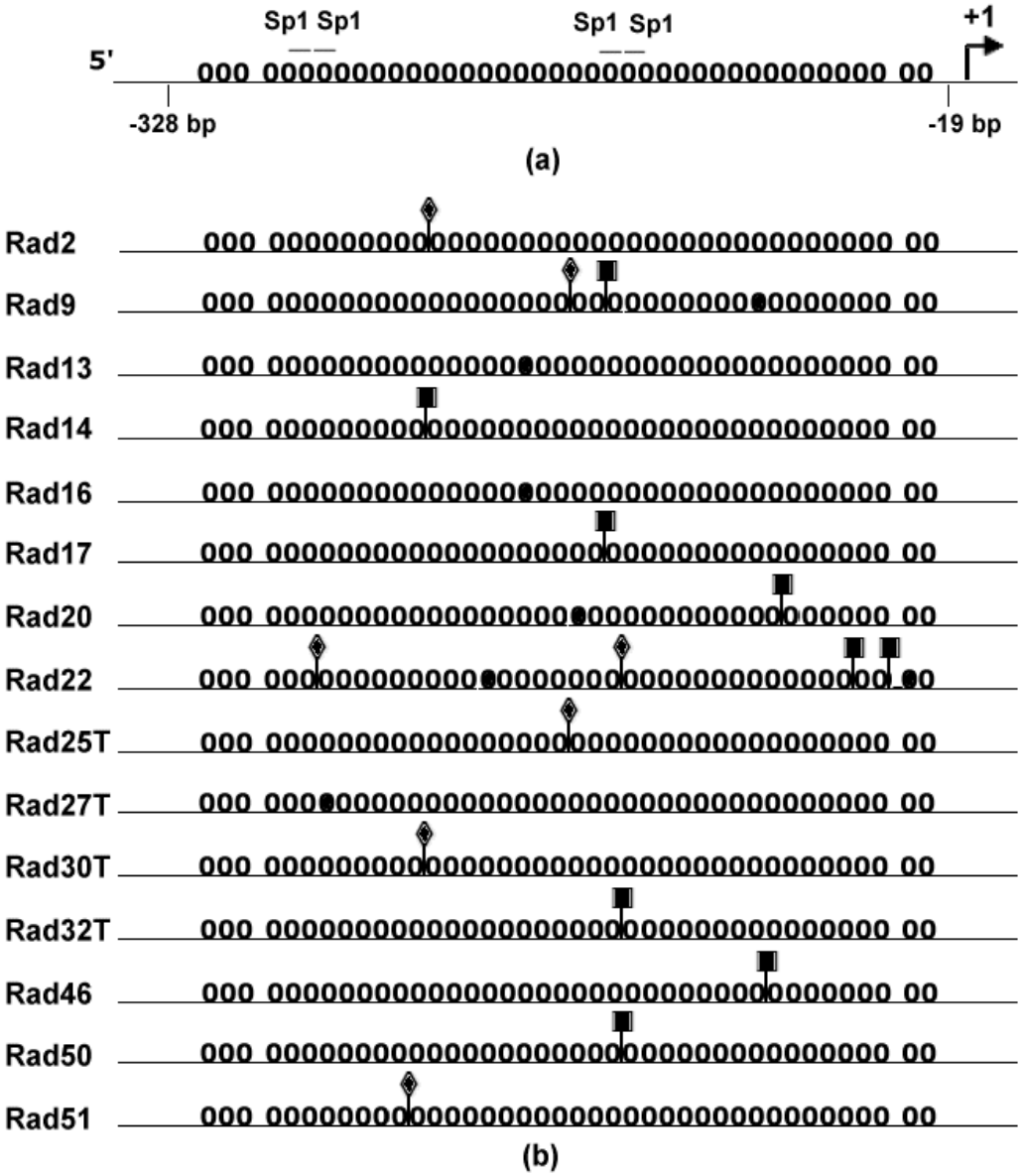

Figure 5.24. Methylation analysis of 5' flanking region of the hHR23B gene. (a) Schematic representation of the hHR23B gene upstream region comprising 40 CpG di-nucleotides. (b) The samples with cytosine methylation. Open circles indicate unmethylated CpGs, and filled circles methylated CpGs. ◆ and ■ represent the methylated CpT and CpC di-nucleotides, respectively.

Table 5.7. The histopathological and epigenetic findings of the tumor tissue analyzed in this study.

#	Age	Tissue type	Histopathological type	Stage	LNM* (+/ -)	Histological Grade	ER	C-erbB2	Cytosine methylation	
									Rad23A	Rad23B
Rad 1	73	Primary tumor	IDC	pT4bN1	+	3	-	?	-	-
Rad 2	55	Primary tumor	IDC	pT1N0	-	2	90 per cent	-	ND	+
Rad 3	50	Primary tumor	IDC	pT2N2	+	2	-	-	ND	ND
Rad 4	59	Primary tumor	IDC	pT3Nx	?	3	-	-	+	-
Rad 5	65	Primary tumor	IDC	pT2N0	-	2	60 per cent	-	-	-
Rad 6	42	Primary tumor	IDC	pT1N1	+	1	<5 per cent	-	+	-
Rad 7	82	Primary tumor	IDC	pT1N0	-	3	60 per cent	-	ND	ND
Rad 9	65	Primary tumor	IDC	pT2N1	+	3	70 per cent	-	ND	+
Rad 10	49	Primary tumor	Invasive apocrin carcinoma	pT1N0	-	2	-	+	ND	-
Rad 11	64	Primary tumor	IDC	pT1N1	+	1	80 per cent	-	-	-
Rad 12	46	Primary tumor	IDC	pT2N2	+	2	-	+	ND	ND
Rad 13	58	Primary tumor	IDC	pT2N2	+	3	60 per cent	-	ND	+
Rad 14	52	Primary tumor	IDC	pT2N1	+	3	80 per cent	-	ND	+
Rad 15	78	Primary tumor	IDC	pT1Nx	?	2	80 per cent	-	+	-
Rad 16	39	Primary tumor	ductal carcinoma *in situ*				10 per cent	-	ND	+
Rad 17	81	Primary tumor	IDC	pT2N0	-	2	70 per cent	-	+	+
Rad 18	71	Primary tumor	Mixed IDC-ILC	pT1N0	-	3	90 per cent	-	ND	-
Rad 19	79	Primary tumor	IDC	pT4bN1	+	3	-	+	ND	ND
Rad 20	66	Primary tumor	IDC	pT2N1	+	3	90 per cent	-	ND	+
Rad 21	43	Primary tumor	IDC	pT2N2	+	3	90 per cent	+	Hyperm.	-

* Lymph Node Metastases; IDC: Invasive (or Infiltrating) Ductal Carcinoma; NA: not available; ND: not determined.

Table 5.7. The histopathological and epigenetic findings of the tumor tissue analyzed in this study (continued).

#	Age	Tissue type	Histopathological type	Stage	LNM* (+/ -)	Histological Grade	ER	C-erbB2	Cytosine methylation	
									Rad23A	Rad23B
Rad 22	60	Primary tumor	IDC	pT3N0	-	3	-	+	ND	+
Rad 23	63	Primary tumor	IDC	pT2N3	+	2	90 per cent	-	-	-
Rad 25N	45	Normal	-	-	-	-			ND	-
Rad 25T		Primary tumor	IDC	pT2N1	+	3	60 per cent	-	ND	+
Rad 26N	40	Normal	-	-	-	-			ND	-
Rad 26T		Primary tumor	IDC	pT1N0	-	1	90 per cent	-	-	-
Rad 27N	37	Normal	-	-	-	-			ND	ND
Rad 27T		Primary tumor	IDC	pT2N1	+	3	20 per cent	-	Hyperm.	+
Rad 28N	63	Normal	-	-	-	-			-	-
Rad 28T		Primary tumor	IDC	pT3N2	+	2	-	-	+	-
Rad 29N	62	Normal	-	-	-	-			+	-
Rad 29T		Primary tumor	IDC	pT2N(Mi)	+	3	100 per cent	-	+	-
Rad 30N	75	Normal	-	-	-	-			-	-
Rad 30T		Primary tumor	IDC	pT1N1	+	2	per cent80	-	-	+
Rad 31N	77	Normal	-	-	-	-			Hyperm.	-
Rad 31T		Primary tumor	IDC	pT2N(Mi)	+	3	100 per cent	-	Hyperm.	-
Rad 32N	81	Normal	-	-	-	-			ND	ND
Rad 32T		Primary tumor	IDC	pT2N1	+	3	90 per cent	-	Hyperm.	+
Rad 33N	48	Normal	-	-	-	-			-	-
Rad 33T		Primary tumor	IDC	pTxNx	+	3	NA	NA	+	-
Rad 43	47	Primary tumor	Invasive Lobular	pT2N1	+	2	80 per cent	-	-	-
Rad 44	52	Primary tumor	Atypical medullar	pT1N1	+	3	-	-	-	-

* Lymph Node Metastases; IDC: Invasive (or Infiltrating) Ductal Carcinoma; NA: not available; ND: not determined.

Table 5.7. The histopathological and epigenetic findings of the tumor tissue analyzed in this study (continued).

#	Age	Tissue type	Histopathological type	Stage	LNM* (+/ -)	Histological Grade	ER	C-erbB2	Cytosine methylation Rad23A	Rad23B
Rad 45	61	Primary tumor	IDC	pT2N0	-	1	30 per cent	-	-	-
Rad 46	55	Primary tumor	Invasive Lobular	pT2N0	-	2	90 per cent	-	-	+
Rad 47	45	Primary tumor	IDC	pT2N2	+	3	-	+	ND	ND
Rad 48	47	Primary tumor	ductal carcinoma *in situ*						+	ND
Rad 49	41	Primary tumor	IDC	pT1N3	+	3	-	+	-	-
Rad 50	54	Primary tumor	IDC	pT2N1	+	2	80 per cent	-	ND	+
Rad 51	53	Primary tumor	IDC	pT1N1	+	3	30 per cent	-	ND	+
Rad 52	51	Primary tumor	IDC	pT1N0	-	3	30 per cent	+	-	-
Rad 53	48	Primary tumor	IDC	pT1N0	-	1	60 per cent	-	ND	-
Rad 54	57	Primary tumor	IDC	pT1N0	-	2	70 per cent	-	-	-
Rad 55	79	Primary tumor	IDC	pT2N1Mx	+	3	70 per cent	-	-	-
Rad 56	63	Primary tumor	IDC	pT1N0	-	2	90 per cent	-	ND	-
Rad 58	49	Primary tumor	Invasive Lobular	pT2N2	+	2	80 per cent	-	ND	-
Rad 59	77	Primary tumor	IDC	pT1N0	-	2	NA	NA	-	-
Rad 62T	76	Primary tumor	IDC	pT2Nx	?	2	60 per cent	-	-	-
Rad 62N		Normal	-	-	-	-			-	-
Rad 60		Normal	-	-	-	-			-	-
Rad 61	41	Normal	-	-	-	-			-	-
Rad24		Normal	-	-	-	-			-	-

* Lymph Node Metastases; IDC: Invasive (or Infiltrating) Ductal Carcinoma; NA: not available; ND: not determined.

5.3. Molecular Basis of Congenital Hypothyroidism

In the present study, the genetic mechanisms leading to congenital hypothyroidism (CH) and prolonged paralysis after mivacurium in a patient was investigated. The patient was screened for the presence of mutations within the TTF2 and BChE genes responsible of hypothyroidism and neuromuscular block after anesthetic administration, respectively.

5.3.1. Clinical Features of the Patient

The proband, a 3900-g female infant, was born to consanguineous parents by normal vaginal delivery at 40 wk gestation after an uncomplicated pregnancy. Postnatal examination revealed the patient to be hypotonic, hypoactive, hypothermic, and areflexic with cleft palate, spiky hairs, and bilateral choanal atresia, subsequently confirmed by paranasal sinus tomography. Meconium staining and perinatal respiratory distress prompted admission to neonatal intensive care for ventilatory support. Immediately after birth, the patient's total serum T4 level was 0.758 µg/dl [normal range (NR), 6.1–14.9 µg/dl], and TSH was greater than 100 mIU/ml (NR, 1.7–9.1 mIU/ml). L-T4 replacement therapy was started, and the baby was discharged at age 2 months. The proband's parents and older male sibling are biochemically euthyroid with no congenital anomalies.

Thyroid ultrasonography and gadolinium-enhanced computed tomography (CT) examination of the proband indicated the thyroid tissue in a eutopic location (Figure 5.25).

5.3.2. Mutation Analysis of the TTF2 Gene

Direct sequencing of coding exon of TTF-2 gene from the patient revealed a C→T transition at nucleotide position 304 (Figure 5.26). The mutation leads to the replacement of amino acid arginine with cysteine at codon 102 (p.R102C) affecting the forkhead domain of the protein. The arginine residue in this position is highly conserved in *H.Sapiens, M.Musculus, R.Norvegicus, C.Elegans* and among human forkhead proteins (Figure 5.27).

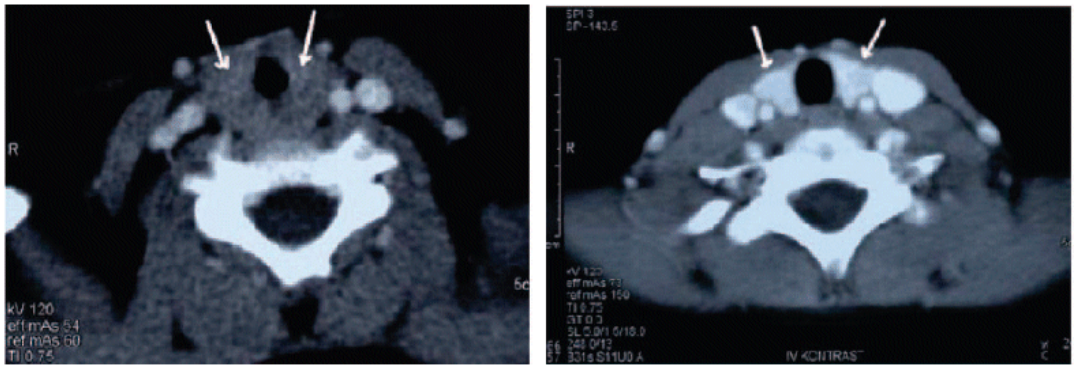

Figure 5.25. Axial postcontrast CT image of the patient reveals a slightly enlarged thyroid gland (arrows) in the paratracheal region with absent contrast enhancement (a). Comparative imaging of the thyroid gland (arrows) in a healthy 9-yr-old child (b) (Barış *et al*., 2006).

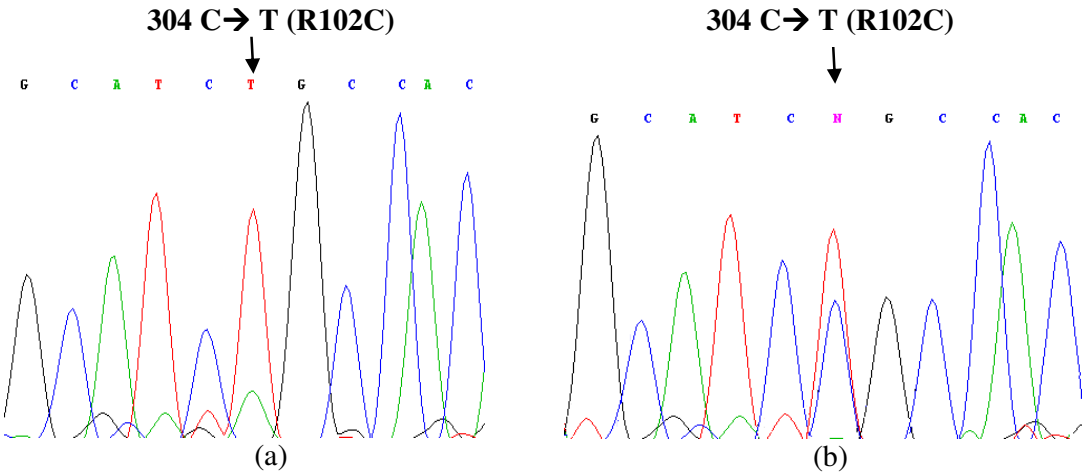

Figure 5.26. DNA sequencing profile of the TTF-2 gene showing mutation in homozygous condition in the patient (a). Her unaffected mother is heterozygous for the mutation (b).

The presence of the mutation was confirmed by restriction enzyme analysis. The mutation creates a novel *AlwN*I site. Her unaffected consanguineous parents were found to be heterozygote (Figure 5.28) and 100 control chromosomes tested negative for the same mutation.

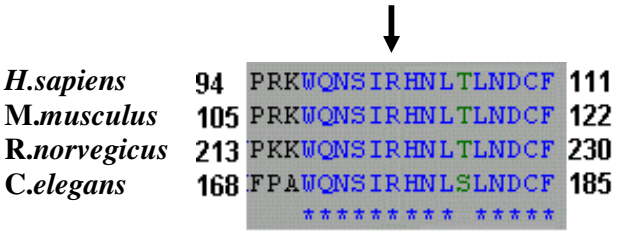

(a)

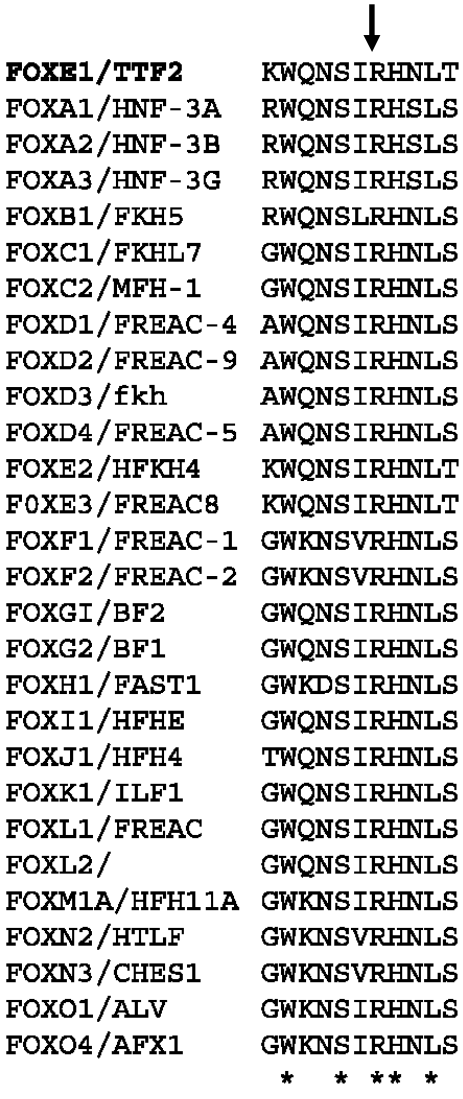

(b)

Figure 5.27. Alignment of the TTF-2 forkhead DNA-binding domain with selected FOX proteins between species (a) and within human proteins (b). At the bottom, '*' indicates conserved residues in all sequences. The arrow shows the Arg 102 residue (Barış *et al*., 2006).

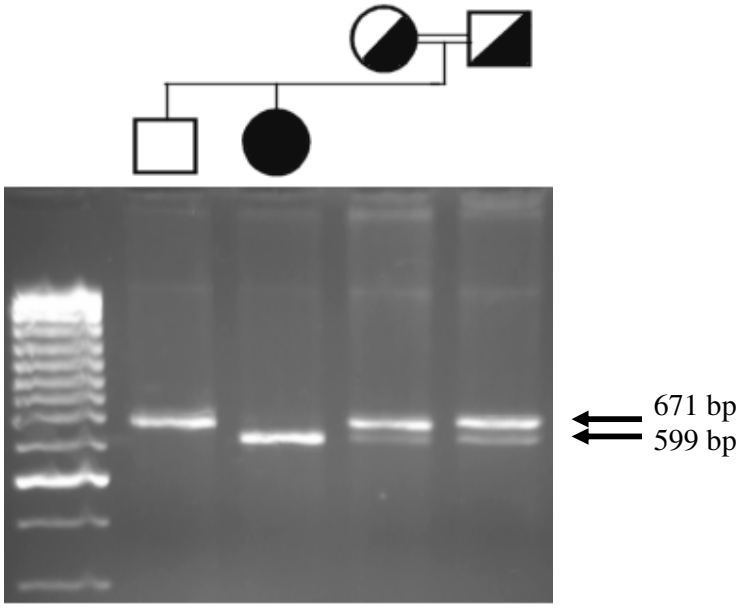

Figure 5.28. Two per cent agarose gel showing *AlwN*I digestion results for the patient and her family members.

5.3.3. Functional Characterization

Functional analyses performed in University of Cambridge revealed that the mutation is highly deleterious, with the p.R102C mutant protein exhibiting negligible DNA binding and transcriptional activity (Barış *et al*., 2006).

5.3.4. Mutation Analysis of Butyrylcholinesterase (BChE) Gene

Patients with CH are candidates for multiple operations due to midline defects (cleft palate and choanal atresia). When our CH patient was a 3-month-old baby, a gastrostomy was required because of a severe nutritional problem secondary to cleft palate. After operations, the patient showed prolonged neuromuscular block (paralysis) for four hours after a single dose of mivacurium as a muscle relaxant. BChE activity was measured and the proband was found to have a marked decrease in BChE activity compared with her parents and brother. The enzyme activities were 408 IU/1 for patient, 4953 IU/l for mother,

4594 IU/1 for father and 6513 IU/1 for brother (normal 5400–13 200 IU/1) (Yıldız *et al*., 2006).

5.3.4.1. PCR-RFLP. The patient and family members were analyzed for the presence of two most common BChE variants; p.Asp70Gly (A-variant) and Ala539Thr. Restriction analysis revealed that the patient, her consanguineous parents and unaffected brother were negative for these variants (Figure 5.29).

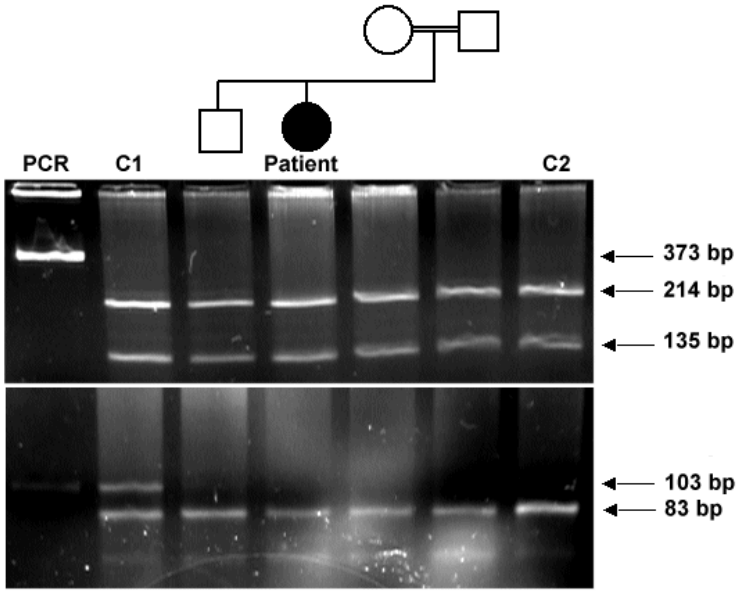

Figure 5.29. *Sau3A*I (upper panel) and *Alu*I (lower panel) digestion analyses for the patient and her parents (C: normal individual) (Yıldız *et al*., 2006).

6. DISCUSSION

Epidemiological studies promise to provide correlative data to permit researchers understand the etiology of human diseases and develop efficient genetic testing assays. Additionally, the accumulated data of genotyping, expression profiling and proteomics allows disease diagnosis, to understand the molecular mechanisms leading to the disease pathogenesis, and to develop efficient therapeutic approaches. In the framework of this thesis, we have investigated genetic and epigenetic changes and provided genotype-phenotype correlations to unravel the molecular mechanisms that lead to three different diseases, Rett Syndrome, breast cancer, and congenital hypothyroidism. To our knowledge, it is the first study on genetic basis of Rett Syndrome in our population. The results of this analysis revealed that gene dosage can be a mechanism that leads to this devastating genetic/epigenetic disease. Investigation of epigenetic changes in two human repair genes has shown CpG and non CpG methylation in tumor samples of breast cancer patients that was important with respect to the available literature. Identification of the causative mutation in the CH patient and its functional study with a collaborative work also helped to understand the genetic mechanisms and provided original evidence that implicated differential effects of TTF-2 mutations on downstream target genes required for normal human thyroid organogenesis. These and other findings are discussed below in respective sections for each disease.

6.1. Molecular Basis of Rett Syndrome

In the framework of this study, the genetic basis of Rett Syndrome (RTT) was investigated in a total of 71 patients. A heterogeneous spectrum of disease-causing mutations was identified in 68.2 per cent of a clinically well defined group of cases. Our results showed that exon duplication/deletions that could not be detected by standard techniques contribute to 19.3 per cent of these MECP2 mutations. Only 12.5 per cent of the patients, referred for differential diagnosis, were positive for MECP2 gene mutations suggesting that this gene does not represent a major cause of the disease among patients with Rett-like features. Comparison of the clinical severity scores of patients with respect

to the presence, type and location of mutation in the gene MECP2, in addition to the pattern of XCI did not reveal a statistically significant correlation.

The molecular analysis revealed 18 different mutations in 30 of 44 (68.2 per cent) female patients in the first group of classical/atypical RTT cases with detailed clinical data. Of the 30 patients with mutations, 10 had a missense, eight had a nonsense mutation, six had small nucleotide deletion/insertions. *MECP2* exon rearrangements were identified in six female patients; three patients with exon 2-4 duplications (R14, R19, R20) and three patients with exon 3 and/or exon 4 deletions (R5, R23, R30). In patient R33, exon duplication identified by Real Time analysis could not be verified by QF-PCR.

The deletions, we have identified in three classical RTT female patients, affect the MBD and TRD domains of the MECP2 protein. For these patients, it is highly unlikely that the protein produced from the mutant allele (if any) would have residual function thus they can be expected to be associated with severe phenotypes. Although Archer *et al.* (2006) noted that their deletion group was clinically indistinguishable from other mutation-positive RTT patients, the patients in our study presented higher clinical severity scores than all other mutation-positive patients. The differences in severity were not significant (8.33±0.58 vs 6.70±1.57, p=0.066), but the findings were in accordance with the data of Hardwick *et al.* (2007) and Scala *et al.* (2007). When we performed statistical analysis of severity scores for specific clinical features, we obtained a significant difference in the field of ‘‘gait function’’ (p=0.016), since none of patients with MECP2 exon deletions have ever walked.

The c.856delA and c.826-829delGTGG deletions identified in patients R3 and R49, respectively, present novel small deletions in exon 4. They cause a frame-shift introducing a premature stop codon at position 288 in TRD domain of the protein and probably alter the ability of the protein to recruit co-repressor complexes and affect its function in the process of transcription repression. The third novel frame-shift mutation due to one-bp deletion (c.744delG), in patient R46, creates a stop codon at the beginning of TRD domain (p.Ser194fsX208) and causes lack of both TRD and NLS domains. It is known that MBD-containing mutant proteins without TRD might accomplish some degree of silencing, either by recruiting the silencing complex by a TRD-independent mechanism or by directly

interfering with binding of transcription factors (Ballestar *et al*., 2000). However, loss of NLS and TRD domains in the case of p.Ser194fsX208 mutation might interfere with proper localization to nucleus and its functioning. The novel deletions in the other patients (R2, R8, and R42) hypothetically affect the C-terminal domain of the protein and may give rise to nonfunctional proteins. The c. 1156-1192del36 (p.Leu386Hisdel12) mutation in patients R2 and R42 are small deletions, however, the mutation in patient R8 causes in a frame-shifted protein starting from Lys345 residue (p.K345fs). Patient R8 is more severely affected in all respects compared to patient R2 and R42, with shorter period of normal development, earlier appearance of epileptic seizures, abnormal gait function with a severity score of 9 versus 7 and 5, in accordance with previous findings for C-terminal deletion mutations (Smeets *et al*., 2005).

In this study, exon duplications were identified in two patients with early seizure and in one with congenital variant of RTT. Although the extent of the duplications and whether they are tandem repeats could not be investigated, we have shown the duplication of exons that are known to be the expressed. Thus, it is the first report implicating gene duplications as causative mutations in female atypical RTT cases. Previously, one female patient with PSV variant of RTT.has been reported to carry three copies of exon four of the MECP2 gene (Ariani *et al*., 2004). In addition to this finding, Meins *et al*. (2005) has shown that duplication in Xq28 causes increased expression of the MECP2 gene in a boy with features of Rett Syndrome. Collins *et al*. (2004) has developed a mouse model that transgenically over-expressed MECP2 under the endogenous human promoter. These mice developed seizures, hypoactivity and spasticity with several other progressive neurological abnormalities. These results support the possibility that duplication of MECP2 may lead to increased expression and underlie some cases of X-linked delayed-onset neurobehavioral disorders including Rett Syndrome. It can be suggested that gene duplications might cause a gain of function rather than a loss of function via (i) repressing its target genes strongly, (ii) preventing their derepression, and/or (iii) repress novel genes that are not the targets in normal cellular conditions. The latter mechanism may be more likely considering the fact that all of our patients with exon duplications present additional neurodevelopmental symptoms leading to atypical phenotypes. Interestingly, eye contact is very difficult to obtain in these patients when compared to that of patients with missense mutation

(p=0.016). Further analysis should be performed to unravel the pathogenic mechanism caused by these duplications.

Previous studies suggest that patients with missense mutations tend to have significantly milder disease than patients with truncating mutations (Cheadle *et al*., 2000; Colvin *et al*., 2004). On the basis of statistical analysis, no significant correlation could be inferred between the overall disease severity and the type of the mutation in our cohort of patients. However, the patients with exon deletions or nonsense mutations affecting the TRD domain of the protein had higher clinical severity scores. Mutation negative patients and patients with skewed XCI patterns had slightly milder phenotypes whereas mutation positive patients had severe problems in their ability in purposeful hand movement and walking skills.

It has been shown that there is a tendency for skewing of XCI in lymphocytes in RTT patients when compared with age-matched controls. Our data is also suggestive for skewed XCI pattern to confer a protective effect on the phenotype especially for severe mutations that lead to production of truncated MECP2 protein. Among our 12 patients presenting skewed XCI pattern along with MECP2 mutations, 10 of them had nonsense/deletion/insertions, and only two of them had missense (p.R306C and p.T158M) mutations. Although we could not show that there is a statistically significant relationship between severity and XCI pattern by mutation, patients with the same mutation and different XCI status had clinical variability. In this situation, each individual might be expected to have differences in inter-tissue and intra-tissue XCI status, as is sometimes observed in mouse models (Young *et al*., 2004; Gibson *et al*., 2005).

The MECP2 mutation detection rate was higher in the first group subjects (68.2 vs. 12.5 per cent). Furthermore, 26 patients of this group were diagnosed using a stringent criteria and the mutations were identified in 79 per cent. Our results show that a strict adherence to the RTT criteria and careful evaluation of the patients improve the rate of MECP2 mutation detection. The diagnosis of RTT is mainly based on clinical criteria and this is a critical step to decide or not to offer genetic testing. From a socio-economic point of view, the use of efficient and well defined clinical criteria is very important since the

cost of MECP2 testing is high. Currently, the cost varies from $300 to $600 and is higher than the official minimum wage in Turkey.

Mutation analyses revealed a total of 31 pathogenic variations of which 15 of 31 (48 .4 per cent) detected by PCR-RFLP, 10 of 31 (32.3 per cent) by SSCP-DNA sequencing and 6 of 31 (19.3 per cent) by quantitative PCR assay. Thus, the PCR-RFLP method can be used as a preliminary step to detect the most common mutations observed in MECP2 gene in Turkish RTT patients. Our results showed that exon duplication/deletions contribute to 19.3 per cent of MECP2 mutations, and these rearrangements escape the PCR-based screening strategy. Quantitative analysis of this gene should also be considered in RTT patients, in order to determine the actual significance of the MECP2 gene in the etiology of RTT.

With excluding 6 exon duplication/deletions, nearly 80 per cent (20 of 25) of the point or small deletion/insertion mutations were detected in the exon 4 of the MECP2 gene. The rest of the mutations (20 per cent) were located within exon 3. This finding suggests that the mutation in MECP2 exon 1 and 2 appears to be rare in Turkish RTT patients and an initial analysis of exon 4 would provide the most efficient approach in a mutation detection protocol.

Huppke *et al.* (2003) recommend using a cutoff point of 8 for genetic testing to exclude girls with *MECP2*-negative results from the test. However, the two patients with exon duplications (patients R19 and R20) and the patient R22 with p.R106W mutation had Huppke scores of 5-7, implicating that genetic diagnosis should be performed even when the scores are lower than 8.

In three prenatal diagnostic tests performed, both chorionic biopsy specimens and parents were tested and found to be negative for the index patient's mutation. Germ line mosaicism of MECP2 mutations is an important problem in genetic counseling for both familial and sporadic RTT cases (Yaron *et al*, 2002). In the recent literature, Caselli *et al.* (2004) reported nine cases that were evaluated for prenatal diagnosis. Only one fetus carried the same mutation with affected sister (1/9, 11 per cent) and the pregnancy was terminated. Although the majority of the patients have *de novo* mutations, the prenatal

diagnosis might be offered for the family with RTT daughter and the parents should be informed about the possibility of germ line mosaicism.

Pathogenic sequence variations could not be identified in 14 of 44 (31.8 per cent) sporadic female patients in the first group. These patients may have MECP2 mutations in the promoter region or introns introducing novel splice sites that could not be detected by PCR-SSCP analysis. RTT can be a genetically heterogeneous disorder, and other causative genes might exist. Several recent studies identified mutations in the CDKL5 gene (OMIM 300203) encoding cyclin-dependent kinase like 5 in patients with an atypical, early seizure variant of RTT (Weaving *et al*., 2005; Evans *et al*., 2005; Scala *et al*., 2005). Thus, mutation screening of CDKL5 should be performed in MECP2 gene mutation-negative patients with early-seizure variant of RTT. Finally, we suggest that quantitative analysis of *MECP2* has to be considered in especially RTT variants in order to determine the actual significance of the gene in the etiology of RTT.

6.1.1. Multiplexed ARMS-PCR Approach for the Detection of Common *MECP2* Mutations

In the present study, we have described the development and validation of a multiplexed multiplex amplification refractory mutation system (ARMS) - PCR assay for identification of seven common mutations that accounts for almost 65 per cent of all MECP2 gene mutations (RettBASE). So far, these mutations could be investigated using PCR-RFLP or DNA sequencing techniques. Although appropriate, DNA sequencing is not well suited for routine use in a clinical laboratory; it is cumbersome, time-consuming, and technically demanding. Carvalho *et al.* (2006) have described a multiplex minisequencing technique for the detection of most common 10 mutations. This assay allows detection of p.R106W, p.A140V and p.G269fs mutations in addition to our assay. However, reagent and equipment costs of minisequencing PCR limit the implementation of this assay into research laboratories. Our multiplex ARMS-PCR assay offers a straightforward, inexpensive, and accurate alternative method. Each mutation-specific primer pair was designed to produce a different-sized fragment, so that the mutation in the sample can be identified unambiguously after agarose gel electrophoresis.

The seven MECP2 mutations included in this assay were selected based on their frequencies in RettBASE database. It is possible that the prevalence of the included mutations may vary among RTT patients from different populations. However, the assay could be improved by the inclusion of primer sets for detection of additional pathogenic mutations. For example, Kim *et al*. (2006) and Yamada *et al*. (2001) did not identify the mutation p.R106W in Korean and Japanese patients, respectively, but the same mutation accounted for 5-6 per cent of the mutations in French and German RTT patients, respectively (Bienvenu *et al*., 2002; Laccone *et al*., 2001). An ARMS assay was also designed and tested the for the p.R106W mutation, however, it could not be implemented to the panels. This mutation can be tested independently from the multiplex assay.

A well-designed ARMS multiplex requires compatible primer sequences in appropriate concentrations. Optimization of the PCR reaction, started with equimolar primer concentrations (10 pmol), revealed uneven amplification of the products, with some of the alleles barely visible. This problem was overcome by increasing the concentration of primers for the ‘weak’ loci and decreasing for the ‘strong’ loci. The specificity of the primer sets used was also found to be highly critical to ensure clear discrimination between target and non-target genomic sequence to avoid any ambiguity of detection. Primer dimers and nonspecific allelic noise was observed with primers for p.T158M and p.R168X mutations. These nonspecific bands could be eliminated by introducing a mismatch at the 3′ end of the allele-specific primers. As for any multiplex PCR, we recommend that users optimize the conditions, especially the primer concentrations for each set, in their laboratory.

In conclusion, the multiplex ARMS test is an efficient and cost-effective screen for molecular genetic testing of patients with RTT. It is a simple and reliable test that does not require any specialized equipment and can be completed in 1–2 days upon receiving the sample.

6.1.2. The Effect of DNA Concentration on Reliability and Reproducibility of SYBR Green Dye-based Real Time PCR Analysis to Detect the Exon Rearrangements

Up to date more than 200 different mutations of *MECP2* have been reported in patients with classical and atypical RTT (RettBASE). MECP2 exon rearrangements are very frequently observed and identified in 2.9- 14 per cent of patients with RTT. Previously, the identification of MECP2 gene rearrangements was carried out by traditional methods including Southern blotting, fluorescent in situ hybridization (FISH), and Long-Range PCR and subsequent DNA sequencing analysis. So far, no rearrangements of the MECP2 gene have been identified by FISH and these approaches are time-consuming and may suffer from a limited sensitivity (e.g., the size of rearrangements). To overcome these problems, rapid and sensitive PCR based assays including quantitative fluorescent PCR (QF-PCR), robust dosage PCR (RD-PCR), and multiple ligation-dependent probe amplification (MLPA) have been developed. In these methods, end-point PCRs are accomplished in 20–25 cycles, when amplification is supposed to be in its exponential phase such that a linear relationship between quantities of template DNA and PCR products is maintained. These assays should be considered semi-quantitative since the actual amplification profile of the reaction is based on a theoretical assumption. Real-time PCR was specifically developed to quantify specific DNA targets through the monitoring of product formation. This technology has been successfully applied for the detection of hemizygous deletions or duplications in different genetic disorders. Recently, quantitative real-time PCR assays based on SYBR Green I dye and TaqMan probe has been developed for the detection of deletions/duplications of the MECP2 gene (Ariani *et al*., 2004; Laccone *et al*., 2004).

Several studies have shown that DNA extraction methods, presence of inhibitors and inefficient homogenization of the sample may lead to false negative results. This may lead to reduced efficiency of real time PCR reaction and underestimation of the quantity of the target DNA upon reaction. The purpose of our study was to analyse the effect of DNA concentration on reliablity and reproducibility of SYBR green dye-based real time PCR analysis to detect the exon rearrangments.

We have tested normal DNA samples along with duplication and deletions using six different DNA concetrations (ranging from 0.1 to 200 ng) in triplicate measurements. The expected copy number ratio (± 2SD) was obtained in all cases when DNA concentration is between 1 to 50 ng. The ratio was out of expected range in six and four of 15 measurements with 0.1 and 100 ng DNA, respectively, and led to misgenotyping of the samples. Expected copy number could never be obtained with 200 ng DNA. These results suggested that Real Time PCR analysis might not be reliable for determination of the exon copy number with DNA in the range of 1-50 ng.

The effect of the DNA concentration on the amplification efficiency and specifity could be observed in amplification curve and melting curve analysis. Using high DNA concentrations (100–200 ng) resulted in inhibition of the amplification and/or nonspecific product formation in some cases. For dilute DNA samples several hypotheses have been proposed to explain misgenotyping. The first issue is the apparent labiality (instability) of the DNA upon prolonged storage periods at low concentrations. Ellison *et al.* (2006) has shown that plastic tube had a strong effect on measured DNA concentration at concentrations below 100 genome equivalents. Teo *et al.* (2002) has observed fluctuations in the concentration of standard solutions even after short time storage in eppendorf tubes due to binding of DNA to the tube walls. Secondly, due to the stochastic distribution of molecules at very low copy number, a sampling error can be introduced when pipetting aliquots of DNA. Measurement variability at low DNA concentration has been demonstrated by the observation that the confidence intervals (representing the measurement uncertainty) associated with amplification from low initial copy numbers of template are much greater than those with high initial copy numbers (Peccoud and Jacob, 1996).

Additionally, we have compared the results obtained using comperative Ct and standard curve methods. A paired sample *t*-test showed that the results by both methods were significantly similar ($P = 0.451 > 0.05$). In addition, the Pearson correlation coefficient of 0.996 ($P = 1E\text{-}6 < 0.01$) demonstrated the equivalence of both methods.

Our study shows that data obtained by the standard curve method and by the comperative Ct method are equally reliable and correlate extremely well. However, the

comperative Ct method appers to be more convenient and efficient to analyze the exon rearrangments in real time PCR experiments. First, it improves the productivity by eliminating the time and effort required to prepare the standards and set up the standard curves. Second, the Ct method reduces the overall cost of assays by reducing the number of reactions run each time and thereby sparing expensive reagents. The only disadvantage of comperative Ct method is use of a single calibrator (reference) DNA sample and the contamination of target DNA with salt, phenol, chloroform and/or ethanol that may cause a low PCR efficiency and miscalculations. In case of standard curve method, serial dilution of the reference sample will also dilute these inhibitors and decrease its effect on the PCR reaction, thereby increasing the PCR efficiency with each dilution step.

6.2. Methylation Analyses of the Putative Promoter Region of hHR23 Genes in Breast Tumor Tissues

Carcinogenesis is a multistep process composed of genetic and epigenetic alterations involving proto-oncogenes, tumor suppressor genes, cell-cycle regulator genes, tissue-invasion-related genes, or mismatch repair genes. Aberrant cytosine methylation of CpG-rich sites was regarded as an epigenetic mechanism for the transcriptional silencing of several repair genes (*BRCA1, hMLH1, O6-MGMT*, *TDG*, and *WRN*) in different types of cancer including breast carcinoma. Recently, Peng *et al*. (2005) has shown that hHR23B gene, a key component in nucleotide excision repair pathway, was epigenetically silenced in Interleukin-6-responsive Multiple Myeloma KAS-6/1 cells lines. This latter finding prompted us to investigate the methylation status of hHR23B and its homolog hHR23A gene in tumor tissues. Additionally, the following cellular functions of both hHR23A and hHR23B make them candidate tumor susceptibility genes: (1) hHR23A/B were also shown to participate not only in NER but also in base excision repair (BER) pathway; (2) The $hHR23B^{KD}$ cell lines and hHR23A/B KO mice exhibit severe UV sensitivity and NER deficiency; (3) hHR23A/B are involved in induction and stability of the damage-signaling tumor-suppressor protein p53; and (4) hHR23B was shown to be required for genotoxic-specific activation of p53 and apoptosis.

In this study, we have analyzed the methylation status of 5' flanking regions (including the CpG islands and putative promoter sequence) of hHR23A and hHR23B

genes in primary breast tumor, tumor adjacent tissues, and normal breast tissues in order to investigate their possible involvement in breast carcinogenesis.

First of all, we have characterized the CpG islands and the putative promoter region in the 5' flanking region of the hHR23A and hHR23B genes using web-based analysis. MethPrimer and PROSCAN softwares revealed two CpG islands (at positions -580/-454 and -341/-55 nts) and a putative eukaryotic Pol II promoter region within the second CpG island (position -48 to -298 nts) with a score of 98.79. The promoter region lacks the CCAAT and TATA-like elements, a common feature of the house-keeping genes. The analysis revealed potential binding sites for the transcription factor Sp1 (two sites), ATF/CREB, Elk-1 and two M22 motifs (5'-TGCGCANK-3'). The analysis of 5' flanking region of hHR23B gene revealed a CCAAT and TATA- box lacking putative Pol II promoter sequence (from position -14 to -264 nts with a score of 217.35) containing four Sp1 binding sites.

The lack of TATA and CAAT boxes, the presence of high C+G content and Sp1 binding sites in the *hHR23A* and *hHR23B* promoters are typical features of house-keeping genes. Yang *et al*. (2007) has shown that three transcription factor binding motifs, Sp1, Elk-1, and M22 are preferentially found in promoters that lack TATA elements. TATA-less promoters are generally enriched in the Sp1 motif that can direct weak transcription initiation from Transcription Start Site *in vitro* from core promoters.(Smale and Kadonaga, 2003). Elk-1, an ETS domain transcription factor of the TCF (ternary complex factor) subfamily, is known to be involved in the regulation of immediate-early genes such as *c-fos* upon mitogen activation, and thus commonly implicated in cell proliferation. The M22 motif (5'-TGCGCANK-3') is the most intriguing one because its potential role in regulation of TATA-independent transcription is not known. The ATF family of transcription factors can form either homodimers or heterodimers with c-Jun and subsequently bind to the cyclic AMP response element (CRE) (5'-TGACGTCA-3') (van Dam *et al*., 1993). The transcription factor ATF-2 is a nuclear target of stress-activated protein kinases (such as p38), that are activated by various extra-cellular stresses, including UV light, osmotic stress, hypoxia, and inflammatory cytokines (Morrison *et al*., 2003). ATF-2 plays a critical role in hypoxia- and high-cell-density-induced apoptosis, growth control, and the development of mammary tumors. The ATF-2 mRNA levels in human

breast cancers were lower than those in normal breast tissue (Maekawa *et al*., 2007). Since hHR23A was shown to interact with stress-related factors (eEF1A, Hsp70, and Hsp71) (Chen and Madura, 2006), it might be a novel target of stress-activated protein kinases via the transcription factor ATF.

The methylation status of the CpG islands was investigated by bisulfite-sequencing method. Semi-nested PCR strategy was used to amplify the bisulfite modified DNA samples. PCR fragments could be produced in 38 samples for hHR23A gene and 58 samples for hHR23B gene out of 61 samples tested. The failure in amplification might be due to poor-quality of DNA samples. It is known that the extraction of high-quality nucleic acid from formalin-fixed tissues might not be possible because of cross-linking between proteins and DNA. The fixation and paraffin embedding processes might also damage the DNA. Additionally, formalin-fixed tissues undergo degradation possibly because of an inadequate neutralization of the formalin, eventually resulting in acid depurination. The acid is known to depurinate the DNA and destroy its structure, thus preventing amplification (Goelz *et al*., 1985). In retrospective studies using fixed tissues, the primers must be carefully chosen to generate smaller amplification products, because larger DNA fragments are more difficult to amplify (Rivero *et al*., 2006). This is in accordance with our results that amplification of hHR23B gene was more successful than hHR23A gene (95% vs 62%) since the hHR23B primers generated smaller PCR products. The agarose gel electrophoresis showed that paraffin embedded tissue DNAs are more fragmented when compared to DNAs isolated from peripheral blood supporting the findings of poor preservation and high degradation of DNA extracted from fixed tissues.

The methylation status of hHR23A and hHR23B genes could be determined in 35 of 38 and 51 of 58 samples, respectively. Briefly, methylation analysis of 5' flanking region of hHR23A gene revealed cytosine methylation in 12 tumor and 2 tumor adjacent tissues. Hypermethylation was observed in four tumors (from patients Rad21, 27T, 31T, and 32T) and one tumor adjacent tissue sample (Rad31N). Two patients (Rad17 and 28T) have single CpG methylation and seven patients (Rad4, 6, 15, 29T, 29N, 33T, and 48) have non-CpG methylation. Cytosine methylation (CpG and non-CpG) in the upstream of hHR23B gene was observed in 15 tumor tissues. CpG methylation was observed in six patients (Rad9, 13, 16, 20, 22, and 27T) and non-CpG methylation was also present in three of

them (Rad9, 20, and 22). Nine patients have only non-CpG methylation. The methylated cytosine residues were within the Sp1 binding sites in patients Rad9, 17, 22, 27T, 32T, and 50. The methylated C*CpWGG motif was present in four samples (Rad2, 9, 25T, and 30T).

The methylation analysis revealed either hypermethylation or cytosine methylation of single CpG and non-CpG methylation in the putative promoter region of hHR23 genes. It is known that hypermethylation of CpG island in the promoter region is generally associated with transcription silencing. Intriguingly, Pogribny *et al*. (2000) and Veerla *et al*. (2008) have shown that single CpG methylation could down regulate the expression of the p53 and IRF7 genes, respectively. It was also reported that methylation of single non-CpG dinucleotides (CpA or CpC) within the transcription binding site could affect the expression pattern of the genes (Veerla *et al*. 2008).

Until recently, a few studies reported cytosine methylation of non-CpG dinucleotides in genomic DNAs from human carcinomas and its involvement in the carcinogenesis. Two recent studies have reported non-CpG methylation pattern in B cell-specific B29 gene in Primary Effusion Lymphoma, and p53 gene in non-small cell lung carcinoma (Malone *et al*., 2001; Kouidou *et al*., 2005 and 2006). Analysis of the p53 exon 5 mutation spectrum in mutation databases for lung cancer revealed frequent G:C > A:T transitions, several of which occur at non-CpG methylated sequences. Additionally, non-CpG methylation was observed in the tissues adjacent to the tumor in the lung, which indicates that non-CpG methylation may appear in the early stage of carcinogenesis and serve as a useful tool for early cancer detection (Kouidou *et al*., 2005). Thus, the findings of present study might be the additional support for the involvement of non-CpG methylation in carcinogenesis.

A specific pattern of non-CpG methylation in the C*CpWGG motif was reported in plants and few human genes including p53 and B29 genes. The cytosine methylation of C*CpWGG motif in the promoter region of p53 and B29 genes resulted in transcriptional silencing (Malone *et al*., 2001; Agirre *et al*., 2003). We have identified methylated C*CpWGG motif in *hHR23B* in four tumor samples (Rad2, 9, 25T, and 30T). The methylated C*CpWGG motif was at positition -212/-208 in Rad2 and 30T whereas C*CpWGG motif at positition -151/-147 was methylated in samples Rad9 and 25T. Based

on the above observations, we could speculate that the presence of methylated C*CpWGG motif in the promoter region might affect the transcription of the hHR23B gene in the tumor tissues.

We have observed that the methylated cytosine residues were within the Sp1 binding sites in hHR23B gene in patients Rad9, 17, 22, 27T, 32T, and 50. The affected Sp1 binding site (at position -135/-126) is the same in five of them whereas the Sp1 site at position -270/-261 was methylated in tumor sample Rad27T. Butta *et al*. (2006) has shown that the in vitro transcription of the human podocalyxin (*Podxl*) promoter is dependent on the presence of Sp1 sites. The progressive rise in the promoter activity directly correlates with the number of recognition sites for Sp1. The methylation or deletion of Sp1 element resulted in repression of Podxl gene (Butta *et al*., 2006). The findings of Butta *et al*. (2006) and Veerla *et al*. (2008) prompted us to speculate that the cytosine methylation in Sp1 binding site might interfere the binding of Sp1 and down regulate the transcription of hHR23B in tumor tissues Rad9, 17, 22, 27T, and 32T.

In five samples, hHR23A gene was partially hypermethylated. However, the extent and the position of the methylation site were different in each sample. The down-stream region (positions +6/+117) of TSS site was hypermethylated in tumor adjacent tissue Rad31N whereas hypermethylation spread to the upstream region (between -249/+117 nts) of TSS site in tumor tissue of the same sample (Rad31T). The upstream region was hypermethylated in sample Rad21 whereas both upstream and downstream regions were hypermethylated in samples Rad27T, 31T, and 32T. The observed non-uniformity in hypermethylation pattern suggest that the methylation initiation site is probably similar in four samples and within downstream of TSS (position +1/+117) whereas it is different in sample Rad21 probably being between -249/-27 nts. It is known that the spreading of methylation from the foci of methylated CpG sites is a common event in tumor tissues.

Two samples have cytosine methylation within upstream region of *hHR23A* in both tumor and adjacent tissues. Patient Rad29 has CpC methylation at position -114/-113 in tumor adjacent tissue (Rad29N) whereas CpT and CpA di-nucleotides were methylated at positions -133/-132 and +11/+12 in the tumor tissue (Rad29T). The region between nucleotide positions +6/+117 was hypermethylated in tumor adjacent tissue Rad31N

whereas hypermethylation spread to the region between -249/+117 nts in tumor tissue of the same sample (Rad31T). The observation of cytosine methylation in tissues adjacent to tumor is consistent with previously reported findings (Kouidou *et al*., 2005). The cytosine methylation pattern in samples Rad25T, 27T, 28T, 30T, 32T, and 33T was not present in corresponding tumor adjacent tissues suggesting that the observed *de novo* methylation is specific to tumor formation. Additionally, cytosine methylation was not observed in five DNA samples isolated from peripheral blood tissue.

We could not obtain statistical differences among patients when compared with respect to the presence, type, and position of methylation in *hHR23A or hHR23B*. On the other hand, correlations based on histopathological features of the samples implicate some preliminary features. For example, in all patients (Rad21, 27T, 31T, and 32T) showing hypermethylation of hHR23A gene, lymph node metastasis (LNM) was positive and showed high grade (III) and stage (pT2Nx) tumor progression. The Estrogen Receptor (*ER*) expression was positive in all samples. *c-erbB-2* expression was negative in tumor samples Rad27T, 31T, and 32T, however,it was expressed in tumor tissue Rad21 showing different methylation initiation site in the upstream region of TSS. Among the patients (Rad9, 17, 22, 27T, 32T, and 50) presenting methylated cytosine residues within the Sp1 binding sites in hHR23B gene, there is no uniformity in histopathological features of tumor tissues. However, the bisulfite sequencing revealed that three of them (samples Rad17, 27T, and 32T) have cytosine methylation in both hHR23A and hHR23B genes. The sample Rad27T showed hypermethylated region (between nts -226/+117) in hHR23A and methylated cytosine residue within the Sp1 binding site (-270/-261) in hHR23B gene. Similarly, upstream region (between -121/+117 nts) of hHR23A gene was hypermethylated along with the cytosine residue within the Sp1 binding site (-135/-126) in hHR23B gene in patient Rad32T. Sample Rad17 has CpC methylation at position -116/-115 and methylated cytosine residue within the Sp1 binding site (-135/-126) in hHR23A and hHR23B genes, respectively. Among the patients (Rad2, 9, 25T, and 30T) having the methylated C*CpWGG motif in the *hHR23B* promoter region, the histological grade of tumor showed differences according to the position of methylated C*CpWGG motif. The tumor grade was II in samples Rad2 and Rad30T whereas the grade is higher in samples Rad9 and Rad25T.

The methylated cytosine residues were not seem to be within the conserved motifs or transcription binding sites in samples Rad4, 6, 15, 17, 28T, 29T, 29N, 33T, and 48 for hHR23A and Rad13, 14, 16, 20, 46, and 51 for hHR23B genes. Bisulfite sequencing of HHR23A and hHR23B revealed no methylation in 21 and 36 tissue samples, respectively. There was no significant histopathological difference among these samples.

In conclusion, there are no known reports investigating the role of methylation of hHR23A and hHR23B genes in the tumor tissues (breast cancer). The observations of the hypermethylation of hHR23A gene and the presence of methylated conserved motifs and transcription binding sites in hHR23B gene among tumor tissues suggested the involvement of methylation of hHR23 genes in the breast carcinogenesis. However, the expression pattern of methylated hHR23 genes should be investigated in fresh or frozen tumor tissues. If the promoter methylation correlates with loss of protein expression, methylation status of hHR23 genes could be a marker in breast carcinomas. It is known that the genetic and epigenetic alterations that initiate and drive cancer can be used as targets for detection of neoplasia in bodily fluids. Several studies showed that tumor cell-specific aberrant promoter hypermethylation can be detected in nipple aspirate and ductal lavage from breast cancer patients and the results were concordant between tumor and circulating DNA methylation (Dulaimi *et al*., 2004; Mirza *et al*., 2007). Hypermethylation-based screening of serum, a readily accessible bodily fluid and pre-invasive method, may enhance early detection of breast cancer.

6.3. Molecular Basis of Congenital Hypothyroidism

We have investigated the genetic mechanisms leading to hypothyroidism in a child with CH associated with bilateral choanal atresia, cleft palate, and spiky hair. Direct sequencing of coding exon of *TTF-2* gene from the patient revealed a novel homozygous missense mutation (c.304C>T; p.R102C) affecting the forkhead DNA binding domain of TTF-2. Both parents were heterozygous for the mutation but euthyroid with no congenital anomalies, and the mutation was absent in 100 control chromosomes. The arginine residue at codon 102 is a highly conserved residue in the forkhead domain family of proteins, and mutations of the equivalent amino acid in other forkhead proteins [e.g. FOXC1 (R127H), FOXC2 (R121H), and FOXP2 (R553H)] have been described. Consonant with this, in

vitro studies (performed in University of Cambridge, UK) indicated that the mutation was highly deleterious, with the p.R102C mutant protein exhibiting negligible DNA binding and transcriptional activity (Appendix 1). Interestingly, thyroid ultrasonography and CT examination of the proband indicated thyroid tissue in a eutopic location, although biochemical measurements and radioisotope scanning show that it is nonfunctional.

Our case represents the third recorded example of a loss-of-function mutation in the human TTF-2 gene, with the two previously described mutations (A65V and S57N) also being located within its forkhead, DNA-binding domain (Clifton-Bligh *et al*., 1998; Castanet *et al*., 2002). The A65V mutation was identified in a nonconsanguineous Welsh family with two male siblings exhibiting CH, cleft palate, choanal atresia, and bifid epiglottis together with spiky hair, whereas the S57N mutation was reported in two male siblings of a consanguineous Tunisian kindred exhibiting CH and cleft palate alone. With both of these TTF-2 mutation cases, 123I scanning and ultrasonography showed complete athyreosis (Clifton-Bligh *et al*., 1998; Castanet *et al*., 2002). In contrast, although the third case we report here shares some of these features, including severe CH and extrathyroidal anomalies, imaging indicates the presence of thyroid tissue in a eutopic location. However, severe biochemical hypothyroidism at birth and also following T4 withdrawal, together with absent ^{131}I uptake and very low serum thyroglobulin levels, indicates that the function of such glandular tissue is markedly compromised.

Mouse models support a critical role for TTF-2 in thyroid and palate organogenesis. Expression of TTF-2, together with the transcription factors TTF-1 and PAX-8, has been demonstrated from the onset of formation of the thyroid primordium (embryonic d 8–8.5), continuing throughout the migration of the thyroid diverticulum (Kimura *et al*., 1996; Zannini et a., 1997; Mansouri *et al*., 1998). TTF-2 is also expressed in craniopharyngeal ectoderm involved in palate formation and Rathke's pouch in mouse embryos (Zannini et a., 1997) and in the outer follicular hair sheath in humans (Sequeira *et al*., 2003). Targeted disruption of the murine Titf2 locus results in homozygous null mice with cleft palate and either complete thyroid agenesis or ectopic sublingual gland development (De Felice *et al*., 1998). The two murine phenotypes were seen with equal frequency and may reflect different developmental manifestations of the disorder. Thus, similar to the murine context,

our human proband illustrates that thyroid morphogenesis can occur in the absence of TTF-2, albeit with migration of thyroid gland tissue to a eutopic location.

Mutations in TTF-2 and a TTF-1/NKX2.1 mutation (Krude *et al*., 2002) are the only known genetic causes of thyroid agenesis. However, involvement of TTF-2 accounts for only a small minority of CH cases, being a strong consideration only in those with cleft palate, which is an infrequent association of CH (Olivieri *et al*., 2002). This case illustrates further phenotypic heterogeneity associated with human TTF-2 mutations and suggests that defects in this gene should also be considered in cases of syndromic CH with cleft palate, but not necessarily complete thyroid agenesis. This variable phenotype may reflect differential effects of TTF-2 mutations on downstream target genes required for normal human thyroid organogenesis, migration, and differentiation, and the further identification of such genes may elucidate these mechanisms and provide novel genetic candidates for CH and cleft palate.

6.3.1. Mutation Analysis of Butyrylcholinesterase (BChE) Gene

The same CH patient with the TTF2 mutation was referred to our lab a year later since she experienced prolonged neuromuscular block after an operation and had a marked decrease in BChE activity compared with her parents and brother. Because BChE is known to hydrolyze the anesthetic reagents we analyzed its two common variants in the patient that can be responsible for reduced plasma cholinesterase and prolonged paralysis. Restriction analysis revealed that the patient, her consanguineous parents and unaffected brother were negative for these variants. However, the whole BChE gene should be screened for variants that might be responsible for the plasma cholinesterase deficiency.

To our knowledge this patient was the first case with CH showing the prolonged neuromuscular block. Patients with CH are candidates for multiple operations due to midline defects (e.g. cleft palate and choanal atresia) and their responses to muscle relaxants are not known. Therefore, careful preoperative evaluation and molecular genetic testing should be performed.

7. CONCLUSION AND FUTURE PROSPECTS

To our knowledge, this is the first study on genetic basis of Rett Syndrome in our population. Our findings suggest that gene dosage can be a mechanism that leads to this devastating genetic/epigenetic disease. We have shown the duplication of exons that are known to be the expressed. As a future prospect, the breakpoints of the duplications, whether they are tandem repeats, and their effect on *MECP2* expression can be investigated in these patients.

The findings of methylation analyses of hHR23A and hHR23B prompted us to speculate that the cytosine methylation of putative promoter region may down regulate transcription of hHR23A and hHR23B genes in tumor tissues. Additional studies can be performed to investigate the expression pattern of methylated hHR23 genes in fresh or frozen tumor tissues. Methylation status of hHR23 genes may be tested as a candidate marker in breast carcinomas upon correlation of promoter methylation with the loss of expression. Additionally, the body fluids could be investigated for the presence of aberrant promoter hypermethylation. If the results were concordant between tumor and circulating DNA methylation, the screening of hHR23 methylation may enhance early detection of breast cancer.

The identification of TTF2 mutation in a CH patient with thyroid tissue suggested that further phenotypic heterogeneity is associated with human TTF-2 mutations and the CH patients with thyroid tissue should also be screened for the mutations within the TTF2 gene. Further mutations should be identified and investigated to unravel the functions of TTF2 in thyroid organogenesis.

REFERENCES

Abramowicz, M. J., L. Duprez, J. Parma, G. Vassart and C. Heinrichs, 1997, "Familial congenital hypotyroidism due to inactivating mutation of the thyrotropin receptor causing profound hypoplasia of the thyroid gland", *The Journal of Clinical Investigation*, Vol. 99, No. 12, pp. 3018-3024, June.

Agirre, X., J. L. Vizmanos, M. J. Calasanz, M. Garcia-Delgado, M. J. Larrayoz and F. J. Novo, 2003, "Methylation of CpG dinucleotides and/or CCWGG motifs at the promoter of TP53 correlates with decreased gene expression in a subset of acute lymphoblastic leukemia patients", *Oncogene*, Vol. 22, No. 7, pp. 1070-1072, February.

Akarsu, A. N., I. Stoilov, E. Yilmaz, B. S. Sayli and M. Sarfarazi, 1996, "Genomic structure of HOXD13 gene: a nine polyalanine duplication causes synpolydactyly in two unrelated families", *Human Molecular Genetics*, Vol. 5, No. 7, pp. 945-952, July.

Allen, R. C., H. Y. Zoghbi, A. B. Moseley and H. M. Rosenblatt, 1992, "Methylation of HpaII and HhaI sites near the polymorphic CAG repeat in the human androgen-receptor gene correlates with X chromosome inactivation", *American Journal of Human Genetics,* Vol. 51, pp. 1229-1239.

Amir, R. E., I. B. Van den Veyver and M. Wan, 1999, "Rett syndrome is caused by mutations in X-linked MECP2, encoding methyl-CpG-binding protein 2", *Nature Genetics,* Vol. 23, No. 2, pp. 185-188, October.

Ang, S., A. Wierda, D. Wong, D. Stevens, S. Cascio, J. Rossant and K. S. Zaret, 1993, "The formation and maintenance of the definitive endoderm lineage in the mouse: involvement of HNF3/forkhead proteins", *Development*, Vol. 119, No. 4, pp. 1301-1315, December.

Antequera, F. and A. Bird, 1993, "Number of CpG islands and genes in human and mouse", *Proceedings of the National Academy of Sciences of the United States of America*, Vol. 90, No. 24, pp. 11995-11999, December.

Araki, M., C. Masutani, M. Takemura, A. Uchida, K. Sugasawa, J. Kondoh, Y. Ohkuma and F. Hanaoka, 2001, "Centrosome protein centrin 2/caltractin 1 is part of the xeroderma pigmentosum group C complex that initiates global genome nucleotide excision repair", *Journal of Biological Chemistry,* Vol. 276, No. 22, pp. 18665-18672, June.

Archer, H. L., J. C. Evans, D. S. Millar, P. W. Thompson, A. M. Kerr, H. Leonard, J. Christodoulou, D. Ravine, L. Lazarou, L. Grove, C. Verity, S. D. Whatley, D. T. Pilz, J. R. Sampson and A. J. Clarke, 2006, "NTNG1 mutations are a rare cause of Rett syndrome", *American Journal of Medical Genetics*, Vol. 140, No. 7, pp. 691-694, April.

Archer, H. L., S. D. Whatley, J. C. Evans and D. Ravine, 2006, "Gross rearrangements of the MECP2 gene are found in both classical and atypical Rett syndrome patients", *Journal of Medical Genetics,* Vol. 43, pp. 451-456.

Ariani, F., F. Mari, C. Pescucci and I. Longo, 2004, "Real-time quantitative PCR as a routine method for screening large rearrangements in Rett syndrome: Report of one case of MECP2 deletion and one case of MECP2 duplication", *Human Mutation,* Vol. 24, pp. 172-177, August.

Armstrong, D. D., 2005, "Neuropathology of Rett syndrome", *Journal of Child Neurology*, Vol. 20, No. 9, pp. 747-753, September.

Asaka, Y., D. G. Jugloff, L. Zhang, J. H. Eubanks and R. M. Fitzsimonds, 2006, "Hippocampal synaptic plasticity is impaired in the Mecp2-null mouse model of Rett syndrome", *Neurobiological Disorders*, Vol. 21, No. 1, pp. 217-227.

Ausio, J., D. B. Levin, G. V. de Amorim, S. Bakker and P. M. Macleod, 2003, "Syndromes of disordered chromatin remodeling", *Clinical Genetics*, Vol. 64, pp. 83-95.

Aza-Blanc, P., R. Di Lauro and P. Santisteban, 1993, "Identification of a cisregulatory element and a thyroid-specific nuclear factor mediating the hormonal regulation of rat thyroid peroxidase promoter activity", *Molecular Endocrinology*, Vol. 7, pp. 1297-1306.

Bale, T. L. and W.W. Vale, 2004, "CRF and CRF receptors: role in stress responsivity and other behaviors", *Annual Review of Pharmacology and Toxicology*, Vol. 44, pp. 525-557.

Ballestar, E., T. M. Yusufzai and A. P. Wolffe, 2000, "Effects of Rett syndrome mutations of the methyl-CpG binding domain of the transcriptional repressor MeCP2 on selectivity for association with methylated DNA", *Biochemistry,* Vol. 39, pp. 7100-7106.

Ballestar, E., S. Ropero, M. Alaminos, J. Armstrong, F. Setien, R. Agrelo, M. F. Fraga, M. Herranz, S. Avila, M. Pineda, E. Monros and M. Etseller, 2005, "The impact of MECP2 mutations in the expression patterns of Rett syndrome patients", *Human Genetics*, Vol. 116, No. 1-2, pp. 91-104.

Balmer, D., J. Goldstine, Y. M. Rao and J. M. LaSalle, 2003, "Elevated methyl-CpG-binding protein 2 expression is acquired during postnatal human brain development and is correlated with alternative polyadenylation", *Journal Molecular Medicine*, Vol. 81, No. 1, pp. 61-68, January.

Bamforth, J. S., I. A. Hughes, J. H. Lazarus, C. M. Weaver and P. S. Harper, 1989, "Congenital hypothyroidism, spiky hair, and cleft palate", *Journal of Medical Genetics*, Vol. 26, pp. 49-51.

Barış, I., A. E. Arisoy, A. Smith, M. Agostini, C.S. Mitchell, S.M. Park, A.M. Halefoglu, E. Zengin, V.K. Chatterjee and E. Battaloglu, 2006, "A novel missense mutation in human TTF-2 (FKHL15) gene associated with congenital hypothyroidism but not

athyreosis", *Journal of Clinical Endocrinology and Metabolism*, Vol. 91, pp. 4183-4187, October.

Beever, C., B. P. Lai, S. E. Baldry and M. S. Penaherrera, 2003, "Methylation of ZNF261 as an assay for determining X chromosome inactivation patterns", *American Journal of Medical Genetics Part A,* Vol. 120, pp. 439-441.

Belichenko, P. V., A. Oldfors, B. Hagberg and A. Dahlström, 1994, "Rett syndrome: 3-D confocal microscopy of cortical pyramidal dendrites and afferents", *Neuroreports*, Vol. 5, No. 12, pp. 1509-1513.

Bell, A. C. and G. Felsenfeld, 2000, "Methylation of a CTCF-dependent boundary controls imprinted expression of the Igf2 gene", *Nature*, Vol. 405, pp. 482-485.

Berry, F. B., R. A. Saleem and M. A. Walter, 2002, "FOXC1 transcriptional regulation is mediated by N- and C-terminal activation domains and contains a phosphorylated transcriptional inhibitory domain", *The Journal of Biological Chemistry*, Vol. 277, pp. 10292-10297.

Bertani, I., L. Rusconi, F. Bolognese, G. Forlani, B. Conca, L. De Monte, G. Badaracco, N. Landsberger and C. Kilstrup-Nielsen, 2006, "Functional consequences of mutations in CDKL5, an X-linked gene involved in infantile spasms and mental retardation", *Journal of Biological Chemistry*, Vol. 281, No. 42, pp. 32048-32056, October.

Biard, D.S., 2007, "Untangling the relationships between DNA repair pathways by silencing more than 20 DNA repair genes in human stable clones", *Nucleic Acids Research*, Vol. 35, No. 11, pp. 3535-3550.

Bienvenu, T., A. Carrie, N. de Roux and M. C. Vinet, 2000, "MECP2 mutations account for most cases of typical forms of Rett syndrome", *Human Molecular Genetics,* Vol. 9, pp. 1377-1384.

Bienvenu, T. and J. Chelly, 2006, "Molecular genetics of Rett syndrome: when DNA methylation goes unrecognized", *Nature Reviews. Genetics*, Vol. 7, No. 6, pp. 415-426.

Biggins, S., I. Ivanovska and M. D. Rose, 1996, "Yeast ubiquitin-like genes are involved in duplication of the microtubule organizing center", *The Journal of Cell Biology*, Vol. 133, No. 6, pp. 1331-46.

Bird, A., 2002, "DNA methylation patterns and epigenetic memory", *Genes and Development*, Vol. 16, pp. 6-21.

Borg, I., K. Freude, S. Kübart, K. Hoffmann, C. Menzel, F. Laccone, H. Firth, M. A. Ferguson-Smith, N. Tommerup, H. H. Ropers, D. Sargan and V. M. Kalscheuer, 2005, "Disruption of Netrin G1 by a balanced chromosome translocation in a girl with Rett syndrome", *European Journal of Human Genetics*, Vol. 13, No. 8, pp. 921-927.

Bradsher, J., J. Auriol, L. Proietti de Santis, S. Iben, J. L. Vonesch, I. Grummt and J. M. Egly, 2002, "CSB is a component of RNA pol I transcription", *Molecular Cell*, Vol. 10, pp. 819-829.

BreastCancer.org, 2008, *what is breast cancer*, www.cancer.org/docroot/CRI/content/CRI_2_4_1X_what_is_breast_cancer_5.asp.

Brignone, C., K. E. Bradley, A. F. Kisselev and S.R. Grossman, 2004, "A post-ubiquitination role for MDM2 and hHR23A in the p53 degradation pathway", *Oncogene*, Vol. 20, No. 23, pp. 4121-4129.

Brooks, A. R., R. N. Harkins, P. Wang,H. S. Qian, P. Liu and G. M. Rubanyi, 2004, "Transcriptional silencing is associated with extensive methylation of the CMV promoter following adenoviral gene delivery to muscle", *Journal of Gene Medicine*, Vol. 6, pp. 395-404.

Brownawell, A.M., G. J. Kops, I. G. Macara and B. M. Burgering, 2001, "Inhibition of nuclear import by protein kinase B (Akt) regulates the subcellular distribution and activity of the forkhead transcription factor AFX", *Molecular and Cellular Biology*, Vol. 21, No. 3534- 3546.

Buschdorf, J. P. and W. H. Strätling, 2004, "A WW domain binding region in methyl-CpG-binding protein MeCP2: impact on Rett syndrome", *Journal Molecular Medicine*, Vol. 82, No. 2, pp. 135-143, February.

Butta, N., S. Larrucea, S. Alonso, R. B. Rodriguez, E. G. Arias-Salgado, M. S. Ayuso, C. González-Manchón and R. Parrilla, 2006, "Role of transcription factor Sp1 and CpG methylation on the regulation of the human podocalyxin gene promoter", *BMC Molecular Biology*, Vol. 9, pp. 7-17.

Carlsson, P. and M. Mahlapuu, 2002, "Forkhead transcription factors: Key players in development and metabolism", *Developmental Biology*, Vol. 250, pp. 1-23.

Castanet, M., S. Lyonnet, C. Bonaı¨ti-Pellie´, M. Polak, P. Czernichow, P. and J. Le´ger, 2000, "Familial forms of thyroid dysgenesis among infants with congenital hypothyroidism", *The New England Journal of Medicine*, Vol. 343, pp. 441-442.

Castanet, M., M. Polak, C. Bonaiti-Pellie, S. Lyonnet, P. Czernichow and J. Leger, 2001, "Nineteen years of national screening for congenital hypothyroidism: familial cases with thyroid dysgenesis suggest the involvement of genetic factors", *The Journal of Clinical Endocrinology and Metabolism*, Vol. 86, pp. 2009-2014.

Castanet, M., S. M. Park, A. Smith, M. Bost, J. Leger, S. Lyonnet, A. Pelet, P. Czernichow, V. K. Chatterjee and M. Polak, 2002, "A novel loss-of-function mutation in TTF-2 is associated with congenital hypothyroidism thyroid agenesis and cleft palate", *Human Molecular Genetics*, Vol. 11, pp. 2051-2059.

Chadwick, B. P., F. Obermayr and A. M. Frischauf, 1997, "FKHL15, a new human member of the forkhead gene family located on chromosome 9q22", *Genomics*, Vol. 41, pp. 90-396.

Chahrour, M. and H. Y. Zoghbi, 2007, "The Story of Rett Syndrome: From Clinic to Neurobiology", *Neuron,* Vol. 56, pp. 422-437.

Chan, S. W. -L., I. R. Henderson and S. E. Jacobsen, 2005, "Gardening the genome: DNA methylation in Arabidopsis thaliana", *Nature Reviews. Genetics*, Vol. 6, pp. 351-360.

Chan, H. W., J. S. Miller, M. B. Moore and C. T. Lutz, 2005, "Epigenetic control of highly homologous killer Ig-like receptor gene alleles" *The Journal of Immunology*, Vol 175, No. 9, pp. 5966-5974.

Chang, Q., G. Khare, V. Dani, S. Nelson and R. Jaenisch, 2006, "The disease progression of Mecp2 mutant mice is affected by the level of BDNF expression" *Neuron*, Vol. 49, No. 3, pp. 341-348, February.

Chao, H. T., H. Y. Zoghbi and C. Rosenmund, 2007, "MeCP2 controls excitatory synaptic strength by regulating glutamatergic synapse number", *Neuron*, Vol. 56, No. 1, pp. 58-65.

Cheadle, J.P., H. Gill, N. Fleming and J. Maynard, 2000, "Long-read sequence analysis of the MECP2 gene in Rett syndrome patients: correlation of disease severity with mutation type and location", *Human Molecular Genetics,* Vol. 9, pp. 1119-1129.

Chen, L., U. Shinde, T. G. Ortolan and K. Madura, 2001, „Ubiquitin-associated (UBA) domains in Rad23 bind ubiquitin and promote inhibition of multi-ubiquitin chain assembly", *EMBO Reports*, Vol. 2, No. 10, pp. 933-938.

Chen, L. and K. Madura, 2002, "Rad23 promotes the targeting of proteolytic substrates to the proteasome" *Molecular and Cellular Biology*, Vol. 22, No. 13, pp. 4902-4913.

Chen, L. and K. Madura, 2006, "Evidence for distinct functions for human DNA repair factors hHR23A and hHR23B", *FEBS Letters*, Vol. 580, No. 14, pp. 3401-3408.

Chen, R. Z., S. Akbarian, M. Tudor and R. Jaenisch, 2001, "Deficiency of methyl-CpG binding protein-2 in CNS neurons results in a Rett-like phenotype in mice", *Nature Genetics*, Vol. 27, No. 3, pp. 327-331, March.

Chen, W.G., Q. Chang, Y. Lin, A. Meissner, A. E. West, E. C. Griffith, R. Jaenisch and M. E. Greenberg, 2003, "Derepression of BDNF transcription involves calcium-dependent phosphorylation of MeCP2", *Science*, Vol. 302, No. 5646, pp. 885-889, October.

Clark, K. L., E. D. Halay, E. Lai and S. K. Burley, 1993, "Co-crystal structure of the HNF-3/fork head DNA-recognition motif resembles histone H5", *Nature*, Vol. 364, pp. 412-420.

Clarke, D. J., G. Mondesert, M. Segal, B. L. Bertolaet, S. Jensen, M. Wolff, M. Henze and S. I. Reed, 2001, "Dosage suppressors of pds1 implicate ubiquitin-associated domains in checkpoint control", *Molecular and Cellular Biology*, Vol. 21, No. 6, pp. 1997-2007.

Clifton-Bligh, R. J., J. M. Wentworth, P. Heinz, M. S. Crisp, R. John, J. H. Lazarus, M. Ludgate and K. Chatterjee, 1998, "Mutation of the gene encoding human TTF-2 associated with thyroid agenesis cleft palate and choanal atresia", *Nature Genetics*, Vol. 19, pp. 399-401.

Cohen, D., G. Lazar, P. Couvert, V. Desportes, D. Lippe, P. Mazet and D. Héron, 2002, "MECP2 mutation in a boy with language disorder and schizophrenia", *American Journal of Psychiatry*, Vol. 159, No. 1, pp. 148-149, January.

Collins, A. L., J. M. Levenson, A. P. Vilaythong, R. Richman, D. L. Armstrong, J. L. Noebels, J. David Sweatt and H. Y. Zoghbi, 2004, "Mild overexpression of MeCP2

causes a progressive neurological disorder in mice", *Human Molecular Genetics*, Vol. 13, No. 21, pp. 2679-2689.

Colvin, L., H. Leonard, N. de Klerk and M. Davis M, 2004, "Refining the phenotype of common mutations in Rett syndrome", *Journal of Medical Genetics,* Vol. 41, pp. 25-30.

Congdon, T., L. Q. Nguyen, C. R. Nogueira, R. L. Habiby, G. Medeiros-Neto and P. Kopp, 2001, "A novel mutation (Q40P) in PAX8 associated with congenital hypothyroidism and thyroid hypoplasia: evidence for phenotypic variability in mother and child", *The Journal of Clinical Endocrinology and Metabolism*, Vol. 86, pp. 3962-3967.

Couvert, P., T. Bienvenu, C. Aquaviva and K. Poirier, 2001, "MECP2 is highly mutated in X-linked mental retardation", *Human Molecular Genetics,* Vol. 10, pp. 941-946.

Dai, G., O. Levy and N. Carrasco, 1996, "Cloning and characterization of the thyroid iodide transporter", *Nature*, Vol. 379, pp. 458-460.

Dani, V. S., Q. Chang, A. Maffei, G. G. Turrigiano, R. Jaenisch and S. B. Nelson, 2005, "Reduced cortical activity due to a shift in the balance between excitation and inhibition in a mouse model of Rett syndrome", *Proceedings of the National Academy of Sciences of the United States of America,* Vol. 102, No. 35, pp. 12560-12565.

Damante, G., R. DiLauro, 1994, "Thyroid-specific gene expression", *Biochimica et Biophysica Acta*, Vol. 1218, pp. 255-266.

De Boer, J. and J. H. Hoeijmakers, 2000, "Nucleotide excision repair and human syndromes", *Carcinogenesis*, Vol. 21, pp. 453-460.

De Felice, M., C. Ovitt, E. Biffali, A. Rodriguez-Mallon, C. Arra, K. Anastassiadis, P. E. Macchia, M. G. Mattei, A. Mariano, H. Scholer, V. Macchia and R. Di Lauro, 1998,

"A mouse model for hereditary thyroid dysgenesis and cleft palate", *Nature Genetics*, Vol. 19, pp. 395-398.

Del Gaudio, D., P. Fang, F. Scaglia and P. A. Ward, 2006, "Increased MECP2 gene copy number as the result of genomic duplication in neurodevelopmentally delayed males", *Genetics in Medicine,* Vol. 8, pp. 784-792.

Devos, H., C. Rodd, N. Gagne, R. Laframboise and G. Van Vliet, 1999, "A search for the possible molecular mechanisms of thyroid dysgenesis: sex ratios and associated malformations", *The Journal of Clinical Endocrinology and Metabolism*, Vol. 84, pp. 2502-2506.

Devriendt, K., C. Vanhole, G. Matthis and F. De Zegher, 1998, "Deletion of thyroid transcription factor-1 gene in an infant with neonatal thyroid dysfunction and respiratory failure", *The New England Journal of Medicine*, Vol. 338, pp. 1317-1318.

Dodge, J. E., B. H. Ramsahoye, Z. G. Wo, M. Okano and E. Li, 2001, "De novo methylation of MMLV provirus in embryonic stem cells: CpG versus non-CpG methylation", *Gene*, Vol. 289, No. 1-2, pp. 41-48.

Dragich, J. M., Y. H. Kim, A. P. Arnold and N. C. Schanen, 2007, "Differential distribution of the MeCP2 splice variants in the postnatal mouse brain", *Journal of Comparative Neurology*, Vol. 501, No. 4, pp. 526-542, April.

Drapkin, R., J. T. Reardon and A. Ansari, 1994, "Dual role of TFIIH in DNA excision repair and in transcription by RNA polymerase II", *Nature*, Vol. 368, pp. 769-772.

Dulaimi, E., J. Hillinck, I. Ibanez de Caceres, T. Al-Saleem and P. Cairns, 2004, "Tumor suppressor gene promoter hypermethylation in serum of breast cancer patients", *Clinical Cancer Research*, Vol. 10, No. 18, pp. 6189-6193.

Egger, G., G. Liang, A. Aparicio and P. A. Jones, 2004, "Epigenetics in human disease and prospects for epigenetic therapy", *Nature*, Vol. 429, pp. 457-463.

Ehrlich, M. and R. Y. Wang, 1981, "5-Methylcytosine in eukaryotic DNA", *Science*, Vol. 212, pp. 1350-1357.

Ekholm, R., 1990, "Biosynthesis of thyroid hormones", *International Review of Cytology*, Vol. 120, pp. 243-288.

Ericson, L. E., and G. Frederiksson, "Phylogeny and ontogeny of the thyroid gland", in M. A. Greer (ed.), *The Thyroid Gland, Comprehensive Endocrinology*, pp. 1-35, Raven Press, New York, 1990.

Evans, J. C., H. L. Archer, J. P. Colley and K. Ravn, 2005, "Early onset seizures and Rettlike features associated with mutations in CDKL5", *European Journal of Human Genetics,* Vol. 13, pp. 1113-1120.

Feaver, W.J., J. Q. Svejstrup and L. Bardwell, 1993, "Dual roles of a multiprotein complex from S. cerevisiae in transcription and DNA repair", *Cell,* Vol. 75, pp. 1379-1387.

Feig, S. A., 2000, "Ductal carcinoma in situ. Implications for screening mammography", *Radiologic Clinics of North America*, Vol. 38, No. 4, pp. 653-68.

Feinberg, A. P. and B. Tycko, 2004, "The history of cancer epigenetics", *Nature reviews. Cancer*, Vol. 4, pp. 143-153.

Finnegan, E. J. and K. A. Kovac, 2000, "Plant DNA methyltransferases", *Plant Molecular Biology*, Vol. 43, pp. 189-201.

Finnegan, E. J., W. J. Peacock and E. S. Dennis, 2000, "DNA methylation, a key regulator of plant development and other processes", *Current Opinion in Genetics and Development*, Vol. 10, No. 2, pp. 217-223.

Fraga, M. F., E. Ballestar, G. Montoya, P. Taysavang, P. A. Wade and M. Esteller, 2003, "The affinity of different MBD proteins for a specific methylated locus depends on

their intrinsic binding properties", *Nucleic Acids Research*, Vol. 31, No. 6, pp. 1765-1774, March.

Francis-Lang, H., M. Price, M. Polycarpou-Schwarz and R. Di Lauro, 1992, "Cell-type-specific expression of the rat thyroperoxidase promoter indicates common mechanisms for thyroid-specific gene expression", *Molecular and Cellular Biology*, Vol. 12, pp. 576-588.

Friez, M. J., J. R. Jones, K. Clarkson and H. Lubs, 2006, "Recurrent infections, hypotonia, and mental retardation caused by duplication of MECP2 and adjacent region in Xq28", *Pediatrics,* Vol. 118, pp. 1687-1695.

Fukuda, T., Y. Yamashita, S. Nagamitsu and K. Miyamoto, 2005, "Methyl-CpG binding protein 2 gene (MECP2) variations in Japanese patients with Rett syndrome: pathological mutations and polymorphisms", *Brain Development,* Vol. 27, pp. 211-217.

Garcia-Closas, M., N. Malats, F. X. Real, R. Welch, M. Kogevinas, N. Chatterjee, R. Pfeiffer, D. Silverman, M. Dosemeci, A. Tardo´n, C. Serra, A. Carrato, R. Garcı´a-Closas, G. Castan˜o-Vinyals, S. Chanock, M. Yeager, and N. Rothman, 2006, "Genetic Variation in the Nucleotide Excision Repair Pathway and Bladder Cancer Risk", *Cancer Epidemiology and Biomarkers Preview*, Vol. 15, No. 3, pp. 536-542.

Gillam, M. P. and P. Kopp, 2001a, "Genetic regulation of thyroid development", *Current Opinion in Pediatrics*, Vol. 13, pp. 358-363.

Gillam, M. P. and P. Kopp, 2001b, "Genetic defects in thyroid hormone synthesis", *Current Opinion in Pediatrics*, Vol. 13, pp. 364-372.

Glaze, D. G., 2005, "Neurophysiology of Rett syndrome", *Journal of Child Neurology*, Vol. 20, pp. 740-746, September.

Glockzin, S., F. X. Ogi, A. Hengstermann, M. Scheffner and C. Blattner, 2003, "Involvement of the DNA repair protein hHR23 in p53 degradation", *Molecular and Cellular Biology*, Vol. 23, No. 24, pp. 8960-8969.

Goelz, S.E., S. R. Hamilton and B. Vogelstein, 1985, "Purification of DNA from formaldehyde fixed and paraffin embedded human tissue", *Biochemical and Biophysical Research Communications*, Vol. 130, No. 1, pp. 118-126.

Grandjean, V., R. Yaman, F. Cuzin and M. Rassoulzadegan, 2007, "Inheritance of an epigenetic mark: The CpG DNA Methyltransferase 1 is required for *de novo* establishment of a complex pattern of non-CpG methylation", *PLoS ONE*, Vol. 2, No. 11, pp. e1136.

Grosso, S., A. Brogna, S. Bazzotti, A. Renieri, G. Morgese and P. Balestri, 2007, "Seizures and electroencephalographic findings in CDKL5 mutations: case report and review", *Brain and Development*, Vol. 29, No. 4, pp. 239-242, May.

Guazzi, S., M. Price, M. De Felice, G. Damante, M. G. Mattei and R. Di Lauro, 1990, "Thyroid nuclear factor 1 (TTF-1) contains a homeodomain and displays a novel DNA binding specificity", *EMBO Journal*, Vol. 9, pp. 3631-3639.

Guy, J., B. Hendrich, M. Holmes, J. E. Martin and A. Bird, 2001, "A mouse Mecp2-null mutation causes neurological symptoms that mimic Rett syndrome", *Nature Genetics*, Vol. 27, No. 3, pp. 322-326, March.

Hagberg, B., J. Aicardi, K. Dias and O. Ramos, 1983, "A progressive syndrome of autism, dementia, ataxia and loss of purposeful hand use in girls: Rett's syndrome: report of 35 cases", *Annals of Neurology*, Vol. 14, pp. 471-479.

Hagberg, B., F. Hanefeld, A. Percy and O. Skjeldal, 2002, "An update on clinically applicable diagnostic criteria in Rett syndrome. Comments to Rett Syndrome Clinical Criteria Consensus Panel Satellite to European Paediatric Neurology Society

Meeting, Baden, Germany, 11 September 2001", *European Journal of Paediatric Neurology,* Vol. 6, pp. 293-297.

Hagberg, B., A. Erlandsson, M. Kyllerman and G. Larsson, 2003, "Odd MECP2-mutated Rett variant-long-term follow-up profile to age 25", *European Journal of Paediatric Neurology*, Vol. 7, No. 6, pp. 417-421.

Hardwick, S. A., K. Reuter, S. L. Williamson and V. Vasudevan, 2007, "Delineation of large deletions of the MECP2 gene in Rett syndrome patients, including a familial case with a male proband", *European Journal of Human Genetics,* Vol. 15, pp. 1218-1229.

Helzlsouer, K. J., E. L. Harris, R. Parshad, S. Fogel, W. L. Bigbee and K. K. Sanford, 1995, "Familial clustering of breast cancer: possible interaction between DNA repair proficiency and radiation exposure in the development of breast cancer", *International Journal of Cancer*, Vol. 64, pp. 14 -17.

Helzlsouer, K. J., E. L. Harris, R. Parshad, H. R. Perry, F. M. Price and K. K. Sanford KK, 1996, "DNA repair proficiency: potential susceptibility factor for breast cancer", *Journal of National Cancer Institute*, Vol. 88, pp. 754-755.

Hermesz, E., S. Mackem and K. A. Mahon, 1996, "Rpx: a novel anteriorrestricted homeobox gene progressively activated in the prechordal plate, anterior neural plate and Rathke's pouch of the mouse embryo", *Development*, Vol. 122, pp. 41-52.

Hoeijmakers, J. H., 2001, "Genome maintenance mechanisms for preventing cancer", *Nature,* Vol. 411, No. 6835, pp. 366-374.

Hofmann, K. and P. Bucher, 1996, "The UBA domain: a sequence motif present in multiple enzyme classes of the ubiquitination pathway", *Trends in Biochemical Sciences,* Vol. 21, pp. 172-173.

Horike, S., S. Cai, M. Miyano, J. F. Cheng and T. Kohwi-Shigematsu, 2005, "Loss of silent-chromatin looping and impaired imprinting of DLX5 in Rett syndrome", *Nature Genetics*, Vol. 37, No. 1, pp. 31-40.

Hsieh, H. C., Y. H. Hsieh, Y. H. Huang, F. C. Shen, H. N. Tsai, J. H. Tsai, Y. T. Lai, Y. T. Wang, W. J. Chuang and W. Huang, 2005, "HHR23A, a human homolog of *Saccharomyces cerevisiae* Rad23, regulates xeroderma pigmentosum C protein and is required for nucleotide excision repair", *Biochemical and Biophysical Research Communications*, Vol. 335, No. 1, pp. 181-187.

Huang, W. Y., S. I. Berndt, D. Kang, N. Chatterjee, S. J. Chanock, M. Yeager, R. Welch, R. S. Bresalier, J. L. Weissfel and R. B. Hayes, 2006, "Nucleotide excision repair gene polymorphisms and risk of advanced colorectal adenoma: XPC polymorphisms modify smoking-related risk", *Cancer Epidemiology and Biomarkers Preview*, Vol. 15, No. 2, pp. 306-311.

Huppke, P., K. Köhler, F. Laccone and N. Kramer, 2003, "Indication for genetic testing: a checklist for rett syndrome", *Journal of Pediatrics,* Vol. 3, pp. 332-335.

Jeffery, L. and S. Nakielny, 2004, "Components of the DNA methylation system of chromatin control are RNA-binding proteins", *Journal of Biological Chemistry*, Vol. 279, No. 47, pp. 49479-49487, November.

Jellinger, K., D. Armstrong, H. Y. Zoghbi and A. K. Percy, 1988, "Neuropathology of Rett syndrome", *Acta Neuropathologica*, Vol. 76, No. 2, pp. 142-158.

Jian, L., H. L. Archer, D. Ravine, A. Kerr, N. de Klerk, J. Christodoulou, M. E. Bailey, C. Laurvick and H. Leonard, 2005, "p.R270X MECP2 mutation and mortality in Rett syndrome", *European Journal of Human Genetics*, Vol. 13, No. 11, pp. 1235-1238.

Jiang, Y., J. Bressler and A. L. Beaudet, 2004, "Epigenetics and human disease", *Annual Review of Genomics and Human Genetics*, Vol. 5, pp. 479-510.

Jin, C., I. Marsden, X. Chen and X. Liao, 1999, "Dynamic DNA contacts observed in the NMR structure of winged helix protein - DNA complex", *Journal of Molecular Biology*, Vol. 289, pp. 683-690.

Kaufmann, W. E. And H. W. Moser, 2000, "Dendritic anomalies in disorders associated with mental retardation", *Cerebral Cortex*, Vol. 10, No. 10, pp. 981-991.

Kaur, M., M. Pop, D. Shi, C. Brignone and S. R. Grossman, 2007, "hHR23B is required for genotoxic-specific activation of p53 and apoptosis", *Oncogene*, Vol. 26, No. 8, pp. 1231-1237.

Kerr, A. M., H. L. Archer, J. C. Evans, R. J. Prescott and F.Gibbon, 2006, "People with MECP2 mutation-positive Rett disorder who converse", *Journal of Intellectual Disability Research*, Vol. 50, Pt. 5, pp. 386-394.

Kim, I., K. Mi and H. Rao, 2004, "Multiple interactions of rad23 suggest a mechanism for ubiquitylated substrate delivery important in proteolysis", *Molecular and Biological Cell*, Vol. 15, No. 7, pp. 3357-3365.

Kimura, S., Y. Hara, T. Pineau, P. Fernandez-Salguero, C. H. Fox, J. M. Ward and F. J. Gonzalez, 1996, "The T/ebp null mouse: thyroid-specific enhancer-binding protein is essential for the organogenesis of the thyroid lung ventral forebrain", *Genes and Development*, Vol. 10, pp. 60-69.

Kohn, L. D., M. Saji, M. Kosugi, T. Ban, C. Giuliani, A. Hidaka, Y. Shimura and F. Okajima, 1993, "Thyroid Disease: Basic Science, Pathology, Clinical and Laboratory Diagnosis", *CRC press*, Boca Raton, pp. 59-118.

Kopp, P., 2001, "The TSH receptor and its role in thyroid disease", *Cellular and Molecular Life Sciences*, Vol. 58, No. 1301-1322.

Kouidou, S., T. Agidou, A. Kyrkou, A. Andreou, T. Katopodi, E. Georgiou, D. Krikelis, A. Dimitriadou, P. Spanos, C. Tsilikas, H. Destouni and G. Tzimagiorgis, 2005, "Non-

CpG cytosine methylation of p53 exon 5 in non-small cell lung carcinoma", *Lung Cancer*, Vol. 50, No. 3, pp. 299-307.

Kouidou, S., A. Malousi and N. Maglaveras, 2006, "Methylation and repeats in silent and nonsense mutations of p53", *Mutation Research*, Vol. 599, No. 1-2, pp. 167-177.

Krude, H., B. Schutz, H. Biebermann, A. von Moers, D. Schnable, H. Neitzel, H. Tonnies, D. Weise, A. Lafferty, S. Schwarz, M. DeFelice, A. con Deimling, F. van Landeghem, R. Li Lauro and A. Gruters, 2002, "Choreoathetosis, hypothyroidism, and pulmonary alterations due to human NKX2–1 haploinsufficiency", *The Journal of Clinical Investigation*, Vol. 109, pp. 475-480.

Kumar, S., A. L. Talis and P. M. Howley, 1999, "Identification of HHR23A as a substrate for E6-associated protein-mediated ubiquitination", *The Journal of Biological Chemistry*, Vol. 274, No. 26, pp. 18785-18792.

Lazzaro, D., M. Price, M. De Felice and R. Di Lauro, 1991, "The transcription factor TTF-1 is expressed at the onset of thyroid and lung morphogenesis and in restricted regions of the fetal brain", *Development*, Vol. 113, No. 1093-1104.

Lambertson, D., L. Chen and K. Madura, 1999, "Pleiotropic defects caused by loss of the proteasome-interacting factors Rad23 and Rpn10 of *Saccharomyces cerevisiae*", *Genetics*. Vol. 153, No. 1, pp. 69-79.

Li, L. C. and R. Dahiya, 2002, "MethPrimer: designing primers for methylation PCRs", Bioinformatics, Vol. 18, No. 11, pp. 1427-1431.

Lommel, L., T. Ortolan, L. Chen, K. Madura and K. S. Sweder, 2002, „Proteolysis of a nucleotide excision repair protein by the 26 S proteasome", Current Genetics, Vol. 42, No. 1, pp. 9-20.

Luikenhuis, S., E. Giacometti, C. F. Beard and R. Jaenisch, 2004, "Expression of MeCP2 in postmitotic neurons rescues Rett syndrome in mice", *Proceedings of the National*

Academy of Sciences of the United States of America, Vol. 101, No. 16, pp. 6033-6038, April.

Macchia, P.E., P. Lapi, H. Krude, M. T. Pirro, C. Missero, L. Chiovato, A. Souabni, M. Baserga, V. Tassi, A. Pinchera, G. Fenzi, A. Gruters, M. Busslinger and R. DiLauro, 1998, "PAX8 mutations associated with congenital hypothyroidism caused by thyroid agenesis", *Nature Genetics*, Vol. 19, No. 83-86.

Macchia, P.E., M. G. Mattei, P. Lapi, G. Fenzi and R. Di Lauro, 1999, "Cloning, chromosomal localization and identiÆcation of polymorphisms in the human thyroid transcription factor 2 gene (TTF-2)", *Biochimie,* Vol. 81, No. 433-440.

Maekawa, T., T. Shinagawa, Y. Sano, T. Sakuma, S. Nomura, K. Nagasaki, Y. Miki, F. Saito-Ohara, J. Inazawa, T. Kohno, J. Yokota and S. Ishii, 2007, "Reduced levels of ATF-2 predispose mice to mammary tumors", *Molecular and Cellular Biology*, Vol. 27, No. 5, pp. 1730-1744.

Magewu, A. N. and P. A. Jones, 1994, "Ubiquitous and tenacious methylation of the CpG site in codon 248 of the p53 gene may explain its frequent appearance as a mutational hot spot in human cancer", *Molecular and Cellular Biology*, Vol. 14, No. 6, pp. 4225-4232, June.

Makedonski, K., L. Abuhatzira, Y. Kaufman, A. Razin and R. Shemer, 2005, "MeCP2 deficiency in Rett syndrome causes epigenetic aberrations at the PWS/AS imprinting center that affects UBE3A expression", *Human Molecular Genetics*, Vol. 14, No. 8, pp. 1049-1058, April.

Malone, C. S., M. D. Miner, J. R. Doerr, J. P. Jackson, S. E. Jacobsen, R. Wall and M. Teitell, 2001, "CmC(A/T)GG DNA methylation in mature B cell lymphoma gene silencing", *Proceedings of the National Academy of Sciences of the USA*, Vol. 98, No. 18, pp. 10404-10409.

Mansouri, A., K. Chowdhury and P. Gruss, 1998, "Follicular cells of the thyroid gland require Pax8 gene function", *Nature Genetics*, Vol. 19, pp. 87-90.

Margueron, R., P. Trojer and D. Reinberg D., 2005, "The key to development: Interpreting the histone code?", *Current Opinion in Genetics and Development*, Vol. 15, pp.163-176.

Mari, F., S. Azimonti, I. Bertani, F. Bolognese, E. Colombo, R. Caselli, E. Scala, I. Longo, S. Grosso, C. Pescucci, F. Ariani, G. Hayek, P. Balestri, A. Bergo, G. Badaracco, M. Zappella, V. Broccoli, A. Renieri, C. Kilstrup-Nielsen and N. Landsberger, 2005, "CDKL5 belongs to the same molecular pathway of MeCP2 and it is responsible for the early-onset seizure variant of Rett syndrome", *Human Molecular Genetics*, Vol. 14, No. 14, pp. 1935-1946, July.

Marsden, I., C. Jin and X. Liao, 1998, "Structural changes in the region directly adjacent to the DNA-binding helix highlight a possible mechanism to explain the observed changes in the sequence-specific binding of winged helix proteins", *Journal of Molecular Biology,* Vol. 278, No. 293-299.

Masutani, C., M. Araki and K. Sugasawa, 1997, "Identification and characterization of XPC-binding domain of hHR23B", *Molecular and Cellular Biology,* Vol. 17, pp. 6915-6923.

Masuyama, T., M. Matsuo, J. J. Jing, Y. Tabara, K. Kitsuki, H. Yamagata, Y. Kan, T. Miki, K. Ishii and I. Kondo, 2005, "Classic Rett syndrome in a boy with R133C mutation of MECP2", *Brain and Development*, Vol. 27, No. 6, pp. 439-442, September.

Matarazzo, V., D. Cohen, A. M. Palmer, P. J. Simpson, B. Khokhar, S. J. Pan and G. V. Ronnett, 2004, "The transcriptional repressor Mecp2 regulates terminal neuronal differentiation", *Molecular and Cellular Neurosciences*, Vol. 27, No. 1, pp. 44-58, September.

Mechanic, L. E., R. C. Millikan, J. Player, A. R. de Cotret, S. Winkel, K. Worley, K. Heard, C. K. Tse and T. Keku, 2006, "Polymorphisms in nucleotide excision repair genes, smoking and breast cancer in African Americans and whites: a population-based case-control study", *Carcinogenesis*, Vol. 27, No. 7, pp. 1377-1385.

Meins, M., J. Lehmann, F. Gerresheim and J. Herchenbach, 2005, "Submicroscopic duplication in Xq28 causes increased expression of the MECP2 gene in a boy with severe mental retardation and features of Rett syndrome", *Journal of Medical Genetics,* Vol. 42, pp. 12.

Miao, F., M. Bouziane, R. Dammann, C. Masutani, F. Hanaoka, G. Pfeifer and T. R. O'Connor, 2000, "3-Methyladenine-DNA glycosylase (MPG protein) interacts with human RAD23 proteins", *The Journal of Biological Chemistry*, Vol. 275, No. 37, pp. 28433-28438.

Mirza, S., G. Sharma, C.P. Prasad, R. Parshad, A. Srivastava, S.D. Gupta and R.Ralhan, 2007, "Promoter hypermethylation of TMS1, BRCA1, ERalpha and PRB in serum and tumor DNA of invasive ductal breast carcinoma patients", *Life sciences,* Vol. 81, No. 4, pp. 280-287.

Moretti, P., J. M. Levenson, F. Battaglia, R. Atkinson, R. Teague, B. Antalffy, D. Armstrong, O. Arancio, J. D. Sweatt and H. Y. Zoghbi, 2006, "Learning and memory and synaptic plasticity are impaired in a mouse model of Rett syndrome", *Journal of Neurosciences*, Vol. 26, No. 1, pp. 319-327.

Moretti, P. and H. Y. Zoghbi, 2006, "MeCP2 dysfunction in Rett syndrome and related disorders", *Current Opinion in Genetics and Development,* Vol. 16, No. 3, pp. 276-281.

Morrison, D. K., and R. J. Davis, 2003, "Regulation of MAP kinase signaling modules by scaffold proteins in mammals", *Annual Review of Cell and Developmental Biology*, Vol. 19, pp. 91-118.

Mount, R. H., R. P. Hastings, S. Reilly, H. Cass and T. Charman, 2001, "Behavioural and emotional features in Rett syndrome", *Disability and Rehabilitation*, Vol. 23, No. 3-4, pp. 129-138.

Nan, X., F. J. Campoy and A.Bird, 1997, "MeCP2 is a transcriptional repressor with abundant binding sites in genomic chromatin", *Cell*, Vol. 88, No. 4, pp. 471-481.

Nikitina, T., R. P. Ghosh, R. A. Horowitz-Scherer, J. C. Hansen, S. A. Grigoryev, and C. L. Woodcock, 2007, "MeCP2-chromatin interactions include the formation of chromatosome-like structures and are altered in mutations causing Rett syndrome", *The Journal of Biological Chemistry*, Vol. 282, No. 38, pp. 28237-28245.

Ng, J. M., W. Vermeulen, G. T. van der Horst, S. Bergink, K. Sugasawa, H. Vrieling and J. H. Hoeijmakers, 2003, "A novel regulation mechanism of DNA repair by damage-induced and RAD23-dependent stabilization of xeroderma pigmentosum group C protein", *Genes and Development,* Vol. 13, pp. 1630-1645.

Nuber, U. A., S. Kriaucionis, T. C. Roloff, J. Guy, J. Selfridge, C. Steinhoff, R. Schulz, B. Lipkowitz, H. H. Ropers, M. C. Holmes and A. Bird, 2005, "Up-regulation of glucocorticoid-regulated genes in a mouse model of Rett syndrome", *Human Molecular Genetics*, Vol. 14, No. 15, pp. 2247-2256, August.

Oka, M., A. M. Meacham, T. Hamazaki, N. Rodić, L. J. Chang and N. Terada, 2005, "De novo DNA methyltransferases Dnmt3a and Dnmt3b primarily mediate the cytotoxic effect of 5-aza-2'-deoxycytidine", *Oncogene*, Vol. 24, No. 19, pp. 3091-3099.

Okano, M., D. W. Bell, D. A. Haber and E. Li, 1999, "DNA methyltransferases Dnmt3a and Dnmt3b are essential for de novo methylation and mammalian development", *Cell*, Vol. 99, No. 3, pp. 247-257.

Okuda, Y., R. Nishi, J.M. Ng, W. Vermeulen, G.T. van der Horst, T. Mori, J.H. Hoeijmakers, F. Hanaoka and K. Sugasawa, 2004, "Relative levels of the two

mammalian Rad23 homologs determine composition and stability of the xeroderma pigmentosum group C protein complex", *DNA Repair*, Vol. 3, No. 10, pp. 1285-1295.

Olivieri, A., M. A. Stazi, P. Mastroiacovo, C. Fazzini, E. Medda, A. Spagnolo, S. De S. Angelis, M. E. Grandolfo, D. Taruscio, V. Cordeddu and M. Sorcini, 2002, "A population-based study on the frequency of additional congenital malformations in infants with congenital hypothyroidism: data from the Italian Registry for Congenital Hypothyroidism (1991-1998)", *The Journal of Clinical Endocrinology and Metabolism*, Vol. 87, pp. 557-562.

Orrico, A., C. Lam, L. Galli, M. T. Dotti, G. Hayek, S. F. Tong, P. M. Poon, M. Zappella, A. Federico and V. Sorrentino, 2000, "MECP2 mutation in male patients with non-specific X-linked mental retardation", *FEBS Letters*, Vol. 481, No. 3, pp. 285-288.

Ortolan, T. G., P. Tongaonkar, D. Lambertson, L. Chen, C. Schauber and K. Madura, 2000, "The DNA repair protein Rad23 is a negative regulator of multi-ubiquitin chain assembly", *Nature Cell Biology*, Vol. 2, pp. 601-608.

Pelka, G. J., C. M. Watson, T. Radziewic, M. Hayward, H. Lahooti, J. Christodoulou and P. P. Tam, 2006, "Mecp2 deficiency is associated with learning and cognitive deficits and altered gene activity in the hippocampal region of mice", *Brain*, Vol. 129, No. 4, pp. 887-898, April

Peng, B., D. R. Hodge, S. B. Thomas, J. M. Cherry, D. J. Munroe, C. Pompeia, W. Xiao and W. L. Farrar, 2005, "Epigenetic silencing of the human nucleotide excision repair gene, hHR23B, in interleukin-6-responsive multiple myeloma KAS-6/1 cells", *Journal of Biological Chemistry*, Vol. 280, No. 6, pp. 4182-4187.

Peterson, C. L. and M. A. Laniel, 2004, "Histones and histone modifications", *Current Biology*, Vol. 14, pp. 546-551.

Pierrou, S., M. Hellqvist, L. Samuelsson, S. Enerback and P. Carlsson, 1994, "Cloning and characterization of seven human forkhead proteins: Binding site specificity and DNA bending", *EMBO Journal*, Vol. 13, No. 5002-5012.

Plachov, D., K. Chowdhury, C. Walther, D. Simon, J-L. Guenet and P. Gruss, 1990, "Pax8, a murine paired box gene expressed in the developing excretory system and thyroid gland", *Development*, Vol. 116, No. 643-651.

Prestridge, D. S., 1995, "Predicting Pol II promoter sequences using transcription factor binding sites", *The Journal of Molecular Bology*, Vol. 249, No. 5, pp. 923-932.

Raasi, S. and C. M. Pickart, 2003, "Rad23 ubiquitin-associated domains (UBA) inhibit 26 S proteasome-catalyzed proteolysis by sequestering lysine 48-linked polyubiquitin chains", *The Journal of Molecular Biology*, Vol. 278, No. 11, pp. 8951-8959.

Ramsahoye, B. H., D. Biniszkiewicz, F. Lyko, V. Clark, A. P. Bird and R. Jaenisch, 2000, "Non-CpG methylation is prevalent in embryonic stem cells and may be mediated by DNA methyltransferase 3a", *Proceedings of the National Academy of Sciences of the USA*, Vol.97, pp. 5237-5242.

Rassoulzadegan, M., M. Magliano and F. Cuzin, 2002, "Transvection effects involving DNA methylation during meiosis in the mouse", *The EMBO Journal*, Vol. 21, No. 3, pp. 440-450.

Refetoff, S., T. Sunthornthepvarakul, M. Gottschalk and Y. Hayashi, 1996, "Resistance to thyrotropin and other abnormabilities of the thyrotropin receptor", *Recent progress in Hormone Research*, Vol. 51, No. 97-122.

RettBASE, 2008, *IRSA MECP2 Variation Database*, http://mecp2.chw.edu.au.html.

Reiss, A. L., F. Faruque, S. Naidu, M. Abrams, T. Beaty, R. N. Bryan and H. Moser, 1993, "Neuroanatomy of Rett syndrome: a volumetric imaging study", *Annals of Neurology*, Vol. 34, No. 2, pp. 227-234.

Rett, A., 1966, "Ueber ein eigenartiges hirnatrophisches syndrom bei hyperammoniamie in kindesalter", *Wien Med Wschr,* Vol. 116, pp. 723-738.

Rivero, E. R., A. C. Neves, M. G. Silva-Valenzuela, S. O. Sousa and F. D. Nunes, 2006, "Simple salting-out method for DNA extraction from formalin-fixed, paraffin-embedded tissues", *Pathology, Research and Practice*, Vol. 202, No. 7, pp. 523-529.

Robbins, J., J. E. Rall and P. Gordon, 1980, "Metabolic Control and Disease", *Sounders,* Philadelphia, pp. 1325-1426.

Rodenhiser, D. and M. Mann, 2006, "Epigenetics and human disease: Translating basic biology into clinical applications", *Canadian Medical Association Journal*, Vol. 174, No. 3, pp. 341-348.

Scala, E., F. Ariani, F. Mari and R. Caselli, 2005, "CDKL5/STK9 is mutated in Rett syndrome variant with infantile spasms", *Journal of Medical Genetics,* Vol. 42, pp. 103-107.

Scala, E., I. Longo, F. Ottimo and C. Speciale, 2007, "MECP2 deletions and genotype-phenotype correlation in Rett syndrome", *American Journal of Medical Genetics Part A,* Vol. 143, pp. 2775-2784.

Schaeffer, L., R. Roy, S. Humbert, V. Moncollin, W. Vermeulen, J. H. Hoeijmakers, P. Chambon and J. M. Egly, 1993, "DNA repair helicase: A component of BTF2 (TFIIH) basic transcription factor", *Science*, Vol. 260, pp. 58–63.

Schanen, C., E. J. Houwink, N. Dorrani and J. Lane, 2004, "Phenotypic manifestations of MECP2 mutations in classical and atypical Rett syndrome", *American Journal of Medical Genetics,* Vol. 126, pp. 129-140.

Schauber, C., L. Chen, P. Tongaonkar, I. Vega, D. Lambertson, W. Potts and K. Madura, 1998, "Rad23 links DNA repair to the ubiquitin/ proteasome pathway", *Nature,* Vol. 391, pp. 715–718.

Schubert, U, L. C. Anton, J. Gibbs, C. C. Norbury, J. W. Yewdell and J. R. Bennink, 2000, "Rapid degradation of a large fraction of newly synthesized proteins by proteasomes", *Nature*, Vol. 404, pp. 770-774.

Schuler, M. and D. R. Green, 2005, "Transcription, apoptosis and p53: catch-22", *Trends in Genetics*, Vol. 21, No. 3, pp. 182-187.

Sdek, P., H. Ying, D. L. Chang, W. Qiu, H. Zheng, R. Touitou, M. J. Allday and Z. X. Xiao, 2005, "MDM2 promotes proteasome-dependent ubiquitin-independent degradation of retinoblastoma protein", *Molecular Cell*, Vol. 20, No. 5, pp. 699-708.

Segawa, M. and Y. Nomura, 2005, "Rett syndrome", *Current Opinion in Neurology*, Vol. 18, No. 2, pp. 97-104.

Sequeira, M., F. Al-Khafaji, S. M. Park, M. D. Lewis, M. H. Wheeler, V. K. K. Chatterjee, B. Jasani and M. Ludgate, 2003, "Production and application of polyclonal antibody to human thyroid transcription factor 2 reveals thyroid transcription factor 2 protein expression in adult thyroid and hair follicles and prepubertal testis", *Thyroid*, Vol. 13, pp. 927-932.

Shahbazian, M. D., B. Antalffy, D. L. Armstrong and H. Y. Zoghbi, 2002a, "Insight into Rett syndrome: MeCP2 levels display tissue- and cell-specific differences and correlate with neuronal maturation", *Human Molecular Genetics*, Vol. 11, No. 2, pp. 115-124, January.

Shahbazian, M. D., J. Young, L. Yuva-Paylor, C. Spencer, B. Antalffy, J. Noebels, D. Armstrong, R. Paylor and H. Zoghbi, 2002b, "Mice with truncated MeCP2

recapitulate many Rett syndrome features and display hyperacetylation of histone H3", *Nature*, Vol. 35, No. 2, pp. 243-254, July.

Shen, M., S. I. Berndt, N. Rothman, D. M. DeMarini, J. L. Mumford, X. He, M. R. Bonner, L. Tian, M. Yeager, R. Welch, S. Chanock, T. Zheng, N. Caporaso and Q. Lan, 2005, "Polymorphisms in the DNA nucleotide excision repair genes and lung cancer risk in Xuan Wei, China". *International Journey of Cancer*, Vol. 116, pp. 768–773.

Shi, S. R., R. J. Cote, L. Wu, C. Liu, R. Datar, Y. Shi, D. Liu, H. Lim and C. R. Taylor, 2002, "DNA extraction from archival formalin-fixed, paraffin-embedded tissue sections based on the antigen retrieval principle: heating under the influence of pH", *The Journal of Histochemistry and Cytochemistry*, Vol. 50, No. 8, pp. 1005-1011.

Shimizu, Y., S. Iwai, F. Hanaoka and K. Sugasawa, 2003, " Xeroderma pigmentosum group C protein interacts physically and functionally with thymine DNA glycosylase", *EMBO Journal,* Vol. 22, No. 1, pp. 164-173.

Simpson, P. T., J. S. Reis-Filho, T. Gale and S. R. Lakhani, 2005, "Molecular evolution of breast cancer", *Journal of Pathology*, Vol. 205, No. 2, pp. 248-254, January.

Sinclair, A., R. Lonigro, D. Civitareale, L. Ghibelli and R. Di Lauro, 1990, "The tissue-specific expression of the thyroglobulin gene requires interaction between thyroid-specific and ubiquitous factors", *European Journal of Biochemistry*, Vol. 193, No. 311-318.

Slee, E. A., D. J. O'Connor and X. Lu, 2004, "To die or not to die: how does p53 decide?", *Oncogene*, Vol. 23, No. 16, pp. 2809-2818.

Smale, S. T. and J. T. Kadonaga, 2003, "The RNA polymerase II core promoter", *Annual Review of Biochemistry*, Vol. 72, pp. 449-479.

Smeets, E., P. Terhal, P. Casaer and A. Peters, 2005, "Rett syndrome in females with CTS hot spot deletions: a disorder profile", *American Journal of Medical Genetics Part A,* Vol. 132, pp. 117-120.

Stein, S.A., E. L. Oates, C. R. Hall, R. M. Grumbles, L. M. Fernandez, N. A. Taylor, D. Puett and S. Jin, 1994, "Identification of a point mutation in the thyrotropin receptor of the hyt/hyt hypothyroid mouse", *Molecular Endocrinology*, Vol. 8, No. 129-138.

Strachan, T. and A. P. Read, *Human Molecular Genetics*, Wiley-Liss, New York, 2003.

Sugasawa, K., J. M. Y. Ng, C. Masutani, T. Maekawa, A. Uchida, P. J. van der Spek, A. P. M. Eker, S. Rademakers, C. Visser, A. Aboussekhra, R. D. Wood, F. Hanaoka, D. Bootsma and J. H. J. Hoeijmakers, 1997, "Two human homologs of Rad23 are functionally interchangeable in complex formation and stimulation of XPC repair activity", *Molecular Cell Biology,* Vol. 17**,** pp. 6924–6931.

Sugasawa, K., J. M. Ng, C. Masutani, S. Iwai, P. J. van der Spek, A. P. Eker, F. Hanaoka, D. Bootsma and J. H. Hoeijmakers, 1998, "Xeroderma pigmentosum group C protein complex is the initiator of global genome nucleotide excision repair", Molecular Cell, Vol. 2, pp. 223–232.

Szyf, M., "Targeting DNA methylation in cancer", 2006, *Bulletin du Cancer*, Vol. 93, No. 9, pp. 961-972.

Thoma, B. S. and K. M. Vasquez, 2003, "Critical DNA damage recognition functions of XPC-hHR23B and XPA-RPA in nucleotide excision repair", *Molecular Carcinogenesis*, Vol. 38, No. 1, pp. 1-13.

Toublanc, J.E., 1992, "Comparaison of epidemiological data on congenital hypothyroidism in Europe with those of other parts in the world", *Hormone Research*, Vol. 38, No. 230-235.

Trappe, R., F. Laccone, J. Cobilanschi, M. Meins, P. Huppke, F. Hanefeld and W. Engel, 2001, "MECP2 mutations in sporadic cases of Rett syndrome are almost exclusively of paternal origin", *American Journal of Human Genetics*, Vol. 68, No. 5, pp. 1093-1091, May.

Tudor, M., S. Akbarian, R. Z. Chen and R. Jaenisch, 2002, "Transcriptional profiling of a mouse model for Rett syndrome reveals subtle transcriptional changes in the brain", *Proceedings of the National Academy of Sciences of the United States of America*, Vol. 99, No. 24, pp. 15536-15541, November.

Van Dam, H., M. Duyndam, R. Rottier, A. Bosch, L. de Vries-Smits, P. Herrlich, A. Zantema, P. Angel, and A. J. van der Eb, 1993, "Heterodimer formation of cJun and ATF-2 is responsible for induction of c-jun by the 243 amino acid adenovirus E1A protein", *EMBO Journal*, Vol. 12, pp. 479-487.

Van der Spek, P. J., C. E. Visser, F. Hanaoka, B. Smit, A. Hagemeijer, D. Bootsma and J. H. Hoeijmakers, 1996, "Cloning, comparative mapping, and RNA expression of the mouse homologous of the *Saccharomyces cerevisiae* nucleotide excision repair gene RAD23", *Genomics,* Vol. 31, pp. 20–27.

Van Dongen, M. J., A. Cederberg, P. Carlsson, S. Enerback and M. Wikstrom, 2000, "Solution structure and dynamics of the DNA-binding domain of the adipocyte-transcription factor FREAC-11", *Journal Molecular Biology*, Vol. 296, No. 351-359.

Van Esch, H., M. Bauters, J. Ignatius and M. Jansen, 2005, "Duplication of the MECP2 region is a frequent cause of severe mental retardation and progressive neurological symptoms in males", *American Journal of Human Genetics,* Vol. 77, pp. 442-453.

Veerla, S., I. Panagopoulos, Y. Jin, D. Lindgren and M. Höglund, 2008, "Promoter analysis of epigenetically controlled genes in bladder cancer", *Genes Chromosomes Cancer*, Vol. 47, No. 5, pp. 368-378.

Vilain, C., C. Rydlewski, L. Duprez, C. Heinrichs, M. Abramowicz, P. Malvaux, B. Renneborg, J. Parma, S. Costagliola and G. Vassart, 2001, "Autosomal dominant transmission of congenital thyroid hypoplasia due to loss-of-function mutation of PAX8", *The Journal of Clinical Endocrinology and Metabolism*, Vol. 86, No. 234-238.

Wan, M., S. S. Lee, X. Zhang, I. Houwink-Manville, H. R. Song, R. E. Amir, S. Budden, S. Naidu, J. L. Pereira, I. F. Lo, H. Y. Zoghbi, N. C. Schanen and U. Francke, 1999, "Rett syndrome and beyond: recurrent spontaneous and familial MECP2 mutations at CpG hotspots", *American Journal of Human Genetics*, Vol. 65, No. 6, pp. 1520-1529, December.

Watkins, J.F., P. Sung, L. Prakash and S. Prakash, 1993, "The Saccharomyces cerevisiae DNA repair gene RAD23 encodes a nuclear protein containing a ubiquitin-like domain required for biological function", *Molecular and cellular biology,* Vol. 13, pp. 7757–7765.

Watson, P., G. Black, S. Ramsden and M. Barrow, 2001, "Angelman syndrome phenotype associated with mutations in MECP2, a gene encoding a methyl CpG binding protein", *Journal of Medical Genetics,* Vol. 38, pp. 224-228.

Weaving, L. S., J. Christodoulou, S. L. Williamson and K. L. Friend, 2004, "Mutations of CDKL5 cause a severe n.eurodevelopmental disorder with infantile spasms and mental retardation", *American Journal of Human Genetics,* Vol. 75, pp. 1079-1093.

Weaving, L. S., C. J. Ellaway, J. Gecz and J. Christodoulou, 2005, "Rett syndrome: clinical review and genetic update", *Journal of Medical Genetics,* Vol. 42, pp. 1-7.

Webb, T. and F. Latif, 2001, "Rett syndrome and the MECP2 gene", *Journal of Medical Genetics,* Vol. 38, pp. 217-223.

Weigel, D., G. Jurgens, F. Kuttner, E. Seifert and H. Jackle, 1989, "The homeotic gene fork head encodes a nuclear protein and is expressed in the terminal regions of the Drosophila embryo", *Cell*, Vol. 57, No. 645-658.

Weigelt, J., I. Climent, K. Dahlman-Wright and M. Wikstrom, 2001, "Solution structure of the dna binding domain of the human forkhead transcription factor afx (foxo4)", *Biochemistry*, Vol. 40, No. 5861-5869.

Weiss, S.J., N. J. Philp and E. F. Grollman, 1984, "Iodide transport in a continuous line of cultured cells from rat thyroid", *Endocrinology*, Vol. 114, No. 1090-1098.

Widschwendter, M. and P.A. Jones, 2002, "DNA methylation and breast carcinogenesis", *Oncogene*, Vol. 21, No. 35, pp. 5462-82, August.

Yamaguchi, R. And A. Dutta, 2000, "Proteasome inhibitors alter the orderly progression of DNA synthesis during S-phase in HeLa cells and lead to replication of DNA", *Experimental Cell Research*, Vol. 261, pp. 271-283.

Yang, C., E. Bolotin, T. Jiang, F. M. Sladek and E. Martinez, 2007, "Prevalence of the initiator over the TATA box in human and yeast genes and identification of DNA motifs enriched in human TATA-less core promoters", *Gene*, Vol. 389, No. 1, pp. 52-65.

Yasui, D. H., S. Peddada, M. C. Bieda, R. O. Vallero, A. Hogart, R. P. Nagarajan, K. N. Thatcher, P. J. Farnham and J. M. Lasalle, 2007, "Integrated epigenomic analyses of neuronal MeCP2 reveal a role for long-range interaction with active genes", *Proceedings of the National Academy of Sciences of the United States of America*, Vol. 104, No. 49, pp. 19416-19421, December.

Yıldız, T. S., M. Solak, I. Baris and K. Toker, 2006, "Unexpected prolonged paralysis after mivacurium in a patient with Bamforth syndrome", *Paediatric Anaesthesia*, Vol. 16, pp. 892-894, August.

Young, J. I., E. P. Hong, J. C. Castle, J. Crespo-Barreto, A. B. Bowman, M. F. Rose, D. Kang, R. Richman, J. M. Johnson, S. Berget and H.Y.Zoghbi, 2005, "Regulation of RNA splicing by the methylation-dependent transcriptional repressor methyl-CpG binding protein 2", *Proceedings of the National Academy of Sciences of the United States of America*, Vol. 102, No. 49, pp. 17551-17558, December.

Zannini, M., H. Francis-Lang, D. Plachov and R. Di Lauro, 1992, "Pax-8, a paired domain-containing protein, binds to a sequence overlapping the recognition site of a homeodomain and activates transcription from two thyroid-specific promoters", *Molecular and Cellular Biology,* Vol. 12, No. 9, pp. 4230-4241, September.

Zannini, M., V. Avantaggiato, E. Biffali, M. I. Arnone, K. Sato, M. Pischetola, B. A. Taylor, S. J. Phillips, A. Simeone and R. Di Lauro, 1997, "TTF-2, a new forkhead protein, shows a temporal expression in the developing thyroid which is consistent with a role in controlling the onset of the differentiation", *EMBO Journal*, Vol. 16, pp. 3185-3197.

Zappella, M., I. Meloni, I. Longo and G. Hayek, 2001, "Preserved speech variants of the Rett syndrome: molecular and clinical analysis", *American Journal of Medical Genetics,* Vol. 104, No. 1, pp. 14-22, November.

Zhu, Q., G. Wani, M. A. Wani and A. A. Wani, 2001, "Human homologue of yeast Rad23 protein A interacts with p300/cyclic AMP-responsive element binding (CREB)-binding protein to down-regulate transcriptional activity of p53", *Cancer Research*, Vol. 61, No. 1, pp. 64-70, January.